

# Design, analysis and simulation of a robust numerical method to solve Zika virus models

Bafana Mthobisi Fundzama



A Thesis submitted in partial fulfillment of the requirements for the degree of Master of Science in Mathematics in the Department of Mathematics and Applied Mathematics at the Faculty of Natural Sciences, University of the Western Cape

Supervisor: Prof. Kailash C. Patidar

June 2019

# KEYWORDS

Mathematical modelling

Zika virus

Qualitative analysis

Equilibrium points

Basic reproduction number

Non-Standard Finite Difference method

Theoretical analysis of the numerical method.



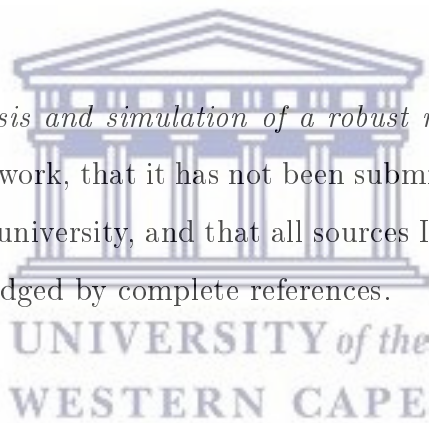
UNIVERSITY *of the*  
WESTERN CAPE

# ABSTRACT

This thesis deals with the analysis and robust simulation of mathematical models describing Zika virus disease. Some background information about the occurrences of this disease and most recent literature indicating some research gaps is presented. Governing models are very complex and their analytical solutions are hard to obtain. This necessitates the use of robust numerical methods. Several models from literature are presented in this work. One particular model is further studied in details for the purpose of understanding key qualitative features of the solutions of these types of models. These features are essential when we wish to develop a robust numerical method. After studying these properties on the dynamics of the solution for a particular model, we developed a novel numerical method, known as the non-standard finite difference method (NSFDM). A detailed theoretical analysis of this method, which is in line with necessary qualitative features of the solution of the governing model, is also presented. Finally, extensive numerical results showing competitiveness of this new method, as compared to other classical methods, are provided. In particular, we have shown how classical methods fail when the discretization step-size is large whereas NSFDM still gives excellent in such cases.

# DECLARATION

I declare that *Design, analysis and simulation of a robust numerical method to solve Zika virus models* is my own work, that it has not been submitted before for any degree or examination at any other university, and that all sources I have used or quoted have been indicated and acknowledged by complete references.



Bafana Mthobisi Fundzama

June 2019

Signed .....



# ACKNOWLEDGEMENT

I would like to take this opportunity to express my profound gratitude and deepest regard to my supervisor Professor Kailash C. Patidar, who made this work possible. His exemplary guidance, valuable feedbacks and suggestions, and constant encouragement throughout the duration of the thesis were of immense help. His perceptive criticism kept me working to make this thesis in a much better way. Working under him was an extremely knowledgeable experience for me.

I would also like to take the opportunity and thank the National Research Fund (NRF) for the financial support they gave me during the duration of my thesis.

I would also like to give my sincere gratitude to my church members especially pastor Okitowamba Onyumba, my friend and brother in Christ Thabo Mboweni and his wife sister Pumla for making my stay in Cape Town enjoyable and pleasant.

I gratefully thank my mother Nurse Fundzama and my siblings Bheki, Bongane, Lindokunhle, Nozipho and Nombulelo Fundzama for their great support and patience during the duration of my thesis.

Lastly, I would also like to give my sincere gratitude to the University of the Western Cape Library for the books and other resources that help in the completion of this thesis.

# DEDICATION

I dedicate this work firstly to the Lord Jesus Christ and to my mother Nurse Fundzama and late father Elias Fundzama.



UNIVERSITY *of the*  
WESTERN CAPE

# Contents

<b>Keywords</b>	<b>i</b>
<b>Abstract</b>	<b>ii</b>
<b>Declaration</b>	<b>iii</b>
<b>Aknowledgement</b>	<b>iv</b>
<b>Dedication</b>	<b>v</b>
<b>List of Tables</b>	<b>ix</b>
<b>List of Figures</b>	<b>xiii</b>
<b>List of Publications</b>	<b>xiv</b>
<b>1 General introduction</b>	<b>1</b>
1.1 Introduction . . . . .	1
1.1.1 History of Zika virus disease . . . . .	2
1.1.2 Symptoms of Zika virus disease . . . . .	4
1.1.3 Transmission of Zika virus disease . . . . .	4
1.1.4 Preventions and Control of Zika virus disease . . . . .	5
1.2 Literature Review . . . . .	6
1.3 Some recent Zika virus disease models . . . . .	19
1.3.1 SI-SI model describing the dynamics of Zika virus disease . . . . .	19



1.3.2	SIR-SI model describing the dynamics of Zika virus disease with the impact of infective immigrants . . . . .	20
1.3.3	SEIR-SEI model describing the dynamics of Zika virus disease . . . . .	22
1.3.4	SEIR-SEI model describing the dynamics of Zika virus disease with the influence of sexual transmission and preventive measures . . . . .	26
1.4	Outline of the thesis . . . . .	27
<b>2</b>	<b>Qualitative analysis of the SEIR-SEI model describing the dynamics of Zika virus disease</b>	<b>28</b>
2.1	Positivity of the solution . . . . .	28
2.2	Equilibrium points . . . . .	31
2.2.1	Disease Free Equilibrium . . . . .	32
2.2.2	Endemic Equilibrium . . . . .	33
2.3	Calculation of the basic reproduction number $R_0$ . . . . .	34
2.4	Local stability analysis of the model . . . . .	38
2.4.1	Local stability of the Disease Free Equilibrium . . . . .	38
2.4.2	Local stability of the Endemic Equilibrium . . . . .	41
2.5	Global stability analysis of the model . . . . .	43
2.5.1	Global stability of the Disease Free Equilibrium . . . . .	43
2.5.2	Global stability of the Endemic Equilibrium . . . . .	45
<b>3</b>	<b>Construction and analysis of a numerical method to simulate the SEIR-SEI model describing the dynamics of Zika virus disease</b>	<b>48</b>
3.1	What are these nonstandard finite difference methods? . . . . .	48
3.2	Derivation of a robust nonstandard finite difference method to solve the Zika virus disease model . . . . .	50
3.3	Analysis of proposed numerical method . . . . .	51
3.3.1	Stability analysis of the fixed points . . . . .	54
<b>4</b>	<b>Simulation results and discussions</b>	<b>60</b>

5 Concluding remarks and scope for further research	92
Bibliography	96



# List of Tables

1.3.1 Description of the model parameters and their values for SEIR-SEI model taken from [57] . . . . .	25
4.0.1 Spectral radii of the Jacobian matrix evaluated at $E_{0,1}$ obtained by Euler, method NSFD-I and NSFD-IIs for different step-sizes $\ell$ for patch 1 with $b_v^1 = 0.38$ and $N_v = 9000000$ . . . . .	63
4.0.2 Spectral radii of the Jacobian matrix evaluated at $E_{0,2}$ obtained by Euler, method NSFD-I and NSFD-IIs for different step-sizes $\ell$ for patch 2 with $b_v^2 = 0.38$ and $N_v = 6000000$ . . . . .	63
4.0.3 Spectral radii of the Jacobian matrix evaluated at $E_{e,1}$ obtained by Euler, method NSFD-I and NSFD-IIs for different step-sizes $\ell$ for patch 1 with $b_v^1 = 0.5$ and $N_v = 60000000$ . . . . .	64
4.0.4 Spectral radii of the Jacobian matrix evaluated at $E_{e,2}$ obtained by Euler, method NSFD-I and NSFD-IIs for different step-sizes $\ell$ for patch 2 with $b_v^2 = 0.5$ and $N_v = 30000000$ . . . . .	64

# List of Figures

1.1.1	Zika virus spread map from Uganda to South America . . . . .	3
1.3.1	Transmission of Zika virus from an infected vector (mosquito) to a susceptible human and back to a susceptible vector. Dotted arrows indicate bites while solid arrows indicate a transfer between different compartments [57]. . . . .	23
4.0.1	The basic reproduction number $R_0$ obtained by method NSFD-II for patch 1 and 2 with a cyclical death rate $\mu_v^i$ and $\ell = 1$ . . . . .	61
4.0.2	Profiles of solutions generated by Euler method (a) and by method NSFD-I and NSFD-II (b) for the human population of patch 1 with $R_{0,1} = 0.57855$ and $\ell = 0.5$ . . . . .	67
4.0.3	Profiles of solutions generated by Euler method (a) and by method NSFD-I and NSFD-II (b) for the vector population of patch 1 with $R_{0,1} = 0.57855$ and $\ell = 0.5$ . . . . .	68
4.0.4	Profiles of solutions generated by Euler method (a) and by method NSFD-I and NSFD-II (b) for the human population of patch 1 with $R_{0,1} = 0.57855$ and $\ell = 6$ . . . . .	69
4.0.5	Profiles of solutions generated by Euler method (a) and by method NSFD-I and NSFD-II (b) for the vector population of patch 1 with $R_{0,1} = 0.57855$ and $\ell = 6$ . . . . .	70

4.0.6	Profiles of solutions generated by Euler method (a) and by method NSFD-I and NSFD-II (b) for the human population of patch 2 with $R_{0,2} = 0.70703$ and $\ell = 0.5$ . . . . .	71
4.0.7	Profiles of solutions generated by Euler method (a) and by method NSFD-I and NSFD-II (b) for the vector population of patch 2 with $R_{0,2} = 0.70703$ and $\ell = 0.5$ . . . . .	72
4.0.8	Profiles of solutions generated by Euler method (a) and by method NSFD-I and NSFD-II (b) for the human population of patch 2 with $R_{0,2} = 0.70703$ and $\ell = 8$ . . . . .	73
4.0.9	Profiles of solutions generated by Euler method (a) and by method NSFD-I and NSFD-II (b) for the vector population of patch 2 with $R_{0,2} = 0.70703$ and $\ell = 8$ . . . . .	74
4.0.10	Profiles of solutions generated by Euler method (a) and by method NSFD-I and NSFD-II (b) for the human population of patch 1 with $R_{0,1} = 1.9655$ and $\ell = 0.5$ . . . . .	75
4.0.11	Profiles of solutions generated by Euler method (a) and by method NSFD-I and NSFD-II (b) for the vector population of patch 1 with $R_{0,1} = 1.9655$ and $\ell = 0.5$ . . . . .	76
4.0.12	Profiles of solutions generated by Euler method (a) and by method NSFD-I and NSFD-II (b) for the human population of patch 1 with $R_{0,1} = 1.9655$ and $\ell = 5.55$ . . . . .	77
4.0.13	Profiles of solutions generated by Euler method (a) and by method NSFD-I and NSFD-II (b) for the vector population of patch 1 with $R_{0,1} = 1.9655$ and $\ell = 5.55$ . . . . .	78
4.0.14	Profiles of solutions generated by Euler method (a) and by method NSFD-I and NSFD-II (b) for the human population of patch 2 with $R_{0,1} = 2.0802$ and $\ell = 0.5$ . . . . .	79



4.0.15	Profiles of solutions generated by Euler method (a) and by method NSFD-I and NSFD-II (b) for the vector population of patch 2 with $R_{0,1} = 2.0802$ and $\ell = 0.5$ . . . . .	80
4.0.16	Profiles of solutions generated by Euler method (a) and by method NSFD-I and NSFD-II (b) for the human population of patch 2 with $R_{0,1} = 2.0802$ and $\ell = 5.8$ . . . . .	81
4.0.17	Profiles of solutions generated by Euler method (a) and by method NSFD-I and NSFD-II (b) for the vector population of patch 2 with $R_{0,1} = 2.0802$ and $\ell = 5.8$ . . . . .	82
4.0.18	Profiles of solutions generated by method NSFD-I and NSFD-II for the human and vector populations of patch 1 with $R_{0,1} = 0.57855$ and $\ell = 50$ . . . . .	83
4.0.19	Profiles of solutions generated by method NSFD-I and NSFD-II for the human and vector populations of patch 2 with $R_{0,2} = 0.70703$ and $\ell = 50$ . . . . .	84
4.0.20	Profiles of solutions generated by method NSFD-I and NSFD-II for the human and vector populations of patch 1 with $R_{0,1} = 1.9655$ and $\ell = 1000$ . . . . .	85
4.0.21	Profiles of solutions generated by method NSFD-I and NSFD-II for the human and vector populations of patch 2 with $R_{0,2} = 2.0802$ and $\ell = 1000$ . . . . .	86
4.0.22	Profiles of solutions generated by Euler, method NSFD-I and NSFD-IIs for the human and vector populations of patch 1 with $b_v = 0.5$ and $\ell = 0.5$ . . . . .	87
4.0.23	Profiles of solutions generated by Euler, method NSFD-I and NSFD-IIs for the human and vector populations of patch 2 with $b_v = 0.5$ and $\ell = 0.5$ . . . . .	88
4.0.24	Profiles of solutions generated by Euler, method NSFD-I and NSFD-IIs for the human and vector populations of patch 1 with $b_v = 0.5$ and $\ell = 6$ . . . . .	89
4.0.25	Profiles of solutions generated by Euler, method NSFD-I and NSFD-IIs for the human and vector populations of patch 2 with $b_v = 0.5$ and $\ell = 6$ . . . . .	90

4.0.26 Profiles of solutions generated by Euler, method NSFD-I and NSFD-IIs  
for the human and vector populations of patch 2 with  $b_v = 0.38$  and  
 $\ell = 6$ . . . . . 91



UNIVERSITY *of the*  
WESTERN CAPE

# List of Publications

We are busy finalizing one research article which we intend to submit soon to an accredited journal.



UNIVERSITY *of the*  
WESTERN CAPE

# Chapter 1

## General introduction

### 1.1 Introduction

Zika virus (also known as ZIKV) was first discovered from sentinel rhesus monkey caged in the Zika forest near Entebbe Peninsula in Uganda in 1947, during a routine surveillance for yellow fever conducted by the East African Virus Research Institute [9, 75]. The word “Zika” comes from the Luganda language, which means overgrown [77]. The single stranded ribonucleic acid (RNA) virus is an arbovirus from the class of flaviviridae that is mainly transmitted to humans by the bites of infected female *Aedes* mosquitoes genus [5, 33]. These types of mosquitoes are also responsible for the transmission of other viruses such as dengue fever, Chikungunya, yellow fever, and Japanese encephalitis and are mainly found in tropical and subtropical regions [25]. Zika virus transmission is endemic to tropical and subtropical regions due to the prevalence of the mosquitoes in those regions, and the role of climate change due to global warming is suspected to be one of the leading contributors to the rising of mosquito-borne diseases [77].

### 1.1.1 History of Zika virus disease

The Zika virus became widely known during the South American outbreak in 2015, which started from the Easter Island in 2014 then moved to the Caribbean and to the Central and South American countries, which was documented as the largest outbreak of the virus since its discovery in 1947 [18].

Thus far, the Zika virus has found its way almost across the whole world, invading a total of 65 countries and territories since its discovery in Uganda [26]. In 1947, the Zika virus was identified in mosquito *Aedes africanus* in the Zika forest and four years later, it was discovered in humans for the first time in Uganda and its neighboring countries, Tanzania and Nigeria [75]. Other African countries that reported isolated cases of human infected by the virus are countries such as Senegal, Ivory Coast, Gabon, Egypt, Central African Republic and Sierra Leone [25, 33].

Outside of Africa, the virus was identified from *A. Aegypti* mosquitoes in Malaysia in 1966, and later in central Java, Indonesia and other Asian countries such as Cambodia, India, Indonesia, Malaysia, Pakistan, Philippines, Singapore, Thailand, and Vietnam reporting several cases of the infection [72, 74]. Not much was known about the virus until the 2007 outbreak in Gabon, Yap Island and some of the Islands of Federated States of Micronesia where approximately 8 000 cases of infection of the virus were reported [33]. In October 2013, a ZIKV outbreak was documented in French Polynesia, South Pacific (with an estimated 70% of the population affected), New Caledonia, and the Cook Islands, followed by the outbreak in 2014 in Easter Island and Vanuatu, Solomon Islands, Samoa, and Fiji in 2015 [25, 31, 81]. It is believed that the virus entered South American and subsequently the whole American continent during the 2014 World Cup soccer games [74]. The outbreak lasted for a period of two years from 2015 to 2016 spreading across the 14 Brazilian states with an estimate of 1 300 000 cases reported. The Pan American Health Organization predicted that roughly 550

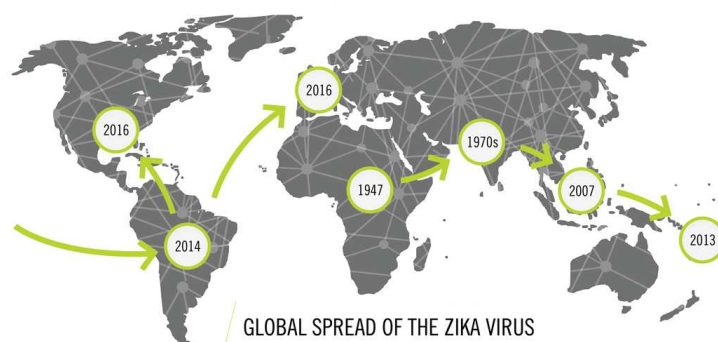


Figure 1.1.1 Zika virus spread map from Uganda to South America

million people were likely to be infected by the Zika virus in the Americas [26].

The Zika virus is believed to be one of the leading cause of close to 6000 cases of microcephaly (a condition where a baby's head is much smaller than expected as a result of an under-developed brain) in Brazil, 200 Guillain-Barré syndrome (sickness of the nervous system in which a person's own immune system damages the nerve cells, causing muscle weakness, and sometimes, paralysis) cases in Columbia and 118 GBS (Guillain-Barré syndrome) cases in El Salvador in newborns between 2015 and 2016. The Zika virus is believed to be one of the leading cause of close to 6000 cases of microcephaly in Brazil, 200 GBS cases in Columbia and 118 GBS cases in El Salvador in newborns between 2015 and 2016. It is worth noting that the virus is believed to have two distinct lineage, the African lineage that was first detected in Uganda in 1947 and the Asian lineage detected in Malaysia in 1966 which is believed to responsible for most outbreak occurred outside Africa [36]. Due to the increase of the cases microcephaly and other neurological diseases resulting from the infection by the virus the World Health Organization (WHO) was prompted to declare a public health emergency of international concern [5].

### 1.1.2 Symptoms of Zika virus disease

Most people that are infected with Zika virus do not show symptoms, only about 20 percent of them have shown some mild symptoms lasting from two to seven days with no cases of death reported that are associated with a direct infection of the virus in the recent large outbreaks [25]. The symptoms includes fever, arthralgia, muscle and joint pain, malaise, headache, edema of extremities, retro-orbital pain, conjunctival hyperaemia and maculopapular rashes usually spreading downward from the face to the limbs and frequently pruritic, vertigo, myalgia, and digestive disorder and it has been associated with neurological and autoimmune complications and confirmed that it causes Guillain-Barré syndrome (GBS) and congenital infection which can course microcephaly and maculopathy [8, 33, 50].

A proper laboratory diagnostic test is essential to diagnose if a patient is infected with Zika virus or not, see [56]. There are two methods used to diagnose the virus, the direct method where the viral genome is detected using a method known as the RT-PCR (where RT stands for reverse transcription and PCR for polymerase chain reaction) in the body fluids and the indirect method where the Zika virus antibodies are detected in the blood [21].

### 1.1.3 Transmission of Zika virus disease

The ZIKV is mainly transmitted to humans by *Aedes* mosquitoes, however the virus can also be transmitted through other means as well, as studies has revealed. The RNA of the virus has been found in the blood, semen, urine, saliva, amniotic fluid, breast milk and cerebro-spinal fluid of infected individuals [26]. A case of a sexually transmitted Zika virus was reported 2008 in Colorado, USA, of a male infecting a female through a virginal sexual intercourse and in the Western Hemisphere ZIKV outbreak in 2016 cases of sexual transmission were also confirmed [75]. In total 9 countries have reported cases of sexual transition of the virus including Chile, France and New

Zealand [67]. The fact that traces of the virus have been found in the semen even after the virus had disappeared in the blood of an infected person, that indicates that the virus can live longer in the semen [77].

The recorded cases of sexual transmission were cases of the transmission from a male to a sexual partner via vaginal or anal intercourse, and it is still unknown if the virus can be transmitted from female to male [26]. Zika virus has gotten more attention for its effects in babies that are born from mother who are infected with the virus during the course of pregnancy resulting in the increase in the number of cases of microcephaly and other neurological disorder in newborns. A pregnant woman can transmit the virus to a fetus. It is still unknown though as to how the Zika virus courses microcephaly, but the presence of the virus from brain tissues of the affected fetus has been identified [77].

The ability of the virus to live in non-human primates possess a great difficulty in annihilating it completely among a population [9]. The potential danger of Zika virus spreading to other regions that the virus did not exist before as it was seen with other viruses transported by the same type of mosquitoes is greater, since the mosquitoes that carries the virus can be found in most part of the world. Other factors that perpetuate outbreaks of infectious diseases are huge human gathering like sports events, religious activities and other forms of entertainment. People travelling to such activities become at risk of contracting and bringing the viruses at their home regions where these vectors that transmit the viruses exist [18]. The study of the outbreaks of ZIKV has shown that infections occur across all age group [25].

#### 1.1.4 Preventions and Control of Zika virus disease

At the moment there is no vaccine, treatment and a quick way to diagnose virus from infected people [25]. Prevention measures include preventing mosquito bite by the use of protective clothing, bed-nets, mosquito-proofing of houses, insect repellents, insect



ticides etc. [77]. ZIKV can be also transmitted via sexual contact, it is necessary to practice safe sex during an outbreak [3]. Avoiding mosquito bites during an outbreak is also necessary to prevent any further spread of the virus [8]. During an outbreak, pregnant women are advised against travelling to areas where the threat of the virus exist, and sexual active women living in affected areas need to use contraceptives and must take measures to avoid mosquito bites [45]. More information on the Zika virus disease can be found in [22, 30, 32, 38, 65, 71, 76].

In the next section, we present a brief literature review on the modelling of Zika virus disease.

## 1.2 Literature Review

To study the transmission dynamics of Zika virus disease, deterministic mathematical models have been presented in [20, 25, 37, 39, 57, 58, 61, 62] and some of the references therein. Most of these models used a susceptible, exposed, infected, recovered (SEIR) model framework for the human population and susceptible, exposed, infected (SEI) model framework for the vector (mosquito) population. However, in some instances, models such as the ones described in [20] and [58] were an SI-SI type of model framework was used with the recovered and the exposed compartment have been omitted. The exposed compartment is left out due to the fact that the period between the infection and the appearance of the first symptoms is short.

Optimal control strategies to reduce the spread of the virus with a minimal cost have been investigated by some of the authors such in [20] and [58] as well. Here we give a literature on the mathematical modelling of the Zika virus and on the discretization of epidemic mathematical models using a robust method known as the nonstandard finite difference (NSFD) method.

The model presented in [20] for example uses an SI type of model for both the human population and mosquito population to describe the dynamics of Zika virus disease. In the model, only consider the susceptible and infected humans and mosquitoes. The basic reproduction number  $R_0$  of the system is derived using a well-known method called the next generation matrix method developed in [73] and a sensitive analysis of the model in terms of some of the important parameters affecting the basic reproduction number is performed. The authors found that some parameters such as the natural death rate of mosquitos and the contact rate between human and mosquitos affects the basic reproduction number  $R_0$  when large. Control measures that were investigated to prevent the spread of the Zika virus such as the use of clothes, mosquito nets, window screens to prevent mosquito bites, increasing the autoimmunity and use of insecticide through source reduction to kill the mosquitos were found to be very effective in reducing the spread of Zika.

Another SI-SI type of a Zika virus model is presented in [58] where the infected individuals are further subdivided into two sub-classes, the infected individuals and isolated individuals. These isolated individuals are infected individuals that are diagnosed and placed in isolation to avoid any further contact with the susceptible human and mosquito population. Treatment is then given to the isolated individuals to treat only the symptoms that they display because of the unavailability of treatment for Zika disease as of yet. In the model, the transmission of Zika virus through sexual contact is also considered. Furthermore, in their model, a distinction is made between individuals that are dying a natural death and individuals that are dying due to the Zika disease.

The qualitative features of the model are investigated and the local stability analysis is performed. Their numerical results show that as the human-induced death rate of mosquitoes is increased, the infected mosquito population reduces. It is also observed that an increase in the mosquito biting rate produced an increased transmission rate.  $R_0$  increases as the biting rate increases and decreases as the human-induced death on

mosquito rate increases. It is then concluded that the increase in the recovery rate, human-induced death on the mosquito population and isolation of infected individuals decreases the spread of the virus.

The model described in [20] and the one described in [58] does not consider the recovered compartment for the human population. However, during the recent large outbreaks such as the one in French Republic and in Brazil, cases of death due to the Zika infection were not reported and even hospitalization of infected individuals was rare [33, 54]. This implied that infected individuals do recover from the infection even without seeking medical attention. The model presented in [10] is an SIR-SI type of a model designed to study the dynamic transmission of the Zika virus between human and mosquitos. This model is used to study the dynamical transmission of Zika virus with some optimal control strategies (prevention, treatment and insecticide). Unlike the model presented in [20] and [58], infected individual do recovers from the infection.

The qualitative features of the model (positivity of solutions, the equilibrium points and the basic reproduction number) were investigated and the stability analysis of the model at the equilibrium points was investigated first without the optimal control strategies and then with the optimal control strategies. The basic reproduction number of the model indicates that the spread of Zika virus is reduced by the increase of the recovery rate and natural death of human and mosquito population. It is found that a combination of all the control strategies (prevention, treatment and insecticide control) yields the best result in combating the disease.

The model presented in [34] is an SEIR-SI deterministic compartmental model to describe the transmission dynamics of Zika virus disease between humans and mosuitos in the Brazil, Cape Verde and Colombia population. In the model, the exposed human compartment is added. These exposed humans are infected humans that are not yet infectious. The qualitative features of the model are investigated and to simulate the

model, data collected by the World Health Organisation (WHO) is used to study three different cases, Colombia, Cape Verde Brazil as case 1, 2 and 3, respectively.

In addition to the model described in [34], the model in [39] described a Zika model where the exposed vector compartment is added. The qualitative features of the model and the local stability of the equilibrium points are investigated with the aid of the Routh-Hurwitz criteria.

Another model presented in [16] offers a similar type of model framework to the one presented in [39] where only the transmission of the virus by mosquito vectors is considered for the Zika virus outbreak in Rio de Janeiro. Data taken from the epidemiological reports of the Ministry of Health in Brazil was used to affirm the representativeness of the described model. It is discovered that due to the lack of information in the report by the Ministry of Health, it made it difficult to choose the right set of parameters and hence that in some instances the model did not fit the data. A model calibration using a non-linear curve fitting procedure was used to analyse the necessary parameters in the model to fit the data.

The qualitative features such as the positivity of the solution, the disease free equilibrium point and the basic reproduction number and the local stability analysis of the model at the disease free equilibrium point were investigated. An economical assessment of the intervention strategies (such as the use of bed-nets, condoms, Indoor Residual Spraying (IRS), symptoms treatments) was done using optimal control and cost effectiveness analysis. Runge-Kutta method was used in the simulations to obtain numerical results for the sub-combination of the control measures and cost effectiveness analysis. It is then discovered that the control strategies that were more cost effective were the use of bed-nets, treatment and IRS.

Another SEIR-SEI compartmental model framework for the human and mosquito pop-

ulation, respectively, is presented in [42]. The model takes into account the developmental stages in a typical life cycle of the mosquitos (egg, larva, pupa, and adult). In the model, susceptible humans get infected by being bitten by infected adult female mosquitos and susceptible mosquitos get infected by biting infected human. To fight against the wide spread of Zika virus into the population, two intervention strategies were investigated: the reduction of mosquito biting rate and the reduction of female mosquito population using relevant methods. The basic reproduction number was used to investigate the effect of the intervention on the spread of the Zika virus in the population. It is found that intervention strategies used such as the reduction of the mosquito biting rate, larvae carrying capacity and adult vector population, and the increase of adult vector mortality rate can reduce the scale of the Zika virus infection.

Similar to the model presented in [42], an SEIR-SEI model framework in which the human population is first divided into male and female subgroups like in the model presented in [13] is described in [3] to study the transmission dynamics of Zika virus disease via vector-borne and sexual (both heterosexual and homosexual) transmission spread. Both the female and male population are partitioned into susceptible, exposed, infected and recovered class and the mosquito population is partitioned into susceptible, exposed and infected class. In the model, male humans are infectious to both males and females, and female humans are assumed to be infectious to males. In the analysis of the model, the positivity analysis of the solution, basic reproduction number, disease free and endemic equilibrium points and their local and global stability analysis was investigated for the sub-models (i.e. mosquito transmission route only model, sexual transmission route only model) and the full model and some numerical results were given to support the analysis.

About 80% of people infected with Zika do not show any symptoms [25]. In the model presented in [62] infected individuals are divided into asymptomatic and symptomatic. An SEIR-SEI type of a model for the human and mosquito population, respectively.

In the model, the exposed compartment cover the incubation phase where the individuals are infected but not yet infectious and the infectious individuals (asymptomatic infected and symptomatic) are assumed to have a different infection rate towards susceptible mosquitos. The infectious individual are assumed to be cable of passing the virus to susceptible human via sexual contact and the susceptible mosquitos can get the virus as well by biting these infected individuals.

As a control measure, two prevention measures recommended by World Health Organisation (WHO) and Central Disease Control (CDC) were incorporated to their model, namely: the Insecticide-Treated Mosquito Nets (ITN) and Indoor Residual Spraying (IRS). The ITN will obviously affect the mosquito biting rate, so this effect was incorporated into the model as a parameter measured as a percent ( $1 - ITN$ ) against the transmission rate from susceptible to exposed individuals, where  $ITN = 1$  implied that the mosquitos will totally fail to bite susceptible individuals and the virus will only spread via sexual contact and  $ITN = 0$  implied the nets have no effect at all on preventing of the mosquitos from biting susceptible individuals. Indoor Residual Spraying (IRS) is used to reduce the population of the mosquitos. It is also assumed that recovered individuals are partially immune to the disease and therefore in the model, once individuals recover from the infection, they are assumed to be no longer susceptible to the virus due to the lack of evidence of such cases where an individual gets infected by the virus after recovery.

To analyse the model in [62], the basic reproduction number is derived using the next generation matrix approach in the present of both the sexual transmission and vector transmission, in the presence of only the vector transmission without any sexual transmission and in the presence of only the sexual transmission without any vector transmission. The fourth order Runge-Kutta method for solving system of Ordinary differential equations was used in their simulation. Computations were done in the presence and absence of the control measures ( $ITN$  and  $IRS$ ), with a large value of

the sexual transmission rate, and for a complete intervention where the exposed and infected mosquito population were totally eliminated from the population with only the sexual transmission presents. In each case, a plot of the basic reproduction number is offered. The results show that in the total absence of the interventions, the spread of the virus is much faster and with a complete intervention (mosquitos totally eradicated from the population), where virus is dependent on the sexual transmission only, the spread is much slower.

The model presented in [37] is a similar type of model to the one presented in [62]. The model was used to study the dynamical transmission of Zika virus during French Polynesia outbreak between the year 2013 to 2014. Infected human are subdivided into symptomatically and asymptotically infected. In the model, unlike in the one presented in [62], both symptomatically and asymptotically infected humans are assumed to transmit the Zika virus to mosquitos at the same rate. Due to the fact that the average human life span is longer than that of the outbreak, both the human birth and mortality rate are ignored in their model. The basic reproduction number  $R_0$  is derived and a sensitive analyses on the parameters of the model is performed.

A model to study the transmission dynamics of Zika virus disease in the population of Colombia, El Salvador, and Suriname during the 2015-2016 outbreak is presented in [66]. In the model, susceptible human become infected after being bitten by infected mosquitos and susceptible mosquitos get infected by biting infected (both symptomatic and asymptomatic) human, sexual transmission is ignored in the model. Exposed human are assumed to be not infectious to susceptible mosquitos. The human birth and death rate is ignored as well in the model. The next generation matrix method is used to calculate the basic reproduction number of the system. In the model, they calculated the population at risk of getting the infection for each respective country instead of assuming the whole population in each country was susceptible. This was done by taking into consideration the presents of the Aedes mosquitos and the geog-

raphy of the respective countries. The parameters of the model were then estimated using the Bayesian computation and the data was taken from Pan American Health Organization database.

In [51] a deterministic model to describe the dynamic of the Zika virus transmission and to study the effectiveness of some optimal control strategy incorporated in the model as an intervention measure against the spread of the Zika virus similar to the one in [66] is presented. The following information was incorporated in the model: Birth rate and natural and disease induced death rate, asymptotically infected human can transmit the virus through sexual contact, treatment is given to symptomatically infected human as a control measure and some human recovery natural without treatment, susceptible mosquitos become infected by biting symptomatically infected human, the reduction of the mosquito population is caused by natural death and by indoor residual spray (IRS) as a control measure, the contact rate between asymptomatic individuals and susceptible individual is greater than the contact rate between symptomatic and susceptible due to the fact that the symptomatic are aware of the disease and may use protections, recovered human gain temporary immunity or no immunity at all.

Another deterministic model is presented in [61] to describe the dynamics of the transmission of Zika virus. In the model, the sexual transmission of the virus from infected individuals to susceptible individual was included. The qualitative features of the model and the stability analysis of the equilibrium points were investigated. The sensitivity analysis revealed that the most sensitive parameters was the rate at which exposed mosquito move to infectious class, the rate at which mosquito infect human and the rate at which infected human infect susceptible mosquito.

To investigate Zika transmission between adult and newly born babies a deterministic compartmental model where the human population is split into adults subgroup and newly born babies subgroup is presented in [4]. The human populations (both



adult and newly born babies) are partitioned into susceptible, exposed, asymptomatic and symptomatic (born with and without microcephaly) infected and recovered class. The dynamic features of model are considered in [3] for the full model. A global sensitivity analysis is performed to assess the impact of uncertainty and the sensitivity of the outcomes of the numerical simulations to variations in each parameter of the model. The sensitive analysis led to the assessment of some control strategies to control certain parameters and their effectiveness as targets. These control strategies include mosquito-reduction strategies, personal protection strategy, combined mosquito control and personal protection strategy and delayed pregnancy. The combined strategy is found to be the most effective strategy to reduce the transmission of Zika.

In the work done in [25], exposed individuals were found to be infectious to both human and mosquitos, but at a lower rate than symptomatically infected individuals. Convalescent individuals can also transmit the virus to human through sexual intercourse. Asymptomatically infected individuals in their study were assumed to be non-infectious to human and mosquitos due to the lack of evidence and individuals after the convalescent stage are left immunised from the virus for life.

A model that incorporated all the information is presented, like the model presented in [62], an SEIR type of model for human and SEI type of model for mosquitos to study the dynamic transmission of the virus. In their model, they have an additional compartment called the convalescent stage were symptomatically infected individual are on the process of recovery from the infection. The infected population is subdivided into four compartments: the exposed, symptomatically infected, convalescent and asymptotically infected compartment. The exposed individuals are assumed to be infectious to susceptible humans via sexual contact due to viremia and virusemenia occurring before the end of the incubation period.

The symptomatically infected were assumed to be infectious to both humans and

mosquitos during the incubation phase lasting two days to a week. Individuals in the convalescent stage were also found to be infectious to susceptible humans via sexual contact, due to the persistence of the virus in the urine, and semen even after it disappears from blood. The lack of evidence of the transmission of the virus from asymptotically infected to susceptible humans and mosquitos led to the assumption that asymptotically infected are not infectious. Since the epidemiological dynamics duration is shorter than the demographical change of that of the human population, birth and mortality rates are ignored in their model as well.

In the paper, data from the outbreak of the Zika virus in Brazil, Colombia and El Salvador was used in the numerical simulations. The basic reproduction number was used to study the effects of certain parameters using the numeric data.

Another SEIR-SEI type of a deterministic model is described in [57] to study the dynamic transmission of Zika virus for two patches, namely Rio de Janeiro and Miami. The model was used to investigate if the visitors from Miami to the Carnival in February 2016 and the Olympics in August of 2016 in Rio de Janeiro would be able contract the virus and bring it back to Miami and course an outbreak. To study the impact of the visitors to both events, a group of 100 people is taken from the population of Miami for both event and added to the population of Rio de Janeiro and allowed to interact with the human and mosquito population and a subpatch was used to monitor these visitors. The basic reproduction number  $R_0$  was then calculated for the model and a plot showing a counter-cyclical condition in both hemispheres shows that  $R_0$  is greater in February and in August for patch 1 and patch 2, respectively.

A sensitive analysis was then performed on the change in the biting rate and the number of visitors to the events. The sensitive analysis was only performed for the parameters of patch 2 (Miami) and it was first discovered that if the parameters are kept the same for both patches, there will be an outbreak in Miami which will see an

approximate of three fourth of the population getting infected. However, if the number of people visiting is reduced by 10%, the size of the outbreak will reduce to 35% of the population getting infected and increased 10 times will results in more than 90% of the population of Miami infected. The model is also discovered to be more sensitive to the change in the rate of bites by mosquito than in the number of bites per human. In the qualitative features of the model, only the basic reproduction number of the model was calculated.

We have already discussed some of the models developed by several authors above to describe the dynamics of Zika virus disease. However, not much work has been done by these authors on the discretization of these models in their work. The importance of the discretization of continuous models lies on the fact that during an epidemic, data is recorded in a discrete time interval (daily, monthly or yearly) and therefore, discrete-time epidemic models gives a more practical scenario than the continuous one in [29]. Continuous models have been discretized in [19], [44], [55] and [28] using a method called as the nonstandard finite difference (NSFD) method known for its robustness. A comparison between the numerical method and other well-known numerical method such as the Euler method and Range Kutta method.

In [19] for example, an NSFD scheme is constructed to solve an SIR epidemic model with vaccination. For the discrete model, the positivity of the solution and the global stability at the equilibrium points was investigated. In the numerical simulation, a comparison between the behaviour of the NSFD scheme and the Range-Kutta of order 4 (RK4) at the equilibrium points was carried out for different step-sizes and it is observed that the NSFD methods converges and preserves the positivity of the solution even for a greater step-size while the RK4 fails to converge and gives negative solution for a large step-size.

Another NSFD methods is constructed in [28] to solve a smoking model in Spain.

In the paper, the qualitative features of the model such as the basic reproduction number and the equilibrium points is studied. After constructing the NSFD methods for the model, then the convergence of the numerical scheme to the equilibrium points is investigated by computing a table showing the spectral radii of the jacobian matrix of the system at the equilibrium points and compare the results with those obtained from the Euler scheme.

The results shows that the Euler scheme will diverges as the step-size increases to 7 and beyond, whereas the NSFD scheme will converge for a larger step-size. The numerical results also shows that the Euler and the standard fourth order Runge-Kutta generates heavy oscillations with negative values when the step-size is 7 and diverges for a step-size of 10. It is then concluded that the NSFD preserves numerical stability, its solution remain positive and is dynamic consistency for even a larger step-size.

In [44] an NSFD method is used to solve numerically a mathematical model for a Cholera epidemic dynamics. In the paper, a mathematical model already develop to study transmission dynamics of the Cholera virus in Zimbabwe during the period of 2008 to 2009 is modified. Then the basic reproduction number and the local and global stability of the disease free equilibrium point was investigated.

Numerical simulations of the numerical method was carried out first with different step-sizes and initial conditions, and then a comparisons between the NSFD methods, Euler method and Runge-Kutta method of order 4 was done by first comparing the spectral radii of the Jacobian matrix of the system at the disease free equilibrium for different step-sizes  $\ell$  and then by plotting the results for each method with different initial conditions. The numerical results shows that when the step-size  $\ell$  increases both Euler and RK4 methods diverge whereas the NSFD method converges. It is then concluded that the NSFD methods produces better results.

In [55] a work similar to the work in [44] is done. In the paper an NSFD method is constructed to solve a HIV transmission dynamics model. The qualitative features of the continuous model, such as basic reproduction number, disease free equilibrium point and the endemic equilibrium point were first investigated. In the construction of the NSFD methods two cases were presented, the first one the denominator function used is the normal step-size function (NSFD-I) and the second case a non-classical denominator function different from the step-size function (NSFD-II).

The fixed points of the NSFD scheme are obtained and a note that the equilibrium points of the continuous system and then performed a numerical stability analysis of the fixed points are the same. It is also further shown that the NSFD-II methods gives better results for a larger step-size by offering tables and plots comparing it with the NSFD-I method and other well-known methods such as the ODE45 and the Runge-Kutta method of order 4 which diverge when the step-size increases. It is then concluded that the NSFD methods gives better results which are consistent with the continuous system, converges to the right equilibrium points even with large step-size and preserves the positivity of the solution.

Different models have been developed to gain insight into the transmission dynamics of Zika virus disease, as some of them are already mentioned above. Qualitative analysis of some of these models was investigated and some numerical computations have been performed to gain deep understanding on the effect of certain parameter in the model. These models are of the form of systems of non-linear differential equations. The use of differential equations in epidemic modelling gives rise to the need to study the models using numerical method as we have already seen from some author's work above.

In the next section we present models already developed by some authors to describe the dynamic of Zika virus.

### 1.3 Some recent Zika virus disease models

In this section we present different Zika virus models.

#### 1.3.1 SI-SI model describing the dynamics of Zika virus disease

The Zika model described by Oluyo and Adeyemi in [58] subdivides the human population  $N_h(t)$  into susceptible  $S_h(t)$ , infected  $I_h(t)$  and isolated  $Q(t)$ , such that,  $N_h(t) = S_h(t) + I_h(t) + Q(t)$ , and the mosquito population  $N_m(t)$  is into two subclasses, namely; the susceptible  $S_m(t)$  and the infectious  $I_m$ , such that,  $N_m(t) = S_m(t) + I_m(t)$ . The model equations are as follows,

$$\left. \begin{aligned} \frac{dS_h}{dt} &= \beta_1(1 - \theta I_h) - \mu_1 S_h - (b\tau_1 I_m + \tau_2 I_h)S_h + \gamma(I_h + Q), \\ \frac{dI_h}{dt} &= (b\tau_1 I_m + \tau_2 I_h)S_h + \theta\beta_1 I_h - (\mu_1 + \sigma_1 + \gamma)I_h - \rho I_h, \\ \frac{dQ}{dt} &= \rho I_h - (\mu_1 + \sigma_1 + \gamma)Q, \\ \frac{dS_m}{dt} &= \beta_2 - (u_2 + \sigma_2)S_m - b\tau_3 I_h S_m, \\ \frac{dI_m}{dt} &= b\tau_3 I_h S_m - (\mu_2 + \sigma_2)I_m. \end{aligned} \right\} \quad (1.3.1)$$

with the initial conditions:  $S_h(t_0) = S_{h0}$ ,  $I_h(t_0) = I_{h0}$ ,  $Q(t_0) = Q_0$ ,  $S_m(t_0) = S_{m0}$  and  $I_m(t_0) = I_{m0}$ .

In the model, humans are recruited into the susceptible class  $S_h$  through birth or immigration at a rate of  $\beta_1$  and out through an natural death rate of  $\mu_1$ . To join the infected class  $I_h$ , susceptible human receive a bite from an infected mosquito at a biting rate of  $b$  with the probability that a bite results in transmission of disease to human  $\tau_1$  or by becoming infected through sexual contact with the infected individuals at a rate of  $\tau_2$ . The infected individuals that are diagnosed are then place in isolation at a rate of  $\rho$  to prevent further contact with the rest of the human and mosquito population and given treatment to treat the symptoms displayed since no Zika disease treatment is available.

The Isolated individuals are assumed to be no longer infecting any susceptible humans or mosquitos due to the isolation. Isolated individuals  $Q$  and infected individuals  $I_h$  are still susceptible to the virus at the rate  $\gamma$ . Both Infected individuals and isolated individuals moves out of the infected class  $I_h$  and isolated class  $Q$ , respectively through a natural and disease induced death rate of  $\mu_1$  and  $\sigma_1$ , respectively. Mosquitoes are recruited into the susceptible class  $S_m$  at a birth rate of  $\beta_2$  and out of both the susceptible  $S_m$  and infected class  $I_m$  at a natural and diseases induced rate of  $\mu_2$  and  $\sigma_2$ , respectively. Susceptible mosquitoes leave the susceptible class  $S_m$  to join the infected class  $I_m$  by biting infected humans at a rate of  $b$  with the probability that a bite results in transmission of the virus to a susceptible mosquito  $\tau_3$ .

### 1.3.2 SIR-SI model describing the dynamics of Zika virus disease with the impact of infective immigrants

The model presented by Ayana and Koya in [6] focuses on the impact of symptomatic and asymptomatic infective immigrants during the spread of Zika virus. In their model, the human population is divides in to the susceptible individuals  $S_h$ , the symptomatic and asymptomatic infected individuals  $I_1$  and  $I_2$ , respectively, and the recovered individuals  $R_h$ , and the mosquito population is divided into two host compartment, the susceptible and infected mosquitoes. The model equations are as follows;

$$\left. \begin{aligned} \frac{dS_h}{dt} &= \Lambda_h N_h - b\phi I_v(S_h/N_h) - \mu_h S_h, \\ \frac{dI_1}{dt} &= b\epsilon \phi I_v(S_h/N_h) + p_1 I_1 - (\mu_h + \sigma) I_1, \\ \frac{dI_2}{dt} &= b(1-\epsilon)\phi I_v(S_h/N_h) + p_2 I_2 - (\mu_h + \sigma) I_2, \\ \frac{dR_h}{dt} &= \sigma(I_1 + I_2) - \mu_h R_h, \\ \frac{dS_v}{dt} &= \Lambda_v N_v - b\theta I_1(S_v/N_h) - b\gamma I_2(S_v/N_h) - \mu_v S_v, \\ \frac{dI_v}{dt} &= b\theta I_1(S_v/N_h) + b\gamma I_2(S_v/N_h) - \mu_v I_v, \end{aligned} \right\} \quad (1.3.2)$$

where  $N_h = S_h + I_1 + I_2 + R_h$ ,  $N_v = S_v + I_v$  and the initial conditions  $S_h(0) = S_{h0}$ ,  $I_1(0) = I_{10}$ ,  $I_2(0) = I_{20}$ ,  $R_h(0) = R_{h0}$ ,  $S_v(0) = S_{v0}$  and  $I_v(0) = I_{v0}$ . From the model, humans are recruited to the susceptible at a rate  $\Lambda_h$  and leave the susceptible compartment  $S_h$  through a natural death  $\mu_h$  or by being infected by the virus through a bite by an infected mosquito at a biting rate of  $b$  with the bite resulting to an infection at a rate of  $\phi$  to join either the symptomatic infected or the asymptomatic infected at a rate of  $\epsilon$  or  $(1 - \epsilon)$ , respectively. Furthermore, individuals joins the symptomatic and asymptomatic infected compartment  $I_1$  and  $I_2$ , respectively, by immigrating in to the population while infected with the virus at a rate of  $P_1$  and  $P_2$ , respectively, and exit the infected (symptomatic and asymptomatic) compartment through a natural death or by recovering from the infection at a rate  $\sigma$  to joint the recovered individuals compartment  $R_h$ . Recovered individuals leaves the recovered compartment  $R_h$  only through natural death.

For the vector population, mosquitoes are recruited to the susceptible compartment  $S_v$  at a rate  $\Lambda_v$  and exit through a natural death rate  $\mu_v$  or by being infected from biting either a symptomatic or asymptomatic infected individual at a biting rate  $b$  with the bite resulting in the mosquito being infected at a rate of  $\theta$  for symptomatic and  $\gamma$  for asymptomatic to join the infected compartment  $I_v$ . Mosquito leaves the infected compartment  $I_v$  through a natural death rate.

### 1.3.3 SEIR-SEI model describing the dynamics of Zika virus disease

The model under investigation is the model presented by Oleson et al. in [57] to describe the transmission of Zika virus between mosquitos to humans which constitute of 7 host compartments. The model describes the transmission of Zika virus in Rio de Janeiro and in Miami: patch 1 and 2, where patch 1 represents the population dynamics for Rio de Janeiro and patch 2 represent the population dynamics for Miami.



The human population ( $N_H^i$ ) has four different compartmental classes, the susceptible ( $S_H^i$ ), exposed ( $E_H^i$ ), infectious ( $I_H^i$ ) and recovered group ( $R_H^i$ ) and the vector population has three different compartmental classes, the susceptible ( $S_v^i$ ), exposed ( $E_v^i$ ) and the infectious ( $I_v^i$ ).

In the model, humans enter the susceptible class through birth at the birth rate of  $\nu_H^i$  and exit the class either by natural death at a rate of  $\mu_H^i$  or by joining the exposed human class  $E_H^i$  through acquiring the Zika virus via a mosquito bite at a rate of  $b_H^i$  where the density-dependent average number of bites on a human by mosquitoes per unit time is given as  $b_H^i(N_V^i/N_H^i)$  and probability that a mosquito is infectious  $\frac{I_v^i}{N_v^i}$  and its bite will successfully transmit the virus to a susceptible human at a probability rate of  $\beta_H^i$ . Exposed humans leave the exposed class  $E_H^i$  either by natural death or by becoming infected to join the Infected humans class  $I_H^i$  at a rate of  $\alpha_H$  and leaves the infected humans class b or recovery at the recovery rate of  $\gamma_H^i$  to join the recovered class  $R_H^i$ . Recovered human are then immune to the virus and can only exit the recovered class through death from natural causes. Similarly, mosquitoes enter the susceptible

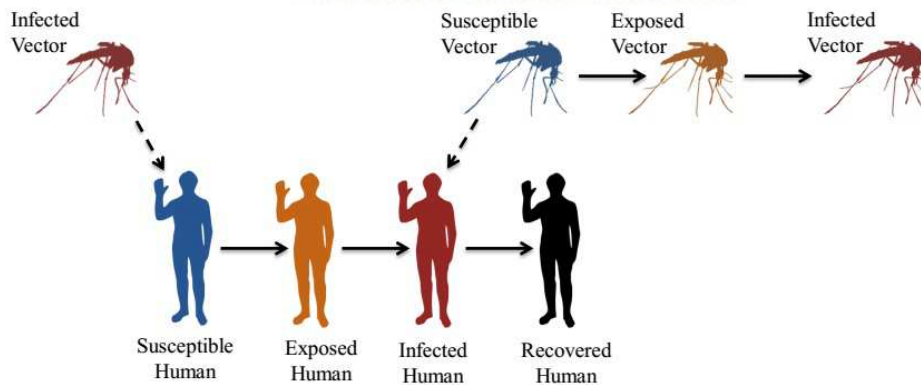


Figure 1.3.1 Transmission of Zika virus from an infected vector (mosquito) to a susceptible human and back to a susceptible vector. Dotted arrows indicate bites while solid arrows indicate a transfer between different compartments [57].

class  $S_H^i$  through birth at the birth rate of  $\nu_v^i$  and exit the susceptible class by natural

death at a death rate of  $\mu_v^i$  or by becoming infected through biting an infected human at a biting rate of  $b_v^i$  with  $b_v^i(N_v^i/N_H^i)$  being the density-dependent average number of bites per mosquito on humans per unit time and a probability  $\frac{I_H^i}{N_H^i}$  that a human is infectious and that the mosquito will successfully contract the virus with probability rate of  $\beta_v^i$  to join the exposed class  $E_v^i$ . Exposed mosquitos leave the exposed mosquitos class either by natural death or by becoming infected to join the Infected mosquitos class  $I_v^i$  at a rate of  $\alpha_v$  and leave the infected mosquitos class through a natural death.

The model equations are as follows:

$$\left. \begin{aligned} \frac{dS_H^i}{dt} &= \nu_H^i N_H^i - b_H^i (N_v^i / N_H^i) \frac{\beta_H^i}{N_v^i} I_v^i S_H^i - \mu_H^i S_H^i, \\ \frac{dE_H^i}{dt} &= b_H^i (N_v^i / N_H^i) \frac{\beta_H^i}{N_v^i} I_v^i S_H^i - \alpha_H^i E_H^i - \mu_H^i E_H^i, \\ \frac{dI_H^i}{dt} &= \alpha_H^i E_H^i - \gamma_H^i I_H^i - \mu_H^i I_H^i, \\ \frac{dR_H^i}{dt} &= \gamma_H^i I_H^i + \mu_H^i R_H^i, \\ \frac{dS_v^i}{dt} &= \nu_v^i N_v^i - b_v^i (N_v^i / N_H^i) \frac{\beta_v^i}{N_H^i} I_H^i S_v^i - \nu_v^i S_v^i, \\ \frac{dE_v^i}{dt} &= b_v^i (N_v^i / N_H^i) \frac{\beta_v^i}{N_H^i} I_H^i S_v^i - \alpha_v^i E_v^i - \mu_v^i E_v^i, \\ \frac{dI_v^i}{dt} &= \alpha_v^i E_v^i - \mu_v^i I_v^i, \end{aligned} \right\} \quad (1.3.3)$$

where  $N_H^i = S_H^i + E_H^i + I_H^i + R_H^i$  and  $N_v^i = S_v^i + E_v^i + I_v^i$ .

Two notes must be made from Oleson [57]: The first one is that, in order to reflect the quality between the total number of bites by mosquitoes on humans and the total number of bites on humans by mosquitoes, the bite rates  $b_H^i(N_v^i/N_H^i)$  and  $b_v^i(N_v^i/N_H^i)$  must satisfy the constancy constraint:

$$b_H^i N_H^i = b_v^i N_v^i, \quad (1.3.4)$$

see [57] for more details. The second note is that, since the mosquito population does not remain constant throughout the year, a time-dependent cyclical death rates was

created by Oleson for both patches that shows a maximum death rate of the mosquitoes in winter for each region. For  $\mu_{v,max}^i$  and  $\mu_{v,min}^i$  for  $i = 1, 2$ , the time-dependent cyclical death rates is given as

$$\mu_v^1(t) = \frac{1}{2} \left[ (\mu_{v,min}^1 - \mu_{v,max}^1) \sin\left(\frac{2\pi t}{365}\right) + \mu_{v,max}^1 + \mu_{v,min}^1 \right], \quad (1.3.5)$$

for patch 1 and as

$$\mu_v^2(t) = \frac{1}{2} \left[ (\mu_{v,min}^2 - \mu_{v,max}^2) \sin\left(\frac{2\pi(t-183)}{365}\right) + \mu_{v,max}^2 + \mu_{v,min}^2 \right], \quad (1.3.6)$$

for patch 2, with an average birth rate  $\nu_v^i$  taken to be the midpoint between the maximum and minimum death rates  $\mu_{v,max}^i$  and  $\mu_{v,min}^i$ , respectively, to make sure the mosquito population remain stable in a long run. See [57] for details.

The following table present the parameter description and the estimated values with the initial population estimation for both patches taken from [57].

#### 1.3.4 SEIR-SEI model describing the dynamics of Zika virus disease with the influence of sexual transmission and preventive measures

The model described by Padmanabhan et al. [62] divides the human population  $N_h$  into five subclasses, namely: The susceptible ( $S_h$ ), exposed ( $E_h$ ), asymptotically infected ( $I_{h,s}$ ), symptomatically infected ( $I_{h,a}$ ) and recovered ( $R_h$ ), and the mosquito population  $N_m$  into susceptible ( $S_m$ ), exposed ( $E_m$ ) and infected ( $I_m$ ).

Table 1.3.1 Description of the model parameters and their values for SEIR-SEI model taken from [57]

Parameter	Description	Values
Human population		
$\nu_H$	Human birth rate	1/19,210
$\mu_H$	Human death rate	1/45,625
$1/\alpha_H$	Human incubation period	5.9
$1/\gamma_H$	Human infectious period	5.9
$\beta_H$	Vector (Mosquito) to Human transmission probability	0.42
$b_H^{max}$	Max bites per human	19
Vector(Mosquito) population		
$\nu_v$	Vector (Mosquito) birth rate	1/7.8
$\mu_v^{min}$	Vector (Mosquito) minimum death rate	1/9.3
$\mu_v^{max}$	Vector (Mosquito) maximum death rate	1/6.5
$1/\alpha_v$	Vector (Mosquito) incubation period	10.5
$\beta_v$	Human to Vector (Mosquito) transmission probability	0.42
$b_v^{max}$	Max bites by Vector (Mosquito)	0.5
Initial values		
Patch 1: Rio de Janeiro ( $i = 1$ )		
$S_H^1$	Susceptible human	12,902,000
$E_H^1$	Exposed human	129,020
$I_H^1$	Infected human	0
$R_H^1$	Recovered human	0
$S_v^1$	Susceptible mosquitos	9,000,000
$E_v^1$	Exposed mosquitos	0
$I_v^1$	Infectious mosquitos	0
Patch 2: Miami ( $i = 2$ )		
$S_H^2$	Susceptible human	5,817,000
$E_H^2$	Exposed human	0
$I_H^2$	Infected human	0
$R_H^2$	Recovered human	0
$S_v^2$	Susceptible mosquitos	60,000,000
$E_v^2$	Exposed mosquitos	0
$I_v^2$	Infectious mosquitos	0

The model equation are as follows:

$$\left. \begin{aligned}
 \dot{S}_h &= -b_{mh}(1 - ITN)S_h I_m - b_h(I_{h,a} + I_{h,s})S_h, \\
 \dot{E}_h &= b_{mh}(1 - ITN)S_h I_m + b_h(I_{h,a} + I_{h,s})S_h - \nu_h E_h, \\
 \dot{I}_{h,s} &= (1 - q)\nu_h E_h - \gamma_{h,s} I_{h,s}, \\
 \dot{I}_{h,a} &= q\nu_h E_h - \gamma_{h,a} I_{h,a}, \\
 \dot{R}_h &= \gamma_{h,s} I_{h,s} + \gamma_{h,a} I_{h,a}, \\
 \dot{S}_m &= \mu_m N_m - \mu_m S_m - b_{hm}(1 - ITN)S_m(I_{h,s} + I_{h,a}) \\
 &\quad - (h \cdot ITN + j \cdot IRS)S_m, \\
 \dot{E}_m &= -\nu_m E_m - \mu_m E_m + b_{hm}(1 - ITN)S_m(I_{h,s} + I_{h,a}) \\
 &\quad - (h \cdot ITN + j \cdot IRS)E_m, \\
 \dot{I}_m &= \nu_m E_m - \mu_m I_m - (h \cdot ITN + j \cdot IRS)I_m,
 \end{aligned} \right\} \quad (1.3.7)$$

with  $N_h = S_h + E_h + I_{h,a} + I_{h,s} + R_h$  and  $N_m = S_m + E_m + I_m$ .

In the model, the individuals leave the susceptible class by becoming exposed to the infection through sexual contact with asymptomatic  $I_{h,a}$  or symptomatic  $I_{h,s}$  infected individuals at a rate of  $b_h$  or by being bitten by Infectious mosquitos  $I_m$  at a rate of  $b_{mh}$ . However, the contact rate between susceptible and infectious mosquitos is reduced by the use of Insecticide-Treated Mosquito Nets ( $ITN$ ). Exposed individuals become asymptomatic  $I_{h,a}$  infected or symptomatic  $I_{h,s}$  infected at a rate of  $(1 - q)$  and  $q$ , respectively, and they recover at a rate of  $\gamma_{h,a}$  and  $\gamma_{h,s}$ , respectively. For the mosquito population, the mosquitoes leaves the susceptible  $S_m$ , exposed  $E_m$  and infected class  $I_m$  at a death rate of  $\mu_m$ , by the use of Insecticide-Treated Mosquito Nets ( $ITN$ ), by the use of Indoor Residual Spraying ( $IRS$ ) at a rate of  $h$  and  $j$ , respectively, or by biting the infectious humans at a rate of  $b_{m,h}$  to join the exposed class  $E_m$ . The exposed mosquitoes become infected at a rate of  $\nu_v$ .

In the next section we give the outline of the thesis.

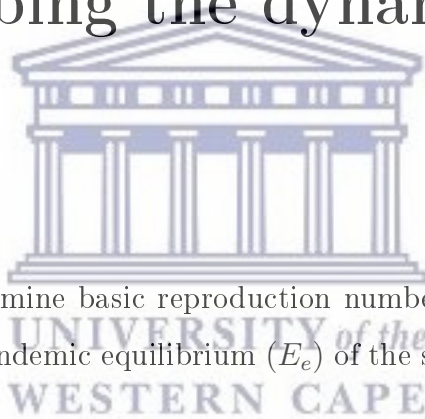
## 1.4 Outline of the thesis

The outline of the research is as follows. In Chapter 2, we present the qualitative analysis of the Zika model (1.3.3) presented by Oleson in [57], the basic reproduction number and the equilibrium points and both the local and global analysis of the equilibrium points and a summary of the results. In Chapter 3, we construct and analyse a robust nonstandard finite difference numerical method to simulate the model, we start by the general philosophy of the method, then the derivation and analysis of proposed numerical method. In Chapter 4, we give comparative numerical results and discussions on them. Finally, some scope for further research is presented in Chapter 5.



## Chapter 2

# Qualitative analysis of the SEIR-SEI model describing the dynamics of Zika virus disease



In this chapter we will determine basic reproduction number  $R_0$  and the disease free equilibrium point ( $E_0$ ) and endemic equilibrium ( $E_e$ ) of the system and their local and Global stability analysis.

In the next section, we deal with the positivity of the solution.

### 2.1 Positivity of the solution

It is biological reasonable that in any epidemic model, when starting with nonnegative initial conditions, say  $S_H^i(0), E_H^i(0), I_H^i(0), R_H^i(0), S_v^i(0), E_v^i(0), I_v^i(0)$  for our model (1.3.3), the solutions  $S_H^i(t), E_H^i(t), I_H^i(t), R_H^i(t), S_v^i(t), E_v^i(t), I_v^i(t)$  remains to be nonnegative for all  $t \in [0; \infty)$ . The following lemma states the condition in which the solution  $S_H^i(t), E_H^i(t), I_H^i(t), R_H^i(t), S_v^i(t), E_v^i(t), I_v^i(t)$  will remain nonnegative when starting with nonnegative initial conditions.

**Lemma 2.1.1** *The solution  $(S_H^i(t), E_H^i(t), I_H^i(t), R_H^i(t), S_v^i(t), E_v^i(t), I_v^i(t))$  of the model (1.3.3) will remain nonnegative when starting with the initial conditions  $(S_H^i(0), E_H^i(0), I_H^i(0), R_H^i(0), S_v^i(0), E_v^i(0), I_v^i(0))$  for all  $t > 0$ .*

**Proof.** Let  $X^i = (S_H^i(t), E_H^i(t), I_H^i(t), R_H^i(t), S_v^i(t), E_v^i(t), I_v^i(t))^T$  and  $f(X^i) = (f_1(X^i), f_2(X^i), f_3(X^i), f_4(X^i), f_5(X^i), f_6(X^i), f_7(X^i))$ . Model (1.3.3) can then be expressed in the following way;

$$\dot{X}^i = f(X^i),$$

where

$$f(X) = \begin{pmatrix} f_1(X^i) \\ f_2(X^i) \\ f_3(X^i) \\ f_4(X^i) \\ f_5(X^i) \\ f_6(X^i) \\ f_7(X^i) \end{pmatrix} = \begin{pmatrix} \nu_H^i N_H^i - b_H^i (N_v^i / N_H^i) \frac{\beta_H^i}{N_v^i} I_v^i S_H^i - \mu_H^i S_H^i \\ b_H^i (N_v^i / N_H^i) \frac{\beta_H^i}{N_v^i} I_v^i S_H^i - \alpha_H^i E_H^i - \mu_H^i E_H^i \\ \alpha_H^i E_H^i - \mu_H^i I_H^i \\ \gamma_H^i I_H^i + \mu_H^i R_H^i \\ \nu_v^i N_v^i - b_v^i (N_v^i / N_H^i) \frac{\beta_v^i}{N_H^i} I_H^i S_v^i - \nu_v^i S_v^i \\ b_v^i (N_v^i / N_H^i) \frac{\beta_v^i}{N_H^i} I_H^i S_v^i - \alpha_v^i E_v^i - \mu_v^i E_v^i \\ \alpha_v^i E_v^i - \mu_v^i I_v^i \end{pmatrix}.$$

We note the following

$$\left. \begin{aligned} \frac{dS_H^i(t)}{dt} \Big|_{S_H^i=0} &= \nu_H^i N_H^i > 0, \\ \frac{dE_H^i(t)}{dt} \Big|_{E_H^i=0} &= k_1^i I_v^i S_H^i > 0, \\ \frac{dI_H^i(t)}{dt} \Big|_{I_H^i=0} &= \alpha_H^i E_H^i > 0, \\ \frac{dR_H^i(t)}{dt} \Big|_{R_H^i=0} &= \gamma_H^i I_H^i > 0, \\ \frac{dS_v^i(t)}{dt} \Big|_{S_v^i=0} &= \nu_v^i N_v^i > 0, \\ \frac{dE_v^i(t)}{dt} \Big|_{E_v^i=0} &= k_2^i I_H^i S_v^i > 0, \\ \frac{dI_v^i(t)}{dt} \Big|_{I_v^i=0} &= \alpha_v^i E_v^i > 0. \end{aligned} \right\} \quad (2.1.1)$$



It then follows by Lemma 2.1 of [43] that the set

$$\mathcal{D}^i = \left\{ (S_H^i, E_H^i, I_H^i, R_H^i, S_v^i, E_v^i, I_v^i) \in \mathfrak{R}_+^7 : N_H^i \leq \frac{\nu_H^i N_H^i}{\mu_H^i}, N_v^i \leq \frac{\nu_v^i N_v^i}{\mu_v^i} \right\}, \quad (2.1.2)$$

is invariant set.

**Lemma 2.1.2** *The solution set  $\{S_H^i(t), E_H^i(t), I_H^i(t), R_H^i(t), S_v^i(t), E_v^i(t), I_v^i(t)\}$  for  $t > 0$  is contained and bounded in the closed set (2.1.2).*

**Proof.** Differentiating

$$N_H^i(t) = S_H^i(t) + E_H^i(t) + I_H^i(t) + R_H^i(t)$$

and

$$N_v^i(t) = S_v^i(t) + E_v^i(t) + I_v^i(t),$$

we obtain the following

$$\frac{dN_H^i}{dt} = \frac{dS_H^i}{dt} + \frac{dE_H^i}{dt} + \frac{dI_H^i}{dt} + \frac{dR_H^i}{dt}$$

and

$$\frac{dN_v^i}{dt} = \frac{dS_v^i}{dt} + \frac{dE_v^i}{dt} + \frac{dI_v^i}{dt},$$

respectively. Hence, from (1.3.3), we obtain

$$\frac{dN_H^i}{dt} = \nu_H^i N_H^i - \mu_H^i N_H^i(t) \quad (2.1.3)$$

and

$$\frac{dN_v^i}{dt} = \nu_v^i N_v^i - \mu_v^i N_v^i(t). \quad (2.1.4)$$

The differential equation (2.1.3) can be solved as follows;

$$\int \frac{1}{\nu_H^i N_H^i - \mu_H^i N_H^i(t)} dN_H^i(t) = \int dt,$$

$$-\frac{\ln|\nu_H^i N_H^i - \mu_H^i N_H^i(t)|}{\mu_H^i} = t + c,$$

$$N_H^i(t) = \frac{\nu_H^i N_H^i}{\mu_H^i} - \frac{A}{\mu_H^i} e^{-\mu_H^i t},$$

where

$$A = \nu_H^i N_H^i - \mu_H^i N_H^i(0).$$

We have the solution

$$N_H^i(t) = \frac{\nu_H^i N_H^i}{\mu_H^i} (1 - e^{-\mu_H^i t}) - N_H^i(0) e^{-\mu_H^i t}.$$

Similarly, the differential equation (2.1.4) has the solution

$$N_v^i(t) = \frac{\nu_v^i N_v^i}{\mu_v^i} (1 - e^{-\mu_v^i t}) - N_v^i(0) e^{-\mu_v^i t}.$$

Since

$$\frac{dN_H^i}{dt} \leq \nu_H^i N_H^i - \mu_H^i N_H^i(t)$$

and

$$\frac{dN_v^i}{dt} \leq \nu_v^i N_v^i - \mu_v^i N_v^i(t),$$

it follows that as  $t \rightarrow 0$ ,  $N_H^i(t) \leq \frac{\nu_H^i N_H^i}{\mu_H^i}$  and  $N_v^i(t) \leq \frac{\nu_v^i N_v^i}{\mu_v^i}$ . From the two results above, lemma (2.1.1) and (2.1.2), we have the following result.

**Theorem 2.1.3** *The feasible region (2.1.2) is positive invariant with respect to the system (1.3.3) with non-negative initial conditions.*

The next section we determine the equilibrium point of the dynamic system.

## 2.2 Equilibrium points

A dynamic system usually has two equilibrium points, namely: the disease free equilibrium point and the endemic equilibrium point. These equilibrium points can be

obtained by setting the model equation of the system to zero. Hence, to calculate the equilibrium points of our dynamic system, we set the right-hand sides of the model equations of model (1.3.3) to zero [3]. We obtain

$$\left. \begin{aligned} \nu_H^i N_H^i - k_1^i I_v^i S_H^i - \mu_H^i S_H^i &= 0, \\ k_1^i I_v^i S_H^i - (\alpha_H^i + \mu_H^i) E_H^i &= 0, \\ \alpha_H^i E_H^i - (\gamma_H^i + \mu_H^i) I_H^i &= 0, \\ \gamma_H^i I_H^i - \mu_H^i R_H^i &= 0, \\ \nu_v^i N_v^i - k_2^i I_H^i S_v^i - \mu_v^i S_v^i &= 0, \\ k_2^i I_H^i S_v^i - (\alpha_v^i + \mu_v^i) E_v^i &= 0, \\ \alpha_v^i E_v^i - \mu_v^i I_v^i &= 0, \end{aligned} \right\} \quad (2.2.1)$$

where

$$k_1^i = b_H^i (N_v^i / N_H^i) \frac{\beta_H^i}{N_v^i}$$

and

$$k_2^i = b_v^i (N_v^i / N_H^i) \frac{\beta_v^i}{N_H^i}.$$

The dynamic system has two equilibrium points, the disease free equilibrium point  $E_{0,i}$  and the endemic equilibrium point  $E_{e,i}$ .

### 2.2.1 Disease Free Equilibrium

The Disease Free equilibrium point (DFE)  $E_{0,i}$ , is defined to be the equilibrium state solution where there is total zero infection in the human population. To obtain the DFE of the system (1.3.3), we set  $I_H^i = 0$ , then equation 3,4,6 and 7 of (2.2.1) gives  $E_H^i = 0$ ,  $R_H^i = 0$ ,  $E_v^i = 0$  and  $I_v^i = 0$ , respectively. Equation 1 and 5 gives  $S_H^i = \frac{\nu_H^i}{\mu_H^i} N_H^i$  and  $S_v^i = \frac{\nu_v^i}{\mu_v^i} N_v^i$ . However, since  $N_H^i = S_H^i + E_H^i + I_H^i + R_H^i$  and  $N_v^i = S_v^i + E_v^i + I_v^i$ , at the DFE point,  $N_H^i = S_H^i$  and  $N_v^i = S_v^i$ . This implies that at the DFE  $\frac{\nu_H^i}{\mu_H^i} = 1$  and

$\frac{\nu_v^i}{\mu_v^i} = 1$ . Therefore, the DFE point is given as

$$E_{0,i} = (S_H^i, E_H^i, I_H^i, R_H^i, S_v^i, E_v^i, I_v^i) = (N_H^i, 0, 0, 0, N_v^i, 0, 0).$$

## 2.2.2 Endemic Equilibrium

The Endemic Equilibrium point (EE) of a system is a positive steady state solution where the disease persists in the population. It can be obtained by solving the equations of (2.2.1) simultaneously. Due to the complexity of the calculation of the endemic equilibrium point of our system (1.3.3), with the aid of MATLAB, we obtain the endemic equilibrium point to be

$$E_{e,i} = (S_H^{*,i}, E_H^{*,i}, I_H^{*,i}, R_H^{*,i}, S_v^{*,i}, E_v^{*,i}, I_v^{*,i}),$$

where

$$\left. \begin{aligned} S_H^{*,i} &= \frac{(N_H^i)^2 \mu_v^i (\alpha_v^i + \mu_v^i) T_H^i}{N_v^i \alpha_H^i b_v^i \beta_v^i Q_H^i}, \\ E_H^{*,i} &= \frac{-N_H^i \nu_v^i (M_H^i - P_H^i)}{N_v^i \alpha_H^i b_v^i \beta_v^i (\alpha_H^i + \mu_H^i) Q_H^i}, \\ I_H^{*,i} &= \frac{-N_H^i \nu_v^i (M_H^i - P_H^i)}{N_v^i b_v^i \beta_v^i (\alpha_H^i + \mu_H^i) Q_H^i}, \\ R_H^{*,i} &= \frac{-N_H^i \gamma_H^i \nu_v^i (M_H^i - P_H^i)}{N_v^i b_v^i \beta_v^i \mu_H^i (\alpha_H^i + \mu_H^i) (\gamma_H^i + \mu_H^i) Q_H^i}, \\ S_v^{*,i} &= \frac{N_H^i (\alpha_H^i + \mu_H^i) (\gamma_H^i + \mu_H^i) T_v^i}{\alpha_v^i b_H^i \beta_H^i Q_v^i}, \\ E_v^{*,i} &= \frac{-\nu_v^i (M_H^i - P_H^i)}{\alpha_v^i b_H^i \beta_H^i (\alpha_v^i + \mu_v^i) Q_v^i}, \\ I_v^{*,i} &= \frac{-\nu_v^i (M_H^i - P_H^i)}{b_H^i \beta_H^i \mu_v^i (\alpha_v^i + \mu_v^i) Q_v^i}, \end{aligned} \right\} \quad (2.2.2)$$

with

$$\left. \begin{aligned}
 T_H^i &= N_H^i \alpha_H^i \gamma_H^i \nu_v^i + N_H^i \alpha_H^i \mu_H^i \nu_v^i + N_H^i \gamma_H^i \mu_H^i \nu_v^i + N_H^i (\mu_H^i)^2 \nu_v^i + N_v^i \alpha_H^i b_v^i \beta_v^i \nu_H^i, \\
 Q_H^i &= N_H^i \alpha_v^i \mu_H^i \mu_v^i + N_H^i \mu_H^i (\mu_v^i)^2 + N_v^i \alpha_v^i b_H^i \beta_H^i \nu_v^i, \\
 M_H^i &= (N_H^i)^2 \alpha_H^i \alpha_v^i \gamma_H^i \mu_H^i \mu_v^i + (N_H^i)^2 \alpha_H^i \alpha_v^i (\mu_H^i)^2 \mu_v^i + (N_H^i)^2 \alpha_H^i \gamma_H^i \mu_H^i (\mu_v^i)^2 \\
 &\quad + (N_H^i)^2 \alpha_H^i (\mu_H^i)^2 (\mu_v^i)^2 + (N_H^i)^2 \alpha_v^i \gamma_H^i (\mu_H^i)^2 \mu_v^i + (N_H^i)^2 \alpha_v^i (\mu_H^i)^2 \mu_v^i \\
 &\quad + (N_H^i)^2 \gamma_H^i (\mu_H^i)^2 (\mu_v^i)^2 + (N_H^i)^2 (\mu_H^i)^3 (\mu_v^i)^2, \\
 F_H^i &= (N_v^i)^2 \alpha_H^i \alpha_v^i b_H^i b_v^i \beta_H^i \beta_v^i \nu_H^i, \\
 Q_v^i &= N_H^i \alpha_H^i \gamma_H^i \nu_v^i + N_H^i \alpha_H^i \mu_H^i \nu_v^i + N_H^i \gamma_H^i \mu_H^i \nu_v^i + N_H^i (\mu_H^i)^2 \nu_v^i + N_v^i \alpha_H^i b_v^i \beta_v^i \nu_H^i, \\
 T_v^i &= N_H^i \alpha_v^i \mu_H^i \mu_v^i + N_H^i \mu_H^i (\mu_v^i)^2 + N_v^i \alpha_v^i b_H^i \beta_H^i \nu_v^i.
 \end{aligned} \right\}$$

In the next section, we derive the basic reproduction number for the dynamic system using the next generation method.

## 2.3 Calculation of the basic reproduction number $R_0$

The basic reproduction number is defined to be the average of secondary infections generated by a single infectious individual during their entire infectious life in a completely susceptible population [73]. If  $R_0 < 1$ , then each infected individual will infect less than one new individuals during their entire infectious life and the disease will die out, and on the other hand,  $R_0 > 1$ , then each infected individual will infect more than one individual during their infectious life and the epidemic invades the population. In other words,  $R_0$  measures the potential of the possible outbreak.

To calculate the basic reproduction number for our system (1.3.3), we employ a well known method called the Next Generation matrix Method presented in [73]. We first find the reduced model of the dynamic system (1.3.3) by considering only the infected host compartments, namely: the exposed and infected host compartments for both

human and mosquitos population. The reduced model is as follows;

$$\left. \begin{aligned} \frac{dE_H^i}{dt} &= b_H^i \left( \frac{N_v^i}{N_H^i} \right) \frac{I_v^i}{N_v^i} \beta_H^i S_H^i - \alpha_H^i E_H^i - \mu_H^i E_H^i, \\ \frac{dI_H^i}{dt} &= \alpha_H^i E_H^i - \gamma_H^i I_H^i - \mu_H^i I_H^i, \\ \frac{dE_v^i}{dt} &= b_v^i \left( \frac{N_v^i}{N_H^i} \right) \frac{I_H^i}{N_H^i} \beta_v^i S_v^i - \alpha_v^i E_v^i - \mu_v^i E_v^i, \\ \frac{dI_v^i}{dt} &= \alpha_v^i E_v^i - \mu_v^i I_v^i. \end{aligned} \right\} \quad (2.3.1)$$

The reduced model (2.3.1) can be written in matrix form as

$$\frac{dx_k(t)}{dt} = \mathcal{F}x_k(t) - \mathcal{V}x_k(t), \quad (2.3.2)$$

where  $k = 1, 2, \dots, m$  with  $m$  representing the number of infected host compartments and  $x = (x_1, x_2, x_3, \dots, x_m)^T$ . The matrix  $F$  is called the infection matrix and its  $(k, j)$  entry represents the number of new infection at stage  $j$  caused by contact with infected individuals in stage  $i$ , and the matrix  $V$  is called the transition matrix and its  $(k, j)$  entry represents the rate individuals in stage  $k$  move to stage  $i$  [73]. For our reduced model (2.3.1), we set:

$$\mathcal{F}^i = \begin{bmatrix} b_H^i \left( \frac{N_v^i}{N_H^i} \right) \frac{I_v^i}{N_v^i} \beta_H^i S_H^i \\ 0 \\ b_v^i \left( \frac{N_v^i}{N_H^i} \right) \frac{I_H^i}{N_H^i} \beta_v^i S_v^i \\ 0 \end{bmatrix} \quad \text{and} \quad \mathcal{V}^i = \begin{bmatrix} \alpha_H^i E_H^i + \mu_H^i E_H^i \\ -\alpha_H^i E_H^i + \gamma_H^i I_H^i \\ \alpha_v^i E_v^i + \mu_v^i E_v^i \\ -\alpha_v^i E_v^i + \mu_v^i I_v^i \end{bmatrix}. \quad (2.3.3)$$

The partial derivatives of  $\mathcal{F}$  and  $\mathcal{V}$ , with respect to  $E_H^i, I_H^i, E_v^i$  and  $I_v^i$  are partitioned as follow;

$$\begin{aligned}
 F^i &= \left[ \frac{\partial \mathcal{F}_k^i}{\partial x_j} \right] \\
 &= \begin{bmatrix} 0 & 0 & 0 & b_H^i \left( \frac{N_v^i}{N_H^i} \right) \frac{S_H^i}{N_v^i} \beta_H^i \\ 0 & 0 & 0 & 0 \\ 0 & b_v^i \left( \frac{N_v^i}{N_H^i} \right) \frac{S_v^i}{N_H^i} \beta_v^i & 0 & 0 \\ 0 & 0 & 0 & 0 \end{bmatrix} \quad (2.3.4)
 \end{aligned}$$

and

$$\begin{aligned}
 V^i &= \left[ \frac{\partial \mathcal{V}_k^i}{\partial x_j} \right] \\
 &= \begin{bmatrix} \alpha_H^i + \mu_H^i & 0 & 0 & 0 \\ -\alpha_H^i & \gamma_H^i + \mu_H^i & 0 & 0 \\ 0 & 0 & \alpha_v^i + \mu_v^i & 0 \\ 0 & 0 & -\alpha_v^i & \mu_v^i \end{bmatrix}, \quad (2.3.5)
 \end{aligned}$$

for  $1 \leq k, j \leq m$ . Evaluating  $F^i$  and  $V^i$  at the disease free equilibrium point  $E_{0,i} = (N_H^i, 0, 0, 0, N_v^i, 0, 0)$ , we obtain

$$\begin{aligned}
 F^i &= \left[ \frac{\partial \mathcal{F}_k^i}{\partial x_j} \right] \\
 &= \begin{bmatrix} 0 & 0 & 0 & b_H^i \beta_H^i \\ 0 & 0 & 0 & 0 \\ 0 & b_v^i \beta_v^i \left( \frac{(N_v^i)^2}{(N_H^i)^2} \right) & 0 & 0 \\ 0 & 0 & 0 & 0 \end{bmatrix} \quad (2.3.6)
 \end{aligned}$$

and

$$\begin{aligned}
 V^i &= \left[ \frac{\partial \mathcal{V}_k^i}{\partial x_j} \right] \\
 &= \begin{bmatrix} \alpha_H^i + \mu_H^i & 0 & 0 & 0 \\ -\alpha_H^i & \gamma_H^i + \mu_H^i & 0 & 0 \\ 0 & 0 & \alpha_v^i + \mu_v^i & 0 \\ 0 & 0 & -\alpha_v^i & \mu_v^i \end{bmatrix}.
 \end{aligned} \tag{2.3.7}$$

The inverse of  $V^i$  is

$$(V^i)^{-1} = \begin{bmatrix} \frac{1}{\alpha_H^i + \mu_H^i} & 0 & 0 & 0 \\ \frac{\alpha_H^i}{(\gamma_H^i + \mu_H^i)(\alpha_H^i + \mu_H^i)} & \frac{1}{\gamma_H^i + \mu_H^i} & 0 & 0 \\ 0 & 0 & \frac{1}{\alpha_v^i + \mu_v^i} & 0 \\ 0 & 0 & \frac{\alpha_v^i}{\mu_v^i(\alpha_v^i + \mu_v^i)} & \frac{1}{\mu_v^i} \end{bmatrix}. \tag{2.3.8}$$

The basic reproduction number  $R_{0,i}$  is then given by the dominant eigenvalue (also called the spectral radius  $\rho(F(V^i)^{-1})$ ) of the matrix  $F(V^i)^{-1}$  below,

$$F(V^i)^{-1} = \begin{bmatrix} 0 & 0 & \frac{\alpha_v^i b_H^i \beta_H^i}{\mu_v^i(\alpha_v^i + \mu_v^i)} & \frac{b_H^i \beta_H^i}{\mu_v^i} \\ 0 & 0 & 0 & 0 \\ \frac{\alpha_H^i b_v^i \beta_v^i (N_v^i)^2}{(\gamma_H^i + \mu_H^i)(\alpha_H^i + \mu_H^i)(N_H^i)^2} & \frac{b_v^i \beta_v^i (N_v^i)^2}{(\gamma_H^i + \mu_H^i)(N_H^i)^2} & 0 & 0 \\ 0 & 0 & 0 & 0 \end{bmatrix}. \tag{2.3.9}$$

Hence

$$R_{0,i} = \sqrt{R_{HV,i}(t)R_{VH,i}(t)}, \tag{2.3.10}$$

where

$$R_{HV,i} = \frac{\alpha_H^i}{\alpha_H^i + \mu_H^i} b_H^i (N_v^i / N_H^i) \beta_v^i \frac{1}{\gamma_H^i + \mu_H^i},$$

and

$$R_{VH,i} = \frac{\alpha_v^i}{\alpha_v^i + \mu_v^i} b_v^i (N_v^i / N_H^i) \beta_H^i \frac{1}{\mu_v^i}.$$



It must be noted that  $R_{HV,i}(t)$  represents the number of new mosquito infections that are caused by the one exposed human and  $R_{VH,i}(t)$  representing the number of secondary infections in humans that are caused by one of the infected mosquitoes [57].

In the next section, we look at the local stability of the steady state solution of the dynamic system.

## 2.4 Local stability analysis of the model

In this section we study the local stability of the dynamic system (1.3.3) at the disease free equilibrium  $E_{0,i}$  and the endemic equilibrium point  $E_{e,i}$ .

### 2.4.1 Local stability of the Disease Free Equilibrium

**Theorem 2.4.1** *The disease free equilibrium point  $E_{0,i}$  of (1.3.3) is locally asymptotically stable if  $R_{0,i} < 1$  and unstable otherwise.*

**Proof.** To prove this result we compute the jacobian matrix of the dynamic system (1.3.3).

Let

$$\left. \begin{aligned} f_1^i &= \frac{dS_H^i}{dt} = \nu_H^i N_H^i - k_1 I_v^i S_H^i - \mu_H^i S_H^i, \\ f_2^i &= \frac{dE_H^i}{dt} = b_H^i (N_v^i / N_H^i) \frac{\beta_H^i}{N_v^i} I_v^i S_H^i - \alpha_H^i E_H^i - \mu_H^i E_H^i, \\ f_3^i &= \frac{dI_H^i}{dt} = \alpha_H^i E_H^i - \gamma_H I_H^i - \mu_H^i I_H^i, \\ f_4^i &= \frac{dR_H^i}{dt} = \gamma_H^i I_H^i + \mu_H^i R_H^i, \\ f_5^i &= \frac{dS_v^i}{dt} = \nu_v^i N_v^i - k_2 I_H^i S_v^i - \nu_v^i S_v^i, \\ f_6^i &= \frac{dE_v^i}{dt} = b_v^i (N_v^i / N_H^i) \frac{\beta_v^i}{N_H^i} I_H^i S_v^i - \alpha_v^i E_v^i - \mu_h^i E_v^i, \\ f_7^i &= \frac{dI_v^i}{dt} = \alpha_v^i E_v^i - \mu_v^i I_v^i. \end{aligned} \right\} \quad (2.4.1)$$

The Jacobian matrix of the system  $J^i$  is as follows:

$$J^i = \begin{bmatrix} \frac{\partial f_1^i}{\partial S_H^i} & \frac{\partial f_1^i}{\partial E_H^i} & \frac{\partial f_1^i}{\partial I_H^i} & \frac{\partial f_1^i}{\partial R_H^i} & \frac{\partial f_1^i}{\partial S_v^i} & \frac{\partial f_1^i}{\partial E_v^i} & \frac{\partial f_1^i}{\partial I_v^i} \\ \frac{\partial f_2^i}{\partial S_H^i} & \frac{\partial f_2^i}{\partial E_H^i} & \frac{\partial f_2^i}{\partial I_H^i} & \frac{\partial f_2^i}{\partial R_H^i} & \frac{\partial f_2^i}{\partial S_v^i} & \frac{\partial f_2^i}{\partial E_v^i} & \frac{\partial f_2^i}{\partial I_v^i} \\ \frac{\partial f_3^i}{\partial S_H^i} & \frac{\partial f_3^i}{\partial E_H^i} & \frac{\partial f_3^i}{\partial I_H^i} & \frac{\partial f_3^i}{\partial R_H^i} & \frac{\partial f_3^i}{\partial S_v^i} & \frac{\partial f_3^i}{\partial E_v^i} & \frac{\partial f_3^i}{\partial I_v^i} \\ \frac{\partial f_4^i}{\partial S_H^i} & \frac{\partial f_4^i}{\partial E_H^i} & \frac{\partial f_4^i}{\partial I_H^i} & \frac{\partial f_4^i}{\partial R_H^i} & \frac{\partial f_4^i}{\partial S_v^i} & \frac{\partial f_4^i}{\partial E_v^i} & \frac{\partial f_4^i}{\partial I_v^i} \\ \frac{\partial f_5^i}{\partial S_H^i} & \frac{\partial f_5^i}{\partial E_H^i} & \frac{\partial f_5^i}{\partial I_H^i} & \frac{\partial f_5^i}{\partial R_H^i} & \frac{\partial f_5^i}{\partial S_v^i} & \frac{\partial f_5^i}{\partial E_v^i} & \frac{\partial f_5^i}{\partial I_v^i} \\ \frac{\partial f_6^i}{\partial S_H^i} & \frac{\partial f_6^i}{\partial E_H^i} & \frac{\partial f_6^i}{\partial I_H^i} & \frac{\partial f_6^i}{\partial R_H^i} & \frac{\partial f_6^i}{\partial S_v^i} & \frac{\partial f_6^i}{\partial E_v^i} & \frac{\partial f_6^i}{\partial I_v^i} \\ \frac{\partial f_7^i}{\partial S_H^i} & \frac{\partial f_7^i}{\partial E_H^i} & \frac{\partial f_7^i}{\partial I_H^i} & \frac{\partial f_7^i}{\partial R_H^i} & \frac{\partial f_7^i}{\partial S_v^i} & \frac{\partial f_7^i}{\partial E_v^i} & \frac{\partial f_7^i}{\partial I_v^i} \end{bmatrix} \quad (2.4.2)$$

$$= \begin{bmatrix} -k_1^i I_v^i - \mu_H^i & 0 & 0 & 0 & 0 & 0 & -k_1^i S_H^i \\ k_1^i I_v^i & -(\alpha_H^i + \mu_H^i) & 0 & 0 & 0 & 0 & k_1^i S_H^i \\ 0 & \alpha_H^i & -(\gamma_H^i + \mu_H^i) & 0 & 0 & 0 & 0 \\ 0 & 0 & \gamma_H^i & -\mu_H^i & 0 & 0 & 0 \\ 0 & 0 & -k_2^i S_v^i & 0 & -k_2^i I_H^i - \mu_v^i & 0 & 0 \\ 0 & 0 & k_2^i S_v^i & 0 & k_2^i I_H^i & -(\alpha_v^i + \mu_v^i) & 0 \\ 0 & 0 & 0 & 0 & 0 & \alpha_v^i & -\mu_v^i \end{bmatrix}. \quad (2.4.3)$$

Evaluating the jacobian matrix (2.4.7) of the dynamic system at disease free equilibrium  $E_{0,i}$  we obtain;

$$J_{E_{0,i}} = \begin{bmatrix} -\mu_H^i & 0 & 0 & 0 & 0 & 0 & -k_1^i N_H^i \\ 0 & -(\alpha_H^i + \mu_H^i) & 0 & 0 & 0 & 0 & k_1^i N_H^i \\ 0 & \alpha_H^i & -(\gamma_H^i + \mu_H^i) & 0 & 0 & 0 & 0 \\ 0 & 0 & \gamma_H^i & -\mu_H^i & 0 & 0 & 0 \\ 0 & 0 & -k_2^i N_v^i & 0 & -\mu_v^i & 0 & 0 \\ 0 & 0 & k_2^i N_v^i & 0 & 0 & -(\alpha_v^i + \mu_v^i) & 0 \\ 0 & 0 & 0 & 0 & 0 & \alpha_v^i & -\mu_v^i \end{bmatrix}. \quad (2.4.4)$$

The eigenvalues of the jacobian matrix  $J_{E_{0,i}}$  are  $\lambda^i = -\mu_H^i$  and the roots of the characteristic equation

$$\lambda^{4,i} + A\lambda^{3,i} + B\lambda^{2,i} + C\lambda^i + D = 0, \quad (2.4.5)$$

where

$$A = a + b + c + d,$$

$$B = ab + ac + ad + bc + bd + cd,$$

$$C = abc + abd + acd + bcd,$$

$$D = abcd - \alpha_H^i \alpha_v^i k_1^i k_2^i N_H^i N_v^i,$$

with  $a = \alpha_H^i + \mu_H^i$ ,  $b = \gamma_H^i + \mu_H^i$ ,  $c = \alpha_v^i + \mu_v^i$  and  $d = \mu_v^i$ . Finding the roots of the polynomial (2.4.5) is too complex. We use the Routh-Hurwitz stability criterion to show that the eigenvalues have a native real part by showing that the roots of the polynomial lies on the left half plane of the imaginary axes. To show this we only need to show that  $A > 0$ ,  $AB - C > 0$ ,  $(AB - C)C - A^2D > 0$  and  $D > 0$ . Since all the parameters are nonnegative, it follows that  $A > 0$  and we also have

$$\begin{aligned} AB - C &= (a + b + c + d)(ab + ac + ad + bc + bd + cd) \\ &\quad - (abc + abd + acd + bcd) \\ &= a^2b + a^2c + a^2d + 2abc + 2abd + 2acd + ab^2 + b^2d + b^2d + \\ &\quad 2bcd + ac^2 + bc^2 + c^2d + ad^2 + bd^2 + cd^2 > 0. \end{aligned}$$

Whenever  $R_{0,i} < 1$ . It follows that

$$\begin{aligned} D &= abcd - \alpha_H^i \alpha_v^i k_1^i k_2^i N_H^i N_v^i \\ &= abcd \left( 1 - \frac{\alpha_H^i \alpha_v^i k_1^i k_2^i N_H^i N_v^i}{abcd} \right) \\ &= abcd \left( 1 - \frac{\alpha_H^i \alpha_v^i b_H^i b_v^i \beta_H^i \beta_v^i (N_v^i)^2}{(\alpha_H^i + \mu_H^i)(\gamma_H^i + \mu_H^i)(\alpha_v^i + \mu_v^i)\mu_v^i (N_H^i)^2} \right) \\ &= abcd(1 - R_{0,i}) > 0. \end{aligned}$$

We are now left to show that  $(AB - C)C - A^2D > 0$ . Applying some basic algebra we obtain:

$$\begin{aligned}
 (AB - C)C - A^2D &= (a^2b + a^2c + a^2d + 2abc + 2abd + 2acd + ab^2 + b^2d + \\
 &\quad b^2d + 2bcd + ac^2 + bc^2 + c^2d + ad^2 + bd^2 + cd^2)(abc + \\
 &\quad abd + acd + bcd) - (a + b + c + d)^2(abcd(1 - R_0)) \\
 &= a^3b^2c + a^3bc^2 + a^2b^3c + ab^3c^2 + a^2bc^3 + ab^2c^3 + a^2bcd^2 + \\
 &\quad ab^2cd^2 + abc^2d^2 + 2a^2b^2c^2 + a^3b^2d + a^3dcd + a^3bd^2 + \\
 &\quad a^2b^3d + ab^3cd + ab^3d^2 + a^2bc^2d + ab^2c^2 + abc^2d^2 + a^2bd^3 + \\
 &\quad ab^3d^2 + 2a^2b^2cd + 2a^2b^2d^2 + a^3bcd + a^3c^2d + a^3cd^2 + \\
 &\quad a^2b^2cd + ab^2c^2d + acd^2d^2 + a^2c^3d + abc^3d + ac^3d^2 + a^2cd^3 + \\
 &\quad abcd^3 + ac^2d^3 + 2a^2bc^2d + 2a^2bcd^2 + 2a^2c^2d^2 + a^2b^2cd + \\
 &\quad a^2bc^2d + a^2bcd^2 + ab^3cd + b^3c^2d + b^3cd^2 + abc^3d + \\
 &\quad b^2c^3d + bc^3d^2 + abcd^3 + b^2cd^3 + bc^2d^3 + 2ab^2c^2d + \\
 &\quad 2ab^2cd^2 + 2abc^2d^2 + 2b^2c^2d^2 + (a^3bcd + ab^3cd + \\
 &\quad abc^3d + abcd^3 + 2a^2b^2cd + 2a^2bc^2d + 2a^2bcd^2 + \\
 &\quad 2ab^2c^2d + 2ab^2cd^2 + 2abc^2d^2)R_0 > 0.
 \end{aligned}$$

This completes our proof. The disease free equilibrium point  $E_{0,i}$  is locally asymptotically stable if  $R_{0,i} < 1$ .

## 2.4.2 Local stability of the Endemic Equilibrium

Next want to establish the local stability of the endemic equilibrium point  $E_{e,i}$ . We first take note that  $E_{e,i}$  can be expressed in terms of the basic reproduction number  $R_{0,i}$  as:

$$E_{e,i} = (S_H^{*,i}, E_H^{*,i}, I_H^{*,i}, R_H^{*,i}, S_v^{*,i}, E_v^{*,i}, I_v^{*,i}),$$

where

$$\left. \begin{aligned}
 S_H^{*,i} &= \frac{(N_H^i)^2 \mu_v^i (\alpha_v^i + \mu_v^i) T_H^i}{N_v^i \alpha_H^i b_v^i \beta_v^i Q_H^i}, \\
 E_H^{*,i} &= \frac{N_H^{3,i} \mu_H^i \nu_v^i U_H^i}{N_v^i \alpha_H^i b_v^i \beta_v^i (\alpha_H^i + \mu_H^i) Q_H^i} (R_{0,i}^2 - 1), \\
 I_H^{*,i} &= \frac{N_H^{3,i} \mu_H^i \nu_v^i U_H^i}{N_v^i b_v^i \beta_v^i (\alpha_H^i + \mu_H^i) (\gamma_H^i + \mu_H^i) Q_H^i} (R_{0,i}^2 - 1), \\
 R_H^{*,i} &= \frac{N_H^{3,i} \mu_H^i \gamma_H^i \nu_v^i U_H^i}{N_v^i b_v^i \beta_v^i \mu_H^i (\alpha_H^i + \mu_H^i) (\gamma_H^i + \mu_H^i) Q_H^i} (R_{0,i}^2 - 1), \\
 S_v^{*,i} &= \frac{N_H^i (\alpha_H^i + \mu_H^i) (\gamma_H^i + \mu_H^i) T_v^i}{\alpha_v^i b_H^i \beta_H^i Q_v^i}, \\
 E_v^{*,i} &= \frac{(N_H^i)^2 \mu_H^i \nu_v^i U_H^i}{\alpha_v^i b_H^i \beta_H^i (\alpha_v^i + \mu_v^i) Q_v^i} (R_{0,i}^2 - 1), \\
 I_v^{*,i} &= \frac{(N_H^i)^2 \mu_H^i \nu_v^i U_H^i}{b_H^i \beta_H^i \mu_v^i (\alpha_v^i + \mu_v^i) Q_v^i} (R_{0,i}^2 - 1),
 \end{aligned} \right\} \quad (2.4.6)$$

with

$$\begin{aligned}
 U_H &= \alpha_H^i \alpha_v^i \gamma_H^i \mu_v^i + \alpha_H^i \gamma_H^i (\mu_v^i)^2 + \alpha_H^i \alpha_v^i \mu_H^i \mu_v^i + \alpha_H^i \mu_H^i (\mu_v^i)^2 + \alpha_v^i \gamma_H^i \mu_H^i \mu_v^i + \\
 &\quad \gamma_H^i \mu_H^i (\mu_v^i)^2 + \alpha_v^i (\mu_H^i)^2 \mu_v^i + (\mu_H^i)^2 (\mu_v^i)^2.
 \end{aligned}$$

This lead to the following result.

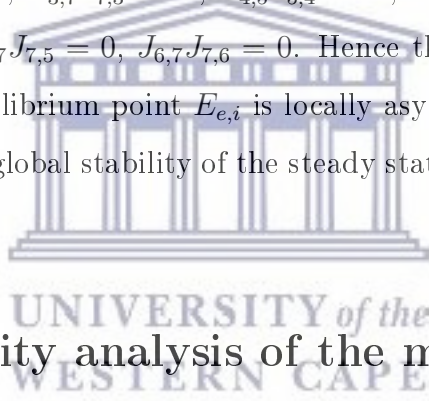
**Theorem 2.4.2** *For  $R_{0,i} > 1$ , there exist a unique endemic equilibrium point  $E_{e,i}$  for the dynamic system (1.3.3) that is locally asymptotically stable.*

**Proof.** To prove that the endemic equilibrium point is local asymptotically stable we adopt the same approach as in [3]. We show that the jacobian matrix (2.4.7) evaluated at the endemic equilibrium point  $E_{e,i}$  is sign stable. The jacobian matrix (2.4.7) at  $E_{e,i}$  gives

$$J_{E_{e,i}} =$$

$$\begin{bmatrix} -k_1^i I_v^{*,i} - \mu_H^i & 0 & 0 & 0 & 0 & 0 & -k_1^i S_H^{*,i} \\ k_1^i I_v^{*,i} & -(\alpha_H^i + \mu_H^i) & 0 & 0 & 0 & 0 & k_1^i S_H^{*,i} \\ 0 & \alpha_H^i & -(\gamma_H^i + \mu_H^i) & 0 & 0 & 0 & 0 \\ 0 & 0 & \gamma_H^i & -\mu_H^i & 0 & 0 & 0 \\ 0 & 0 & -k_2^i S_v^{*,i} & 0 & -k_2^i I_H^{*,i} - \mu_v^i & 0 & 0 \\ 0 & 0 & k_2^i S_v^{*,i} & 0 & k_2^i I_H^{*,i} & -(\alpha_v^i + \mu_v^i) & 0 \\ 0 & 0 & 0 & 0 & 0 & \alpha_v^i & -\mu_v^i \end{bmatrix}. \quad (2.4.7)$$

We have the following sign pattern:  $J_{1,1} = -k_1^i I_v^{*,i} - \mu_H^i < 0$ ,  $J_{2,2} = -(\alpha_H^i + \mu_H^i) < 0$ ,  $J_{3,3} = -(\gamma_H^i + \mu_H^i) < 0$ ,  $J_{4,4} = -\mu_H^i < 0$ ,  $J_{5,5} = -k_2^i I_H^{*,i} - \mu_v^i < 0$ ,  $J_{6,6} = -(\alpha_v^i + \mu_v^i) < 0$ ,  $J_{2,2} = -\mu_v^i < 0$ ,  $J_{1,2}J_{2,1} = 0$ ,  $J_{1,3}J_{3,1} = 0$ ,  $J_{1,4}J_{4,1} = 0$ ,  $J_{1,5}J_{5,1} = 0$ ,  $J_{1,6}J_{6,1} = 0$ ,  $J_{1,7}J_{7,1} = 0$ ,  $J_{2,3}J_{3,2} = 0$ ,  $J_{2,4}J_{4,2} = 0$ ,  $J_{2,5}J_{5,2} = 0$ ,  $J_{2,6}J_{6,2} = 0$ ,  $J_{2,7}J_{7,2} = 0$ ,  $J_{3,4}J_{4,3} = 0$ ,  $J_{3,5}J_{5,3} = 0$ ,  $J_{3,6}J_{6,3} = 0$ ,  $J_{3,7}J_{7,3} = 0$ ,  $J_{4,5}J_{5,4} = 0$ ,  $J_{4,6}J_{6,4} = 0$ ,  $J_{4,7}J_{7,4} = 0$ ,  $J_{5,6}J_{6,5} = 0$ ,  $J_{5,7}J_{7,5} = 0$ ,  $J_{6,7}J_{7,6} = 0$ . Hence the jacobian matrix is sign stable and therefore the equilibrium point  $E_{e,i}$  is locally asymptotically stable. In the next section, we look at the global stability of the steady state solution of the dynamic system.



## 2.5 Global stability analysis of the model

In this section we look at the global stability of the disease free equilibrium point and the endemic equilibrium point of the dynamic system.

### 2.5.1 Global stability of the Disease Free Equilibrium

**Theorem 2.5.1** *The Disease Free Equilibrium  $E_{0,i}$  of the model (1.3.3) is globally asymptotically stable whenever  $R_{0,i} < 1$ .*

**Proof.** Following the work in [11], we construct the following Lyapunov function.

$$L = A_1 E_H^i + A_2 I_H^i + A_3 E_v^i + A_4 I_v^i, \quad (2.5.1)$$

where  $A_1 = \mu_v^i$ ,  $A_2 = k_1^i N_H^i$ ,  $A_3 = \gamma_H^i + \mu_H^i$  and  $A_4 = k_2^i N_v^i$ .

The derivative of  $L$  with respect to time  $t$ , we obtain the following;

$$\begin{aligned}
 \frac{dL}{dt} &= A_1 \frac{dE_H^i}{dt} + A_2 \frac{dI_H^i}{dt} + A_3 \frac{dE_v^i}{dt} + A_4 \frac{dI_v^i}{dt} \\
 &= A_1 [k_1^i I_v^i S_H^i - (\alpha_H^i + \mu_H^i) E_H^i] + A_2 [\alpha_H^i E_H^i - (\gamma_H^i + \mu_H^i) I_H^i] + \\
 &\quad A_3 [k_2^i I_H^i S_v^i - (\alpha_v^i + \mu_v^i) E_v^i] + A_4 [\alpha_v^i E_v^i - \mu_v^i I_v^i] \\
 &= [A_2 \alpha_H^i - A_1 (\alpha_H^i + \mu_H^i)] E_H^i + [A_3 k_2^i S_v^i - B (\gamma_H^i + \mu_H^i)] I_H^i + \\
 &\quad [A_4 \alpha_v^i - A_3 (\alpha_v^i + \mu_v^i)] E_v^i + [A_1 k_1^i S_H^i - A_4 \mu_v^i] I_v^i \\
 &= [k_2^i N_v^i \alpha_H^i - \mu_v^i (\alpha_H^i + \mu_H^i)] E_H^i + [(\gamma_H^i + \mu_H^i) k_2^i S_v^i - k_2^i N_v^i (\gamma_H^i + \mu_H^i)] I_H^i \\
 &\quad + [k_1^i N_H^i \alpha_v^i - (\gamma_H^i + \mu_H^i) (\alpha_v^i + \mu_v^i)] E_v^i + [\mu_v^i k_1^i S_H^i - k_1^i N_H^i \mu_v^i] I_v^i \\
 &= [k_2^i N_v^i \alpha_H^i - \mu_v^i (\alpha_H^i + \mu_H^i)] E_H^i + (\gamma_H^i + \mu_H^i) k_2^i [(S_v^i - N_v^i) I_H^i] \\
 &\quad + [k_1^i N_H^i \alpha_v^i - (\gamma_H^i + \mu_H^i) (\alpha_v^i + \mu_v^i)] E_v^i + \mu_v^i k_1^i [S_H^i - N_H^i] I_v^i.
 \end{aligned}$$

Since  $S_H^i \leq N_H^i$  and  $S_v^i \leq N_v^i$ ,  $\frac{dL}{dt} \leq 0$  whenever  $k_2^i N_v^i \alpha_H^i \leq \mu_v^i (\alpha_H^i + \mu_H^i)$  and  $k_1^i N_H^i \alpha_v^i \leq (\gamma_H^i + \mu_H^i) (\alpha_v^i + \mu_v^i)$ . It follows that since all the parameters are nonnegative,

$$\alpha_H^i \alpha_v^i k_1^i k_2^i N_H^i N_v^i \leq (\alpha_H^i + \mu_H^i) (\gamma_H^i + \mu_H^i) (\alpha_v^i + \mu_v^i) \mu_v^i,$$

or

$$\frac{\alpha_H^i \alpha_v^i k_1^i k_2^i N_H^i N_v^i}{(\alpha_H^i + \mu_H^i) (\gamma_H^i + \mu_H^i) (\alpha_v^i + \mu_v^i) \mu_v^i} \leq 1.$$

Hence

$$R_{0,i}^2 \leq 1,$$

which implies

$$R_0^i \leq 1.$$

Furthermore  $\frac{dL}{dt} = 0$  whenever  $S_H^i = N_H^i, E_H^i = 0, I_H^i = 0, R_H^i = 0, S_v^i = N_v^i, E_v^i = 0, I_v^i = 0$ . Therefore the largest compact invariant set  $\{(S_H^i, E_H^i, I_H^i, R_H^i, S_v^i, E_v^i, I_v^i) \in \mathcal{D} : \frac{dL}{dt} = 0\}$  is the singleton  $E_{0,i}$ . Hence by LaSalle's invariant principle,  $E_{0,i}$  is globally

asymptotically stable [41]. This completes the proof

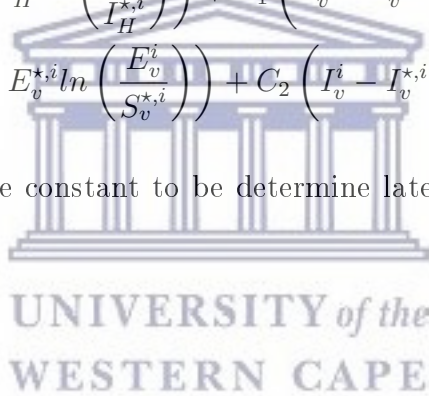
## 2.5.2 Global stability of the Endemic Equilibrium

**Theorem 2.5.2** *The dynamic system (1.3.3) has an endemic equilibrium point  $E_{e,i}$  that is global asymptotically stable whenever  $R_{0,i} > 1$ .*

**Proof.** Using the same approach as in [35], we define a Lyapunov function as follows:

$$\begin{aligned}
 V &= B_1 \left( S_H^i - S_H^{*,i} - S_H^{*,i} \ln \left( \frac{S_H^i}{S_H^{*,i}} \right) \right) + B_1 \left( E_H^i - E_H^{*,i} - E_H^{*,i} \ln \left( \frac{E_H^i}{E_H^{*,i}} \right) \right) \\
 &+ B_2 \left( I_H^i - I_H^{*,i} - I_H^{*,i} \ln \left( \frac{I_H^i}{I_H^{*,i}} \right) \right) + C_1 \left( S_v^i - S_v^{*,i} - S_v^{*,i} \ln \left( \frac{S_v^i}{S_v^{*,i}} \right) \right) \\
 &+ C_1 \left( E_v^i - E_v^{*,i} - E_v^{*,i} \ln \left( \frac{E_v^i}{S_v^{*,i}} \right) \right) + C_2 \left( I_v^i - I_v^{*,i} - I_v^{*,i} \ln \left( \frac{I_v^i}{I_v^{*,i}} \right) \right),
 \end{aligned}$$

where  $B_1$ ,  $B_2$ ,  $C_1$  and  $C_2$  are constant to be determine later. Differentiating  $V$  with





respect to time,  $t$ , we obtain

$$\begin{aligned}
 \frac{dV}{dt} &= B_1 \left(1 - \frac{S_H^{*,i}}{S_H^i}\right) \frac{dS_H^i}{dt} + B_1 \left(1 - \frac{E_H^{*,i}}{E_H^i}\right) \frac{dE_H^i}{dt} + B_2 \left(1 - \frac{I_H^{*,i}}{I_H^i}\right) \frac{dI_H^i}{dt} \\
 &+ C_1 \left(1 - \frac{S_v^{*,i}}{S_v^i}\right) \frac{dS_v^i}{dt} + C_1 \left(1 - \frac{E_v^{*,i}}{E_v^i}\right) \frac{dE_v^i}{dt} + C_2 \left(1 - \frac{I_v^{*,i}}{I_v^i}\right) \frac{dI_v^i}{dt} \\
 &= B_1 \left(1 - \frac{S_H^{*,i}}{S_H^i}\right) (\nu_H^i N_H^i - k_1^i I_v^i S_H^i - \mu_H^i S_H^i) \\
 &+ B_1 \left(1 - \frac{E_H^{*,i}}{E_H^i}\right) (k_1^i I_v^i S_H^i - (\alpha_H^i + \mu_H^i) E_H^i) \\
 &+ B_2 \left(1 - \frac{I_H^{*,i}}{I_H^i}\right) (\alpha_H^i E_H^i - (\gamma_H^i + \mu_H^i) I_H^i) \\
 &+ C_1 \left(1 - \frac{S_v^{*,i}}{S_v^i}\right) (\nu_v^i N_v^i - k_2^i I_H^i S_v^i - \mu_v^i S_v^i) \\
 &+ C_1 \left(1 - \frac{E_v^{*,i}}{E_v^i}\right) (k_2^i I_H^i S_v^i - (\alpha_v^i + \mu_v^i) E_v^i) \\
 &+ C_2 \left(1 - \frac{I_v^{*,i}}{I_v^i}\right) (\alpha_v^i E_v^i - \mu_v^i I_v^i) \\
 &= B_1 \nu_H^i N_H^i \left(1 - \frac{S_H^{*,i}}{S_H^i}\right) + B_1 k_1^i I_v^i S_H^{*,i} - B_1 \mu_H^i S_H^i + B_1 \mu_H^i S_H^{*,i} \\
 &- B_1 k_1^i I_v^i S_H^i \frac{E_H^{*,i}}{E_H^i} - B_1 (\alpha_H^i + \mu_H^i) E_H^i + B_1 (\alpha_H^i + \mu_H^i) E_H^{*,i} + B_2 \alpha_H^i E_H^i \\
 &- B_2 \alpha_H^i E_H^i \frac{I_H^{*,i}}{I_H^i} - B_2 (\gamma_H^i + \mu_H^i) I_H^i + B_2 (\gamma_H^i + \mu_H^i) I_H^{*,i} \\
 &+ C_1 \nu_v^i N_v^i \left(1 - \frac{S_v^{*,i}}{S_v^i}\right) + C_1 k_2^i I_H^i S_v^{*,i} - C_1 \mu_v^i S_v^i + C_1 \mu_v^i S_v^{*,i} \\
 &- C_1 k_2^i I_H^i S_v^i \frac{E_v^{*,i}}{E_v^i} - C_1 (\alpha_v^i + \mu_v^i) E_v^i + C_1 (\alpha_v^i + \mu_v^i) E_v^{*,i} \\
 &+ C_2 \alpha_v^i E_v^i - C_2 \alpha_v^i E_v^i \frac{I_v^{*,i}}{I_v^i} - C_2 \mu_v^i I_v^i + C_2 \mu_v^i I_v^{*,i}. \tag{2.5.2}
 \end{aligned}$$

At the endemic equilibrium point  $E_{e,i}$  we note that  $\nu_H^i N_H^i = k_1^i I_v^{*,i} S_H^{*,i} + \mu_H^i S_H^{*,i}$ ,  $\nu_v^i N_v^i = k_2^i I_H^{*,i} S_v^{*,i} + \mu_v^i S_v^{*,i}$ ,  $(\alpha_H^i + \mu_H^i) E_H^{*,i} = k_1^i I_v^{*,i} S_H^{*,i}$ ,  $(\alpha_v^i + \mu_v^i) E_v^{*,i} = k_2^i I_H^{*,i} S_v^{*,i}$ ,  $(\gamma_H^i + \mu_H^i) I_H^{*,i} = \alpha_H^i E_H^{*,i}$  and  $\mu_v^i I_v^{*,i} = \alpha_v^i E_v^{*,i}$ . Hence, the equation (2.5.2) can be written

as

$$\begin{aligned}
 \frac{dV}{dt} = & B_1 k_1^i I_v^{*,i} S_H^{*,i} \left( 1 - \frac{S_H^{*,i}}{S_H^i} \right) + B_1 \mu_H^i S_H^{*,i} \left( 2 - \frac{S_H^{*,i}}{S_H^i} - \frac{S_H^i}{S_H^{*,i}} \right) + B_1 k_1 I_v^i S_H^{*,i} \\
 & - B_1 k_1 I_v^i S_H^i \frac{E_H^{*,i}}{E_H^i} - B_1 k_1 I_v^{*,i} S_H^{*,i} \frac{E_H^i}{E_H^{*,i}} + B_1 k_1^i I_v^{*,i} S_H^{*,i} + B_2 \alpha_H^i E_H^i \\
 & - B_2 (\gamma_H^i + \mu_H^i) I_H^i - B_2 \alpha_H^i E_H^i \frac{I_H^{*,i}}{I_H^i} + B_2 \alpha_H^i E_H^{*,i} \\
 & + C_1 k_2^i I_H^{*,i} S_v^{*,i} \left( 1 - \frac{S_v^{*,i}}{S_v^i} \right) + C_1 \mu_v^i S_v^{*,i} \left( 2 - \frac{S_v^{*,i}}{S_v^i} - \frac{S_v^i}{S_v^{*,i}} \right) + C_1 k_2 I_H^i S_v^{*,i} \\
 & - C_1 k_2 I_H^i S_v^i \frac{E_v^{*,i}}{E_v^i} - C_1 k_2 I_H^{*,i} S_v^{*,i} \frac{E_v^i}{E_v^{*,i}} + C_1 k_2^i I_H^{*,i} S_v^{*,i} \\
 & + C_2 \alpha_v^i E_v^i - C_2 \mu_v^i I_v^i - C_2 \alpha_v^i E_v^i \frac{I_v^{*,i}}{I_v^i} + C_2 \alpha_v^i E_v^{*,i}.
 \end{aligned}$$

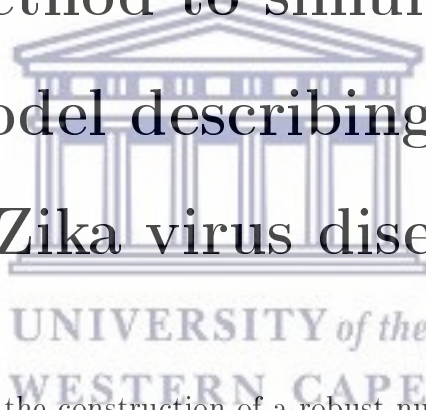
Choosing  $B_1 = \frac{1}{k_1^i I_v^{*,i} S_H^{*,i}}$ ,  $B_2 = \frac{\alpha_H^i + \mu_H^i}{\alpha_H^i k_1^i I_v^{*,i} S_H^{*,i}}$ ,  $C_1 = \frac{1}{k_2^i I_H^{*,i} S_v^{*,i}}$  and  $C_2 = \frac{\alpha_v^i + \mu_v^i}{\alpha_v^i k_2^i I_H^{*,i} S_v^{*,i}}$ . We can rewrite  $\frac{dV}{dt}$  as follows:

$$\begin{aligned}
 \frac{dV}{dt} = & \frac{\mu_H^i}{k_1 I_v^{*,i}} \left( 2 - \frac{S_H^{*,i}}{S_H^i} - \frac{S_H^i}{S_H^{*,i}} \right) + \frac{\mu_v^i}{k_2 I_H^i} \left( 2 - \frac{S_v^{*,i}}{S_v^i} - \frac{S_v^i}{S_v^{*,i}} \right) \\
 & + 6 - \frac{S_H^{*,i}}{S_H^i} - \frac{S_v^{*,i}}{S_v^i} - \frac{E_H^i I_H^{*,i}}{E_H^{*,i} I_H^i} - \frac{E_v^i I_v^{*,i}}{E_v^{*,i} I_v^i} - \frac{I_v^i S_H^i E_H^{*,i}}{I_v^{*,i} S_H^{*,i} E_H^i} - \frac{I_H^i S_v^i E_v^{*,i}}{I_H^{*,i} S_v^{*,i} E_v^i}.
 \end{aligned}$$

Since the arithmetic mean is greater than or equal to the geometric mean of the quantities,  $\frac{dV}{dt} \leq 0$ . Also it can be further noted that  $\frac{dV}{dt} = 0$  whenever  $S_H^i = S_H^{*,i}$ ,  $E_H^i = E_H^{*,i}$ ,  $I_H^i = I_H^{*,i}$ ,  $R_H^i = R_H^{*,i}$ ,  $S_v^i = S_v^{*,i}$ ,  $E_v^i = E_v^{*,i}$ ,  $I_v^i = I_v^{*,i}$ . Then, it follows that the equilibrium point  $E_{e,i}$  is the only positively invariant set  $\{(S_H^i, E_H^i, I_H^i, R_H^i, S_v^i, E_v^i, I_v^i) \in \mathcal{D} : \frac{dV}{dt} = 0\}$  of the system (1.3.3) and hence by the asymptotic stability theorem,  $E_{e,i}$  is globally asymptotically stable [41]. In the next chapter we construct a nonstandard finite difference method consistent with the dynamic system.

## Chapter 3

# Construction and analysis of a numerical method to simulate the SEIR-SEI model describing the dynamics of Zika virus disease



In this chapter we deal with the construction of a robust numerical method known as the nonstandard finite difference method for the dynamic system and the analysis of the numerical method.

In the next section, we give a general philosophy of the nonstandard finite difference method.

### 3.1 What are these nonstandard finite difference methods?

In the study of epidemic, mathematical models play a very significant role. These mathematical models are used to gain an in-depth knowledge about the dynamics of

infectious disease spreading within a population and they can be used to draw some important conclusions. However, often times these mathematical models uses autonomous systems of nonlinear ordinary differential equations which can be very complicated or even impossible to solve for an exact solutions. This factor about solving such systems has resulted in the discretization of these systems using well-known numerical methods.

While an exact solution to the system of nonlinear ordinary differential equations might not be obtainable, with the use of numerical methods, a finite discrete system of the model can be constructed and solved using numerical techniques to find an approximate solutions. It is very important therefore that this numerical methods mimic certain behavioural features of the original continuous model. However, most of these numerical methods such as the Euler and Runge-Kutta method often fail to preserve some of the qualitative properties of the solution corresponding to the original continuous system such as positivity and the local stability of equilibrium points [28].

To avoid numerical instabilities and inconsistencies generated by standard finite difference methods such as Euler method and Runge-Kutta method, a class of robust numerical methods, known as the Non-Standard Finite Difference Method (NSFDM), which are dynamically consistent with the original differential systems was developed in [47].

The NSFDM methods have already being applied to some epidemic models in the following papers: [1, 2, 7, 14, 15, 17, 19, 23, 27, 29, 44, 55, 60, 69, 70, 78, 79, 84, 85]. These NSFDMs have become very popular and powerful tool to solve systems of nonlinear equations due to the fact that unlike Euler and Runge-Kutta, NSFDM do not generate oscillations, chaos, and false steady states [55]. These methods are thoroughly reviewed in the two survey articles [63, 64] where the author has presented different constructions of these methods provided by numerous researchers in the field.

In the next section, we construct a robust Nonstandard Finite Difference method for

the dynamic system.

## 3.2 Derivation of a robust nonstandard finite difference method to solve the Zika virus disease model

We construct a non-standard finite difference (NSFD) scheme consistent with the continuous dynamical system of (1.3.3) for the Zika virus to approximate numerically the model equations of the system. The time domain  $[a, b]$  is subdivided into  $M$  number of small sub-intervals of width  $\ell = t_{n+1} - t_n$  where  $n = 0, 1, \dots, M$  called the step-size such that each continuous time variable  $t$  is replaced by a discrete time  $t_n = n\ell$ . To find an approximate solution  $S_H^{m,i}, E_H^{m,i}, I_H^{m,i}, R_H^{m,i}, S_v^{m,i}, E_v^{m,i}, I_v^{m,i}$  to  $S_H^i, E_H^i, I_H^i, R_H^i, S_v^i, E_v^i, I_v^i$  at time  $t = t_n$ , we construct the discrete model in the following manner:

$$\left. \begin{aligned} \frac{S_H^{m+1,i} - S_H^{m,i}}{\phi(\ell)} &= \nu_H^i N_H^{m,i} - b_H^i \left( \frac{N_v^{m,i}}{N_H^{m,i}} \right) \frac{I_v^{m,i}}{N_v^{m,i}} \beta_H^i S_H^{m+1,i} - \mu_H^i S_H^{m+1,i}, \\ \frac{E_H^{m+1,i} - E_H^{m,i}}{\phi(\ell)} &= b_H^i \left( \frac{N_v^{m,i}}{N_H^{m,i}} \right) \frac{I_v^{m,i}}{N_v^{m,i}} \beta_H^i S_H^{m+1,i} - \alpha_H^i E_H^{m+1,i} - \mu_H^i E_H^{m+1,i}, \\ \frac{I_H^{m+1,i} - I_H^{m,i}}{\phi(\ell)} &= \alpha_H^i E_H^{m+1,i} - \gamma_H^i I_H^{m+1,i} - \mu_H^i I_H^{m+1,i}, \\ \frac{R_H^{m+1,i} - R_H^{m,i}}{\phi(\ell)} &= \gamma_H^i I_H^{m+1,i} - \mu_H^i R_H^{m+1,i}, \\ \frac{S_v^{m+1,i} - S_v^{m,i}}{\phi(\ell)} &= \nu_v^i N_v^{m,i} - b_v^i \left( \frac{N_v^{m,i}}{N_H^{m,i}} \right) \frac{I_m^{m,i}}{N_H^{m,i}} \beta_v^i S_v^{m+1,i} - \mu_v^i S_v^{m+1,i}, \\ \frac{E_v^{m+1,i} - E_v^{m,i}}{\phi(\ell)} &= b_v^i \left( \frac{N_v^{m,i}}{N_H^{m,i}} \right) \frac{I_m^{m,i}}{N_H^{m,i}} \beta_v^i S_v^{m+1,i} - \alpha_v^i E_v^{m+1,i} - \mu_v^i E_v^{m+1,i}, \\ \frac{I_v^{m+1,i} - I_v^{m,i}}{\phi(\ell)} &= \alpha_v^i E_v^{m+1,i} - \mu_v^i I_v^{m+1,i}, \end{aligned} \right\} \quad (3.2.1)$$

where  $N_H^{m,i} = S_H^{m,i} + E_H^{m,i} + I_H^{m,i} + R_H^{m,i}$ ,  $N_v^{m,i} = S_v^{m,i} + E_v^{m,i} + I_v^{m,i}$  and  $\phi(\ell)$  is a real-valued denominator function satisfying

$$\Phi(\ell) = \ell + O(\ell^2) \text{ for all } \ell > 0, \quad (3.2.2)$$

as noted in [48].

In the next section, we look at the analysis of the proposed numerical method.

### 3.3 Analysis of proposed numerical method

To help with the analysis we can simplify (3.2.1) to the following explicit form:

$$\left. \begin{aligned}
 S_H^{m+1,i} &= \frac{\phi \nu_H^i N_H^{m,i} + S_H^{m,i}}{1 + \phi(k_1^{m,i} I_v^{m,i} + \mu_H^i)}, \\
 E_H^{m+1,i} &= \frac{\phi k_1^{m,i} I_v^{m,i} S_H^{m+1,i} + E_H^{m,i}}{1 + \phi(\alpha_H^i + \mu_H^i)}, \\
 I_H^{m+1,i} &= \frac{\phi \alpha_H^i E_H^{m+1,i} + I_H^{m,i}}{1 + \phi(\gamma_H^i + \mu_H^i)}, \\
 R_H^{m+1,i} &= \frac{\phi \gamma_H^i I_H^{m+1,i} + R_H^{m,i}}{1 + \phi \mu_H^i}, \\
 S_v^{m+1,i} &= \frac{\phi \nu_v^i N_v^{m,i} + S_v^{m,i}}{1 + \phi(k_2^{m,i} I_H^{m,i} + \mu_v^i)}, \\
 E_v^{m+1,i} &= \frac{\phi k_2^{m,i} I_H^{m,i} S_v^{m+1,i} + E_v^{m,i}}{1 + \phi(\alpha_v^i + \mu_v^i)}, \\
 I_v^{m+1,i} &= \frac{\phi \alpha_v^i E_v^{m+1,i} + I_v^{m,i}}{1 + \phi \mu_v^i},
 \end{aligned} \right\} \quad (3.3.1)$$

where  $k_1^{m,i} = b_H^i \beta_H^i (N_v^{m,i} / N_H^{m,i})(1 / N_v^{m,i})$  and  $k_2^{m,i} = b_v^i \beta_v^i (N_v^{m,i} / N_H^{m,i})(1 / N_H^{m,i})$ .

The positivity of the solution can easily be seen from the explicit form (3.3.1) that starting with non-negative initial conditions  $S_H^{m,i}(0) \geq 0$ ,  $E_H^{m,i}(0) \geq 0$ ,  $I_H^{m,i}(0) \geq 0$ ,  $R_H^{m,i}(0) \geq 0$ ,  $S_v^{m,i}(0) \geq 0$ ,  $E_v^{m,i}(0) \geq 0$ ,  $I_v^{m,i}(0) \geq 0$  at  $t_0$ , since all parameters are positive, that all solutions of system (3.2.1) subject to initial condition remain non-negative for all  $n \in M$ .

Following the work in [55] we take two cases of the NSFD methods:

**Case1** : We set  $\phi(\ell) = \ell$ .

**Case2** : We define

$$\phi(\ell) = \frac{e^{\ell\mu_H^i} - 1}{\mu_H^i}. \quad (3.3.2)$$

Case 1 is called the NSFD-I and case 2 is called NSFD-II.

The fixed point of the discrete scheme can be obtained by first setting,

$$\left. \begin{aligned} S_H^{m+1,i} &= f_1(S_H^{m,i}, E_H^{m,i}, I_H^{m,i}, R_H^{m,i}, S_v^{m,i}, E_v^{m,i}, I_v^{m,i}), \\ E_H^{m+1,i} &= f_2(S_H^{m,i}, E_H^{m,i}, I_H^{m,i}, R_H^{m,i}, S_v^{m,i}, E_v^{m,i}, I_v^{m,i}), \\ I_H^{m+1,i} &= f_3(S_H^{m,i}, E_H^{m,i}, I_H^{m,i}, R_H^{m,i}, S_v^{m,i}, E_v^{m,i}, I_v^{m,i}), \\ R_H^{m+1,i} &= f_4(S_H^{m,i}, E_H^{m,i}, I_H^{m,i}, R_H^{m,i}, S_v^{m,i}, E_v^{m,i}, I_v^{m,i}), \\ S_v^{m+1,i} &= f_5(S_H^{m,i}, E_H^{m,i}, I_H^{m,i}, R_H^{m,i}, S_v^{m,i}, E_v^{m,i}, I_v^{m,i}), \\ E_v^{m+1,i} &= f_6(S_H^{m,i}, E_H^{m,i}, I_H^{m,i}, R_H^{m,i}, S_v^{m,i}, E_v^{m,i}, I_v^{m,i}), \\ I_v^{m+1,i} &= f_7(S_H^{m,i}, E_H^{m,i}, I_H^{m,i}, R_H^{m,i}, S_v^{m,i}, E_v^{m,i}, I_v^{m,i}). \end{aligned} \right\} \quad (3.3.3)$$

We can then write (3.3.1) as:

$$\left. \begin{aligned} f_1(S_H^{m,i}, E_H^{m,i}, I_H^{m,i}, R_H^{m,i}, S_v^{m,i}, E_v^{m,i}, I_v^{m,i}) &= \frac{\phi\nu_H^i N_H^{m,i} + S_H^{m,i}}{1 + \phi(k_1^{m,i} I_v^{m,i} + \mu_H^i)}, \\ f_2(S_H^{m,i}, E_H^{m,i}, I_H^{m,i}, R_H^{m,i}, S_v^{m,i}, E_v^{m,i}, I_v^{m,i}) &= \frac{\phi k_1^{m,i} I_v^{m,i} S_H^{m+1,i} + E_H^{m,i}}{1 + \phi(\alpha_H^i + \mu_H^i)}, \\ f_3(S_H^{m,i}, E_H^{m,i}, I_H^{m,i}, R_H^{m,i}, S_v^{m,i}, E_v^{m,i}, I_v^{m,i}) &= \frac{\phi\alpha_H^i E_H^{m+1,i} + I_H^{m,i}}{1 + \phi(\gamma_H^i + \mu_H^i)}, \\ f_4(S_H^{m,i}, E_H^{m,i}, I_H^{m,i}, R_H^{m,i}, S_v^{m,i}, E_v^{m,i}, I_v^{m,i}) &= \frac{\phi\gamma_H^i I_H^{m+1,i} + R_H^{m,i}}{1 + \phi\mu_H^i}, \\ f_5(S_H^{m,i}, E_H^{m,i}, I_H^{m,i}, R_H^{m,i}, S_v^{m,i}, E_v^{m,i}, I_v^{m,i}) &= \frac{\phi\nu_v^i N_v^{m,i} + S_v^{m,i}}{1 + \phi(k_2^{m,i} I_H^{m,i} + \mu_v^i)}, \\ f_6(S_H^{m,i}, E_H^{m,i}, I_H^{m,i}, R_H^{m,i}, S_v^{m,i}, E_v^{m,i}, I_v^{m,i}) &= \frac{\phi k_2^{m,i} I_H^{m,i} S_v^{m+1,i} + E_v^{m,i}}{1 + \phi(\alpha_v^i + \mu_v^i)}, \\ f_7(S_H^{m,i}, E_H^{m,i}, I_H^{m,i}, R_H^{m,i}, S_v^{m,i}, E_v^{m,i}, I_v^{m,i}) &= \frac{\phi\alpha_v^i E_v^{m+1,i} + I_v^{m,i}}{1 + \phi\mu_v^i}. \end{aligned} \right\} \quad (3.3.4)$$

The fixed points of discrete model are all the point satisfying the following condition,

$$\left. \begin{aligned} S_H^{m,i} &= f_1(S_H^{m,i}, E_H^{m,i}, I_H^{m,i}, R_H^{m,i}, S_v^{m,i}, E_v^{m,i}, I_v^{m,i}), \\ E_H^{m,i} &= f_2(S_H^{m,i}, E_H^{m,i}, I_H^{m,i}, R_H^{m,i}, S_v^{m,i}, E_v^{m,i}, I_v^{m,i}), \\ I_H^{m,i} &= f_3(S_H^{m,i}, E_H^{m,i}, I_H^{m,i}, R_H^{m,i}, S_v^{m,i}, E_v^{m,i}, I_v^{m,i}), \\ R_H^{m,i} &= f_4(S_H^{m,i}, E_H^{m,i}, I_H^{m,i}, R_H^{m,i}, S_v^{m,i}, E_v^{m,i}, I_v^{m,i}), \\ S_v^{m,i} &= f_5(S_H^{m,i}, E_H^{m,i}, I_H^{m,i}, R_H^{m,i}, S_v^{m,i}, E_v^{m,i}, I_v^{m,i}), \\ E_v^{m,i} &= f_6(S_H^{m,i}, E_H^{m,i}, I_H^{m,i}, R_H^{m,i}, S_v^{m,i}, E_v^{m,i}, I_v^{m,i}), \\ I_v^{m,i} &= f_7(S_H^{m,i}, E_H^{m,i}, I_H^{m,i}, R_H^{m,i}, S_v^{m,i}, E_v^{m,i}, I_v^{m,i}). \end{aligned} \right\} \quad (3.3.5)$$

In other words, to calculate the fixed points we can set the right-hand side of the model equations of (3.2.1) to zero. From this it can be easily verified that the fixed point of the discrete system are the same as the equilibrium points of the continuous system. Hence, the model (3.3.1) has the disease free equilibrium point given by

$$E_{0,i}^m = (N_H^{m,i}, 0, 0, 0, N_v^{m,i}, 0, 0).$$

and the endemic equilibrium point given by

$$E_{e,i}^m = (S_H^{m*,i}, E_H^{m*,i}, I_H^{m*,i}, R_H^{m*,i}, S_v^{m*,i}, E_v^{m*,i}, I_v^{m*,i}),$$



where

$$\left. \begin{aligned}
 S_H^{m*,i} &= \frac{(N_H^{m,i})^2 \mu_v^i (\alpha_v^i + \mu_v^i) T_H^{m,i}}{N_v^{m,i} \alpha_H^i b_v^i \beta_v^i Q_H^{m,i}}, \\
 E_H^{m*,i} &= \frac{(N_H^{m,i})^3 \mu_H^i \nu_v^i U_H^{m,i}}{N_v^{m,i} \alpha_H^i b_v^i \beta_v^i (\alpha_H^i + \mu_H^i) Q_H^{m,i}} (R_{0,i}^2 - 1), \\
 I_H^{m*,i} &= \frac{(N_H^{m,i})^3 \mu_H^i \nu_v^i U_H^{m,i}}{N_v^i b_v^i \beta_v^i (\alpha_H^i + \mu_H^i) (\gamma_H^i + \mu_H^i) Q_H^{m,i}} (R_{0,i}^2 - 1), \\
 R_H^{m*,i} &= \frac{(N_H^{m,i})^3 \mu_H^i \gamma_H^i \nu_v^i U_H^{m,i}}{N_v^i b_v^i \beta_v^i \mu_H^i (\alpha_H^i + \mu_H^i) (\gamma_H^i + \mu_H^i) Q_H^{m,i}} (R_{0,i}^2 - 1), \\
 S_v^{m*,i} &= \frac{N_H^{m,i} (\alpha_H^i + \mu_H^i) (\gamma_H^i + \mu_H^i) T_v^{m,i}}{\alpha_v^i b_H^i \beta_H^i Q_v^{m,i}}, \\
 E_v^{m*,i} &= \frac{(N_H^{m,i})^2 \mu_H^i \nu_v^i U_H^{m,i}}{\alpha_v^i b_H^i \beta_H^i (\alpha_v^i + \mu_v^i) Q_v^{m,i}} (R_{0,i}^2 - 1), \\
 I_v^{m*,i} &= \frac{(N_H^{m,i})^2 \mu_H^i \nu_v^i U_H^{m,i}}{b_H^i \beta_H^i \mu_v^i (\alpha_v^i + \mu_v^i) Q_v^{m,i}} (R_{0,i}^2 - 1),
 \end{aligned} \right\} \quad (3.3.6)$$

with

$$\begin{aligned}
 U_H^{m,i} &= \alpha_H^i \alpha_v^i \gamma_H^i \mu_v^i + \alpha_H^i \gamma_H^i (\mu_v^i)^2 + \alpha_H^i \alpha_v^i \mu_H^i \mu_v^i + \alpha_H^i \mu_H^i (\mu_v^i)^2 + \alpha_v^i \gamma_H^i \mu_H^i \mu_v^i + \\
 &\quad \gamma_H^i \mu_H^i (\mu_v^i)^2 + \alpha_v^i (\mu_H^i)^2 \mu_v^i + (\mu_H^i)^2 (\mu_v^i)^2, \\
 Q_v^{m,i} &= N_H^{m,i} \alpha_H^i \gamma_H^i \nu_v^i + N_H^{m,i} \alpha_H^i \mu_H^i \nu_v^i + N_H^{m,i} \gamma_H^i \mu_H^i \nu_v^i + N_H^i (\mu_H^i)^2 \nu_v^i + N_v^{m,i} \alpha_H^i b_v^i \beta_v^i \nu_H^i, \\
 T_v^{m,i} &= N_H^{m,i} \alpha_v^i \mu_H^i \mu_v^i + N_H^{m,i} \mu_H^i (\mu_v^i)^2 + N_v^{m,i} \alpha_v^i b_H^i \beta_H^i \nu_v^i.
 \end{aligned}$$

### 3.3.1 Stability analysis of the fixed points

**Theorem 3.3.1** *The system (3.2.1) is unconditionally locally asymptotically stable at the disease free equilibrium,  $E_0^{m,i} = (N_H^{m,i}, 0, 0, 0, N_v^{m,i}, 0, 0)$  for the real-valued function  $\phi(\ell) = \ell + O(\ell^2)$  if  $R_0 \leq 1$ , and unstable otherwise.*

**Proof.** The jacobian matrix  $J^m$  of the discrete system (3.2.1) is given as;

$$J^m = \begin{bmatrix} J_{1,1}^m & 0 & 0 & 0 & 0 & 0 & J_{1,7}^m \\ J_{2,1}^m & J_{2,2}^m & 0 & 0 & 0 & 0 & J_{2,7}^m \\ J_{3,1}^m & J_{3,2}^m & J_{3,3}^m & 0 & 0 & 0 & J_{3,7}^m \\ J_{4,1}^m & J_{4,2}^m & J_{4,3}^m & J_{4,4}^m & 0 & 0 & J_{4,7}^m \\ 0 & 0 & J_{5,3}^m & 0 & J_{5,5}^m & 0 & 0 \\ 0 & 0 & J_{6,3}^m & 0 & J_{6,5}^m & J_{6,6}^m & 0 \\ 0 & 0 & J_{7,3}^m & 0 & J_{7,5}^m & J_{7,6}^m & J_{7,7}^m \end{bmatrix}, \quad (3.3.7)$$



UNIVERSITY *of the*  
 WESTERN CAPE

where

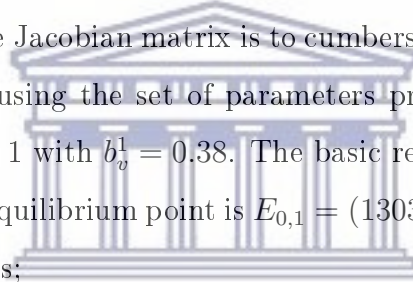
$$\begin{aligned}
 J_{1,1}^m &= \frac{1}{L_1^i + \phi k_1^{m,i} I_v^{m,i}}, & J_{4,4}^m &= \frac{1}{L_4^i}, \\
 J_{1,7}^m &= -\frac{\phi k_1^{m,i} (\phi \nu_H^i N_H^{m,i} + S_H^{m,i})}{(L_1^i + \phi k_1^{m,i} I_v^{m,i})^2}, & J_{4,7}^m &= \frac{\phi^3 \alpha_H^i \gamma_H^i k_1^{m,i} (\phi \nu_H^i N_H^{m,i} + S_H^{m,i})}{L_2^i L_3^i L_4^i (L_1^i + \phi k_1^{m,i} I_v^{m,i})} - \\
 J_{2,1}^m &= \frac{\phi k_1^{m,i} I_v^{m,i}}{L_2^i (L_1^i + \phi k_1^{m,i} I_v^{m,i})}, & & \frac{\phi^4 \alpha_H^i \gamma_H^i (k_1^{m,i})^2 I_v^{m,i} (\phi \nu_H^i N_H^{m,i} + S_H^{m,i})}{L_2^i L_3^i L_4^i (L_1^i + \phi k_1^{m,i} I_v^{m,i})^2}, \\
 J_{2,2}^m &= \frac{1}{L_2^i}, & J_{5,3}^m &= -\frac{\phi k_2^{m,i} (\phi \nu_v^i N_v^{m,i} + S_v^{m,i})}{(L_5^i + \phi k_2^{m,i} I_H^{m,i})^2}, \\
 J_{2,7}^m &= \frac{\phi k_1^{m,i} (\phi \nu_H^i N_H^{m,i} + S_H^{m,i})}{L_2^i (L_1^i + \phi k_1^{m,i} I_v^{m,i})} - \\
 & \frac{\phi^2 (k_1^{m,i})^2 I_v^{m,i} (\phi \nu_H^i N_H^{m,i} + S_H^{m,i})}{L_2^i (L_1^i + \phi k_1^{m,i} I_v^{m,i})^2}, & J_{5,5}^m &= \frac{1}{L_5^i + \phi k_2^{m,i} I_H^{m,i}}, \\
 J_{3,1}^m &= \frac{\phi^2 \alpha_H^i k_1^{m,i} I_v^{m,i}}{L_2^i L_3^i (L_1^i + \phi k_1^{m,i} I_v^{m,i})}, & J_{6,3}^m &= \frac{\phi k_2^{m,i} (\phi \nu_v^i N_v^{m,i} + S_v^{m,i})}{L_6^i (L_5^i + \phi k_2^{m,i} I_H^{m,i})} - \\
 J_{3,2}^m &= \frac{\phi \alpha_H^i}{L_2^i L_3^i}, & & \frac{\phi^2 (k_2^{m,i})^2 I_H^{m,i} (\phi \nu_v^i N_v^{m,i} + S_v^{m,i})}{L_6^i (L_5^i + \phi k_2^{m,i} I_H^{m,i})^2}, \\
 J_{3,3}^m &= \frac{1}{L_3^i}, & J_{6,5}^m &= \frac{\phi k_2^{m,i} I_H^{m,i}}{L_6^i (L_5^i + \phi k_2^{m,i} I_H^{m,i})}, \\
 J_{3,7}^m &= \frac{\phi^2 \alpha_H^i k_1^{m,i} (\phi \nu_H^i N_H^{m,i} + S_H^{m,i})}{L_2^i L_3^i (L_1^i + \phi k_1^{m,i} I_v^{m,i})} - \\
 & \frac{\phi^3 \alpha_H^i (k_1^{m,i})^2 I_v^{m,i} (\phi \nu_H^i N_H^{m,i} + S_H^{m,i})}{L_2^i L_3^i (L_1^i + \phi k_1^{m,i} I_v^{m,i})^2}, & J_{6,6}^m &= \frac{1}{L_6^i}, \\
 & & J_{7,3}^m &= \frac{\phi^2 \alpha_v^i k_2^{m,i} (\phi \nu_v^i N_v^{m,i} + S_v^{m,i})}{L_6^i L_7^i (L_5^i + \phi k_2^{m,i} I_H^{m,i})} - \\
 J_{4,1}^m &= \frac{\phi^3 \alpha_H^i \gamma_H^i k_1^{m,i} I_v^{m,i}}{L_2^i L_3^i L_4^i (L_1^i + \phi k_1^{m,i} I_v^{m,i})}, & & \frac{\phi^3 \alpha_v^i (k_2^{m,i})^2 I_H^{m,i} (\phi \nu_v^i N_v^{m,i} + S_v^{m,i})}{L_6^i L_7^i (L_5^i + \phi k_2^{m,i} I_H^{m,i})^2}, \\
 J_{4,2}^m &= \frac{\phi^2 \alpha_H^i \gamma_H^i}{L_2^i L_3^i L_4^i}, & J_{7,5}^m &= \frac{\phi^2 \alpha_v^i k_2^{m,i} I_H^{m,i}}{L_6^i L_7^i (L_5^i + \phi k_2^{m,i} I_H^{m,i})}, \\
 J_{4,3}^m &= \frac{\phi \gamma_H^i}{L_3^i L_4^i}, & J_{7,6}^m &= \frac{\phi \alpha_v^i}{L_6^i L_7^i}, \\
 & & J_{7,7}^m &= \frac{1}{L_7^i}
 \end{aligned}$$

At the disease free equilibrium,  $E_{0,i}^m = (N_H^{m,i}, 0, 0, 0, N_v^{m,i}, 0, 0)$ , the Jacobian matrix

becomes

$$J_{E_o}^m = \begin{bmatrix} \frac{1}{L_1^i} & 0 & 0 & 0 & 0 & 0 & -\frac{\phi k_1^{m,i} N_H^{m,i} (\phi \nu_H^i + 1)}{(L_1^i)^2} \\ 0 & \frac{1}{L_2^i} & 0 & 0 & 0 & 0 & \frac{\phi k_1^{m,i} N_H^{m,i} (\phi \nu_H^{m,i} + 1)}{L_2^i L_1^i} \\ 0 & \frac{\phi \alpha_H^i}{L_2^i L_3^i} & \frac{1}{L_3^i} & 0 & 0 & 0 & \frac{\phi^2 \alpha_H^i k_1^{m,i} N_H^{m,i} (\phi \nu_H^i + 1)}{L_2^i L_3^i L_1^i} \\ 0 & \frac{\phi^2 \alpha_H^i \gamma_H^i}{L_2^i L_3^i L_4^i} & \frac{\phi \gamma_H^i}{L_3^i L_4^i} & \frac{1}{L_4^i} & 0 & 0 & \frac{\phi^3 \alpha_H^i \gamma_H^i k_1^{m,i} N_H^{m,i} (\phi \nu_H^i + 1)}{L_2^i L_3^i L_4^i L_1^i} \\ 0 & 0 & -\frac{\phi k_2^{m,i} N_v^{m,i} (\phi \nu_v^i + 1)}{(L_5^i)^2} & 0 & \frac{1}{L_5^i} & 0 & 0 \\ 0 & 0 & \frac{\phi k_2^{m,i} N_v^{m,i} (\phi \nu_v^i + 1)}{L_6^i L_5^i} & 0 & 0 & \frac{1}{L_6^i} & 0 \\ 0 & 0 & \frac{\phi^2 \alpha_v^i k_2^{m,i} N_v^{m,i} (\phi \nu_v^i + 1)}{L_6^i L_7^i L_5^i} & 0 & 0 & \frac{\phi \alpha_v^i}{L_6^i L_7^i} & \frac{1}{L_7^i} \end{bmatrix}.$$

Finding the eigenvalues of the Jacobian matrix is to cumbersome. However, we can find the eigenvalues numerically using the set of parameters presented in table 1.3.1 and the initial condition of patch 1 with  $b_v^1 = 0.38$ . The basic reproduction number  $R_{0,1} = 0.57855$  and the disease free equilibrium point is  $E_{0,1} = (13031020, 0, 0, 0, 9000000, 0, 0)$ . The eigenvalues are as follows;



$$\begin{bmatrix} 0.999978082431974 + 0.0000000000000000i \\ 0.999978082431974 + 0.0000000000000000i \\ 0.884417314275595 + 0.0000000000000000i \\ 0.740471581762740 + 0.0000000000000000i \\ 0.844622231515447 + 0.114367304538911i \\ 0.844622231515447 - 0.114367304538911i \\ 0.980520626808754 + 0.0000000000000000i \end{bmatrix}.$$

The modulus of largest eigenvalue is 0.999978082431974 which is less than one. The disease free equilibrium point is stable.

**Theorem 3.3.2** *The endemic equilibrium of the system (3.2.1),  $E_{e,i}^m$ , is unconditionally locally asymptotically stable if  $R_{0,i} > 1$ .*

Proof. We can find the eigenvalues numerically using the set of parameters presented in table 1.3.1 and the initial conditions of patch 2. The corresponding basic reproduction

number is  $R_{0,2} = 2.0802$  and endemic equilibrium point is

$E_{e,2}^m = (1344471.44, 578.29, 578.22, 4471372.05, 29995208.94, 2771.4, 2019.66)$ . Evaluating the jacobian matrix (3.3.7) at the endemic equilibrium point  $E_{e,2}^m$  with  $\phi(\ell) = \ell = 0.5$  we obtain

$$J_{E_{e,2}^m}^m = \begin{bmatrix} 0.99981 & 0.00000 & 0.00000 & 0.00000 & 0.00000 & 0.00000 & -0.02424 \\ 0.00014 & 0.85516 & 0.00000 & 0.00000 & 0.00000 & 0.00000 & 0.02073 \\ 0.00002 & 0.12385 & 0.85516 & 0.00000 & 0.00000 & 0.00000 & 0.00300 \\ 0.00000 & 0.02097 & 0.14482 & 0.99998 & 0.00000 & 0.00000 & 0.00051 \\ 0.00000 & 0.00000 & -1.91264 & 0.00000 & 0.88448 & 0.00000 & 0.00000 \\ 0.00000 & 0.00000 & 1.76419 & 0.00000 & 0.00002 & 0.81583 & 0.00000 \\ 0.00000 & 0.00000 & 0.14849 & 0.00000 & 0.00000 & 0.06867 & 0.88450 \end{bmatrix},$$

With the following sets of eigenvalues

$$\begin{bmatrix} 0.999978100623357 + 0.0000000000000000i \\ 0.726275511712589 + 0.0000000000000000i \\ 0.842167836818293 + 0.131572900108535i \\ 0.842167836818293 - 0.131572900108535i \\ 0.999916330807311 + 0.002542406511835i \\ 0.999916330807311 - 0.002542406511835i \\ 0.884502168340660 + 0.0000000000000000i \end{bmatrix}.$$

The modulus of largest eigenvalue is 0.999978100623357 which is less than one. The endemic equilibrium point is stable. Readers may note that the Euler's method for the

model (1.3.3) reads

$$\left. \begin{aligned} \frac{S_H^{m+1,i} - S_H^{m,i}}{\ell} &= \nu_H^i N_H^{m,i} - k_1^{m,i} I_v^{m,i} S_H^{m,i} - \mu_H^i S_H^{m,i}, \\ \frac{E_H^{m+1,i} - E_H^{m,i}}{\ell} &= k_1^{m,i} I_v^{m,i} S_H^{m,i} - \alpha_H^i E_H^{m,i} - \mu_H^i E_H^{m,i}, \\ \frac{I_H^{m+1,i} - I_H^{m,i}}{\ell} &= \alpha_H^i E_H^{m,i} - \gamma_H^i I_H^{m,i} - \mu_H^i I_H^{m,i}, \\ \frac{R_H^{m+1,i} - R_H^{m,i}}{\ell} &= \gamma_H^i I_H^{m,i} - \mu_H^i R_H^{m,i}, \\ \frac{S_v^{m+1,i} - S_v^{m,i}}{\ell} &= \nu_v^i N_v^{m,i} - k_2^{m,i} I_H^{m,i} S_v^{m,i} - \mu_v^i S_v^{m,i}, \\ \frac{E_v^{m+1,i} - E_v^{m,i}}{\ell} &= k_2^{m,i} I_H^{m,i} S_v^{m,i} - \alpha_v^i E_v^{m,i} - \mu_v^i E_v^{m,i}, \\ \frac{I_v^{m+1,i} - I_v^{m,i}}{\ell} &= \alpha_v^i E_v^{m,i} - \mu_v^i I_v^{m,i}, \end{aligned} \right\}, \quad (3.3.8)$$

where  $N_H^{m,i} = S_H^{m,i} + E_H^{m,i} + I_H^{m,i} + R_H^{m,i}$ ,  $N_v^{m,i} = S_v^{m,i} + E_v^{m,i} + I_v^{m,i}$  and  $\ell$  is the step-size. The explicit form takes the following form;

$$\left. \begin{aligned} S_H^{m+1,i} &= S_H^{m,i} + \ell(\nu_H^i N_H^{m,i} - k_1^{m,i} I_v^{m,i} S_H^{m,i} - \mu_H^i S_H^{m,i}), \\ E_H^{m+1,i} &= E_H^{m,i} + \ell(k_1^{m,i} I_v^{m,i} S_H^{m,i} - \alpha_H^i E_H^{m,i} - \mu_H^i E_H^{m,i}), \\ I_H^{m+1,i} &= I_H^{m,i} + \ell(\alpha_H^i E_H^{m,i} - \gamma_H^i I_H^{m,i} - \mu_H^i I_H^{m,i}), \\ R_H^{m+1,i} &= R_H^{m,i} + \ell(\gamma_H^i I_H^{m,i} - \mu_H^i R_H^{m,i}), \\ S_v^{m+1,i} &= S_v^{m,i} + \ell(\nu_v^i N_v^{m,i} - k_2^{m,i} I_H^{m,i} S_v^{m,i} - \mu_v^i S_v^{m,i}), \\ E_v^{m+1,i} &= E_v^{m,i} + \ell(k_2^{m,i} I_H^{m,i} S_v^{m,i} - \alpha_v^i E_v^{m,i} - \mu_v^i E_v^{m,i}), \\ I_v^{m+1,i} &= I_v^{m,i} + \ell(\alpha_v^i E_v^{m,i} - \mu_v^i I_v^{m,i}). \end{aligned} \right\} \quad (3.3.9)$$

In the next chapter we perform some numerical simulations of the NSFD methods and compare with the numerical results obtained by the Euler method.

# Chapter 4

## Simulation results and discussions

In this chapter, we present extensive numerical simulation results to demonstrate the effectiveness of proposed numerical method and to see whether it gives the results that correspond to our theoretical results. We also present some comparisons with the results obtained by some classical methods such as Euler and RK4. We present tables showing the spectral radii of the jacobian matrices at the equilibrium points of the system for different step-sizes  $\ell$  to study the convergence of the numerical methods (Euler method, method NSFD-I and NSFD-II) to the fixed points of the system. It is however very important to first note the impact of a cyclical death rate discussed in Section (1.3.3) on the basic reproduction number  $R_{0,i}$  and on the convergence of the numerical method to the fixed points of the system. The cyclical death rates implies that the basic reproduction number  $R_{0,i}$  will not remain the same throughout of the year, it will be higher in summer and lower in winter due to the change of the vector population density. Figure 4 of [57] shows that the mosquito population is higher between January and June and lower between July and December for patch 1 while for patch 2 is vice versa. From these observations, it can then be noted the numerical methods will fail to converge to any fixed point on the system due to the fact that the susceptible vector population will go up and down between the seasons. Using the NSFD-II with the parameters in Table 1.3.1, Figure 4.0.1 shows that the basic reproduction number  $R_0$  will not remain constant throughout the year but change with the change in the

population of the vectors for patch 1 and 2, and these results are consistent with the findings in [57]. As highlighted in [57], the fact that the natural death rate for the

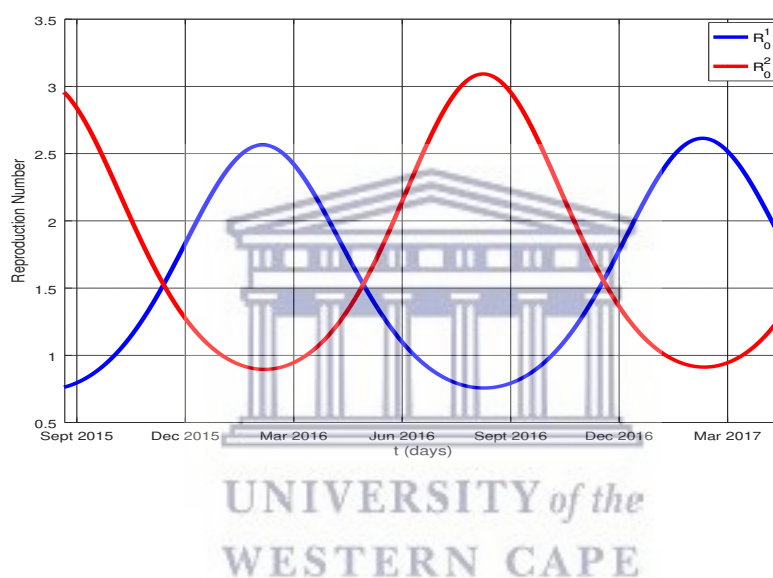


Figure 4.0.1 The basic reproduction number  $R_0$  obtained by method NSFD-II for patch 1 and 2 with a cyclical death rate  $\mu_v^i$  and  $\ell = 1$ .

mosquito population is cyclical, it makes it very difficult to proceed with the analysis of the behaviour of the numerical methods at the equilibrium points. In order to carry out this work, we take the assumption of a constant vector population for both patches throughout the year by taking both the natural birth rate  $\mu_v^i$  and death rate  $\nu_v^i$  to be the average between  $\mu_{v,min}^i$  and  $\mu_{v,max}^i$ .

In order to study the convergence of the numerical methods to the disease free equilibrium points  $E_{0,i}$ , we use the reduced value  $b_v^i = 0.38$  which is chosen in such a way that it captures the presence of the two mosquito species (*Aedes aegypti* and *Aedes*



albopictus) that are responsible for the transmission of Zika virus. This reduced  $b_v^i$  is the average between the average *Aedes aegypti* and *Aedes albopictus*, see [57]. For the vector population, it can be seen from figure 4 of [57] that the vector population ranges between 9 000 000 to 130 000 000 for patch 1 and between 6 000 000 to 60 000 000 for patch 2. When the vector population is kept at minimum, that is 9 000 000 for patch 1 and 6 000 000 for patch 2, the basic reproduction number with  $b_v^i = 0.38$  is calculated to be  $R_{0,1} = 0.57855$  and  $R_{0,2} = 0.70703$  which is less than 1. With these change of parameters, we expect the numerical methods to converge to the Disease free equilibrium points.

To study the convergence of our numerical methods to the endemic equilibrium points, we take a constant vector population of 60 000 000 for patch 1 and 30 000 000 for patch 2, chosen in such a way that a reasonable mosquito presence in both region is kept in order to allow a balance interaction between the humans and vectors. In this case, with  $b_v^i = 0.5$  from the table, the basic reproduction number is  $R_{0,1} = 1.9655$  and  $R_{0,2} = 2.0802$  which is greater than 1. The basic reproduction numbers for both patches will remain the same throughout the year because of the noncyclic death rate.

In order to investigate the convergence of the numerical methods, we compute Table 4.0.1, 4.0.2, 4.0.3 and 4.0.4 below showing the spectral radii obtained from evaluating the jacobian matrices of the system 3.2.1 and 3.3.9 numerically at the fixed points for different step-sizes  $\ell$  for both patches.

With  $S_{v0} = 9000000$  for patch1 and  $S_{v0} = 6000000$  for patch 2 which is the average susceptible mosquito population, the numerical disease free equilibrium points are  $E_{0,1} = (13031020, 0, 0, 0, 9000000, 0, 0)$  and  $E_{0,2} = (5817000, 0, 0, 0, 6000000, 0, 0)$ . It can be seen from Table 4.0.1 and 4.0.2 that the Euler method will only converge to the equilibrium points for a smaller step-size, but with a large step-size, for example  $\ell = 10$  its expected to diverge. However, the NSFD methods (NSFD-I and NSFD-II)

will converge even for a large step-size of  $\ell = 100$ . To study the convergence of

Table 4.0.1 Spectral radii of the Jacobian matrix evaluated at  $E_{0,1}$  obtained by Euler, method NSFD-I and NSFD-IIs for different step-sizes  $\ell$  for patch 1 with  $b_v^1 = 0.38$  and  $N_v = 9000000$ .

$E_{0,1}$	Euler		NSFD-I		NSFD-II	
$\ell$	$\rho(h)$	Comment	$\rho(h)$	Comment	$\rho(h)$	Comment
0.001	0.99999	Converge	0.99999	Converge	0.99999	Converge
0.01	0.99999	Converge	0.99999	Converge	0.99999	Converge
0.5	0.99999	Converge	0.99999	Converge	0.99999	Converge
1	0.99998	Converge	0.99997	Converge	0.99997	Converge
5	0.99989	Converge	0.99989	Converge	0.99989	Converge
10	2.23516	Diverge	0.99978	Converge	0.99978	Converge
25	7.08790	Diverge	0.99945	Converge	0.99945	Converge
100	31.35161	Diverge	0.99781	Converge	0.99781	Converge

Table 4.0.2 Spectral radii of the Jacobian matrix evaluated at  $E_{0,2}$  obtained by Euler, method NSFD-I and NSFD-IIs for different step-sizes  $\ell$  for patch 2 with  $b_v^2 = 0.38$  and  $N_v = 6000000$ .

$E_{0,2}$	Euler		NSFD-I		NSFD-II	
$\ell$	$\rho(h)$	Comment	$\rho(h)$	Comment	$\rho(h)$	Comment
0.001	0.99999	Converge	0.99999	Converge	0.99999	Converge
0.01	0.99999	Converge	0.99999	Converge	0.99999	Converge
0.5	0.99998	Converge	0.99999	Converge	0.99999	Converge
1	0.99997	Converge	0.99997	Converge	0.99997	Converge
5	0.99989	Converge	0.99989	Converge	0.99989	Converge
10	2.43240	Diverge	0.99978	Converge	0.99978	Converge
25	7.58099	Diverge	0.99945	Converge	0.99945	Converge
100	33.32400	Diverge	0.99781	Converge	0.99781	Converge

our numerical method to the endemic equilibrium  $E_{e,i}$  for both patches, we use the parameters of Table 1.3.1 with the fixed vector population. The numerical endemic equilibrium points are

$E_{e,1} = (3373477.19, 1248.70, 1248.54, 9655045.57, 59990763.70, 5342.75, 3893.54)$  and

$E_{e,2} = (1344471.44, 578.29, 578.22, 4471372.05, 29995208.94, 2771.4, 2019.66)$  for patch

1 and 2 respectively. Table 4.0.3 and 4.0.4 shows the Euler method will fail to converge to the endemic equilibrium points  $E_{e,i}$  for even a small step-size of  $\ell = 0.001$  while the method NSFD-I and NSFD-II converge even for a larger step-size. Figures 4.0.2 and

Table 4.0.3 Spectral radii of the Jacobian matrix evaluated at  $E_{e,1}$  obtained by Euler, method NSFD-I and NSFD-IIs for different step-sizes  $\ell$  for patch 1 with  $b_v^1 = 0.5$  and  $N_v = 60000000$ .

$E_{e,1}$	Euler		NSFD-I		NSFD-II	
$\ell$	$\rho(h)$	Comment	$\rho(h)$	Comment	$\rho(h)$	Comment
0.001	1.00002	Diverge	0.99999	Converge	0.99999	Converge
0.01	1.00029	Diverge	0.99999	Converge	0.99999	Converge
0.5	1.01700	Diverge	0.99998	Converge	0.99998	Converge
1	1.03799	Diverge	0.99997	Converge	0.99997	Converge
5	1.31971	Diverge	0.99989	Converge	0.99989	Converge
10	3.22254	Diverge	0.99978	Converge	0.99978	Converge
25	9.55635	Diverge	0.99945	Converge	0.99945	Converge
100	41.22540	Diverge	0.99781	Converge	0.9781	Converge

Table 4.0.4 Spectral radii of the Jacobian matrix evaluated at  $E_{e,2}$  obtained by Euler, method NSFD-I and NSFD-IIs for different step-sizes  $\ell$  for patch 2 with  $b_v^2 = 0.5$  and  $N_v = 30000000$ .

$E_{e,2}$	Euler		NSFD-I		NSFD-II	
$\ell$	$\rho(h)$	Comment	$\rho(h)$	Comment	$\rho(h)$	Comment
0.001	1.00003	Diverge	0.99999	Converge	0.99999	Converge
0.01	1.00034	Diverge	0.99999	Converge	0.99999	Converge
0.5	1.01938	Diverge	0.99998	Converge	0.99998	Converge
1	1.04298	Diverge	0.99997	Converge	0.99997	Converge
5	1.34923	Diverge	0.99989	Converge	0.99989	Converge
10	3.26911	Diverge	0.99978	Converge	0.99978	Converge
25	9.67278	Diverge	0.99945	Converge	0.99945	Converge
100	41.69113	Diverge	0.99781	Converge	0.99781	Converge

4.0.3 show that the Euler method and method NSFD-I and NSFD-II will successfully converge to the disease free equilibrium  $E_{0,1}$  for patch 1 when the step-size is  $\ell = 0.5$ . When the step-size is increased to  $\ell = 6$ , Figure 4.0.4 and 4.0.5 shows that the Euler method generate oscillation with negative values while method NSFD-I and NSFD-II converges successfully without generating any oscillation with negative values for the same step-size.

Figures 4.0.6 and 4.0.6 show that the Euler method and method NSFD-I and NSFD-II will successfully converge to the disease free equilibrium  $E_{0,2}$  for patch 2 when the step-size is  $\ell = 0.5$ . When the step-size is increased to  $\ell = 8$ , Figure 4.0.8 and 4.0.8 shows that the Euler method generate heavy oscillation with negative values and fails

to converge to  $E_{0,2}$  while method NSFD-I and NSFD-II converges successfully without generating any oscillation with negative values for the same step-size.

Figures 4.0.10 and 4.0.11 show that the Euler method and method NSFD-I and NSFD-II will successfully converge to the endemic equilibrium point  $E_{e,1}$  for patch 1 when the step-size is  $\ell = 0.5$ . When the step-size is increased to  $\ell = 5.55$ , Figure 4.0.12 and 4.0.13 shows that the Euler method generate negative values while method NSFD-I and NSFD-II converges successfully without generating any oscillation with negative values for the same step-size.

Figures 4.0.14 and 4.0.15 show that the Euler method and method NSFD-I and NSFD-II will successfully converge to the endemic equilibrium point  $E_{e,2}$  for patch 2 when the step-size is  $\ell = 0.5$ . When the step-size is increased to  $\ell = 5.8$ , Figure 4.0.16 and 4.0.17 shows that the Euler method generate heavy oscillation with negative values and fail to converge to  $E_{e,2}$  while method NSFD-I and NSFD-II converges successfully without generating any oscillation with negative values for the same step-size.

Figures 4.0.18 and 4.0.19 show that the method NSFD-I and NSFD-IIs converges to the disease free equilibrium points  $E_{0,1}$  and  $E_{0,2}$  even for a step-size of  $\ell = 50$ . Furthermore, both numerical method produces similar results.

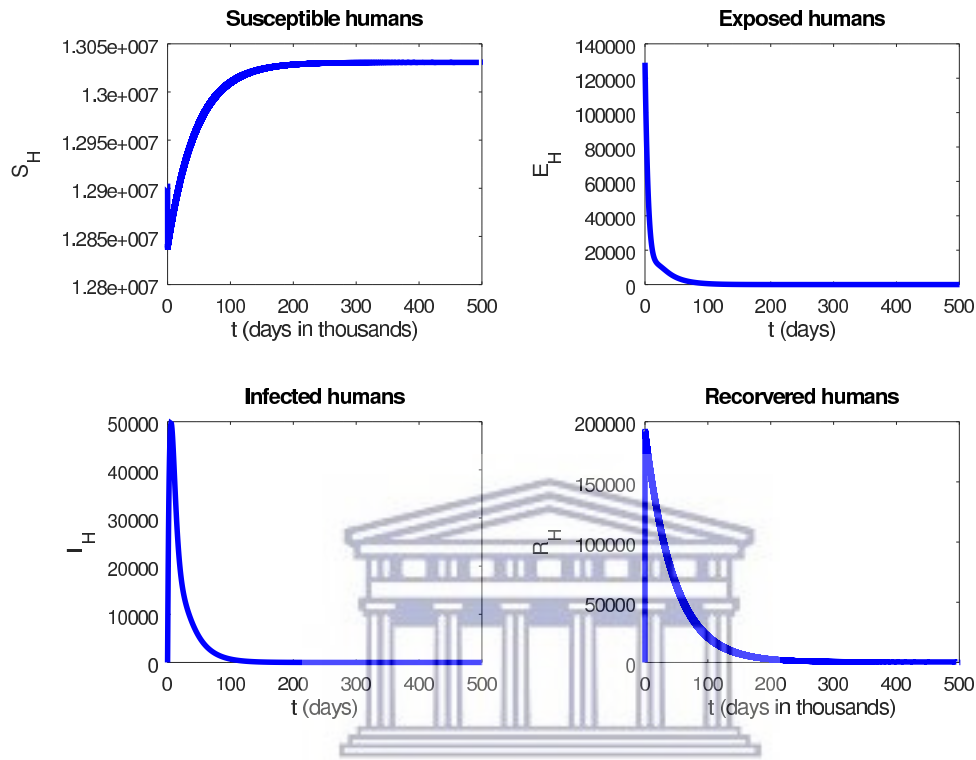
Figures 4.0.21 and 4.0.21 show that the method NSFD-I and NSFD-IIs converges to endemic equilibrium points  $E_{e,1}$  and  $E_{e,2}$  even for a big step-size of  $\ell = 1000$ .

Figures 4.0.22, 4.0.23, 4.0.24 and 4.0.25 are obtained using the parameters of Table 1.3.1 with the cyclical death rates 1.3.5 and 1.3.6 for  $\ell = 0.5$  and  $\ell = 6$ . When the parameters are not changed, Oleson observed that there is an outbreak in patch 1 that will infect almost the entire population and visitors to the Carnival will get infected and the virus with them home in Miami (patch 2) where they will course an outbreak that will infect more that 75 % of the population. It can be seen that from 4.0.22 that all the numerical method produces results identical to the ones obtained by Oleson for patch 1. Figure 4.0.23 shows that the NSFD-I and NSFD-II produces better result than the Euler method. For  $\ell = 6$ , Figure 4.0.24 and 4.0.25 shows that the Euler method produces oscillations and negative solutions while the NSFDs solution remain positive.

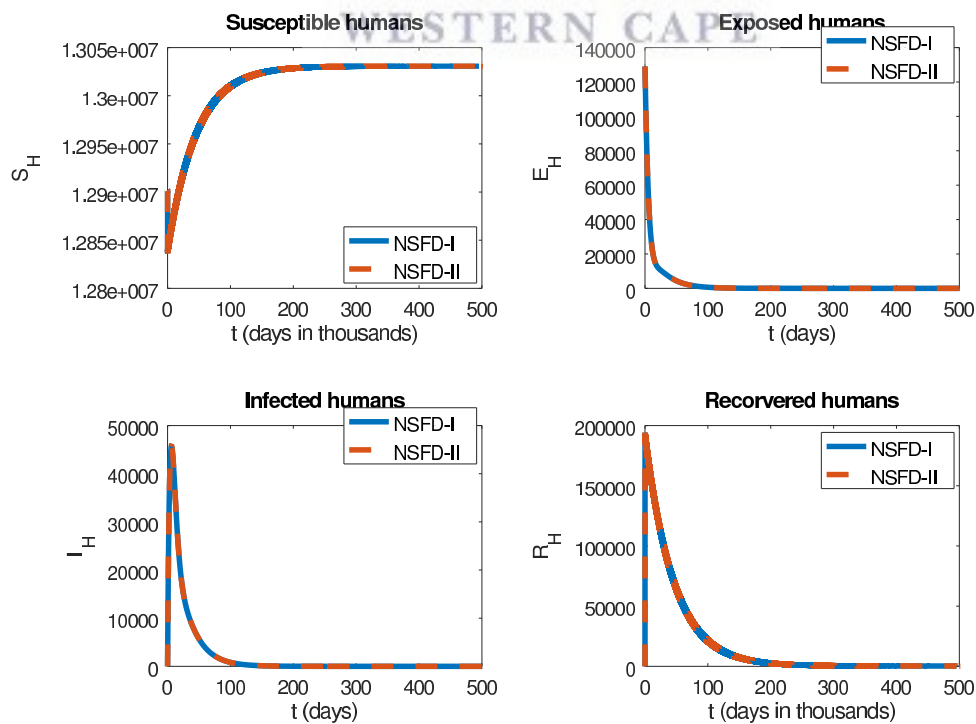
When the  $b_v^2$  is reduced from 0.5 to 0.38, Oleson observes that there will be no outbreak of the Zika virus in patch 2. Consistent with the results of Oleson, Figure 4.0.26 shows that according to the NSFD-I and NSFD-II less than 500 people will be infected by the virus before it dies out, whereas the Euler method produces heavy oscillation and negative solutions.

In the next chapter, we indicate some scope for further research.





(a)



(b)

Figure 4.0.2 Profiles of solutions generated by Euler method (a) and by method NSFD-I and NSFD-II (b) for the human population of patch 1 with  $R_{0,1} = 0.57855$  and  $\ell = 0.5$ .

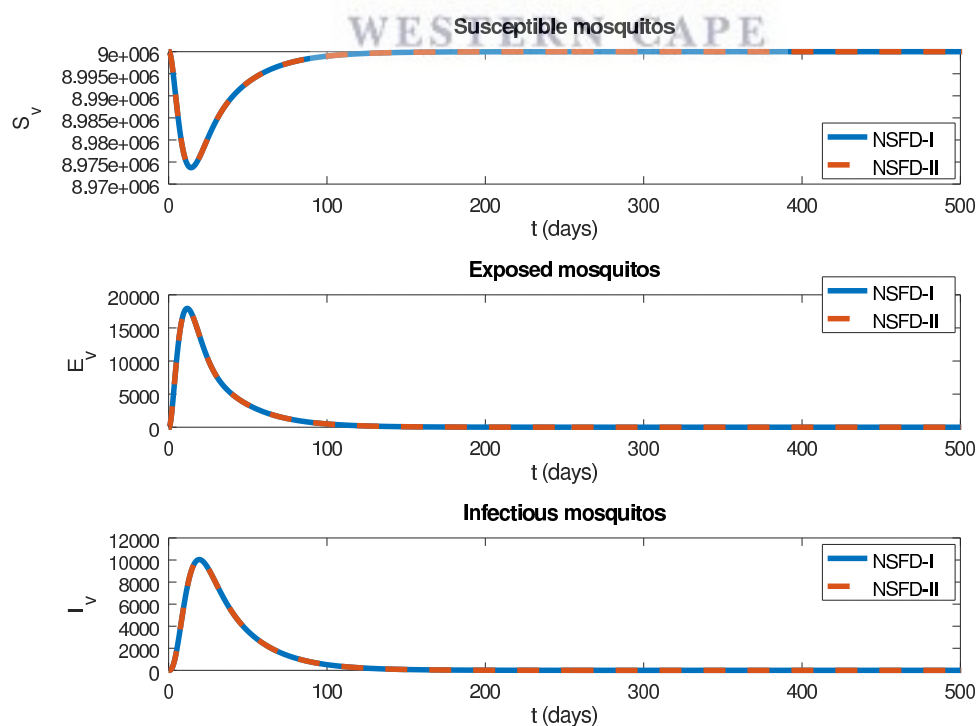
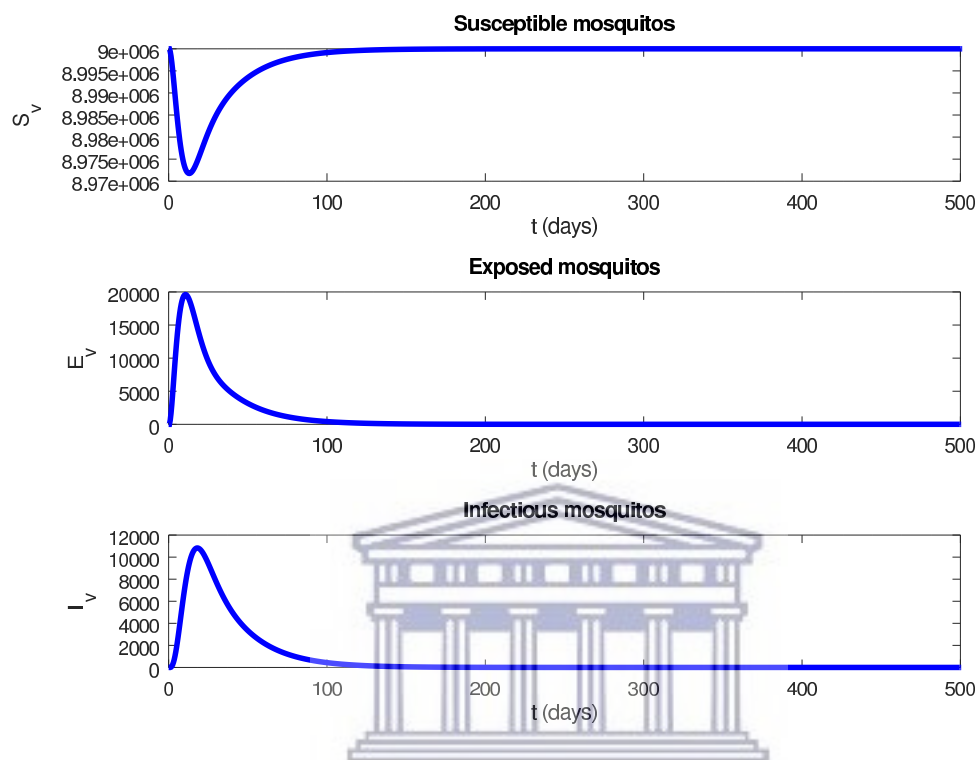
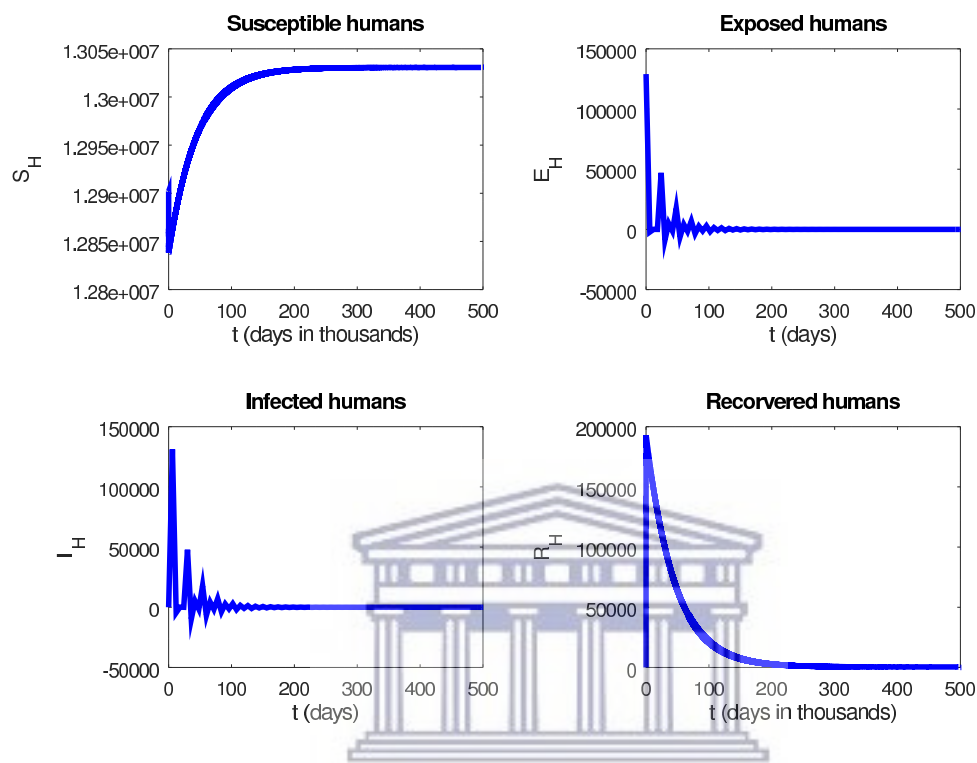
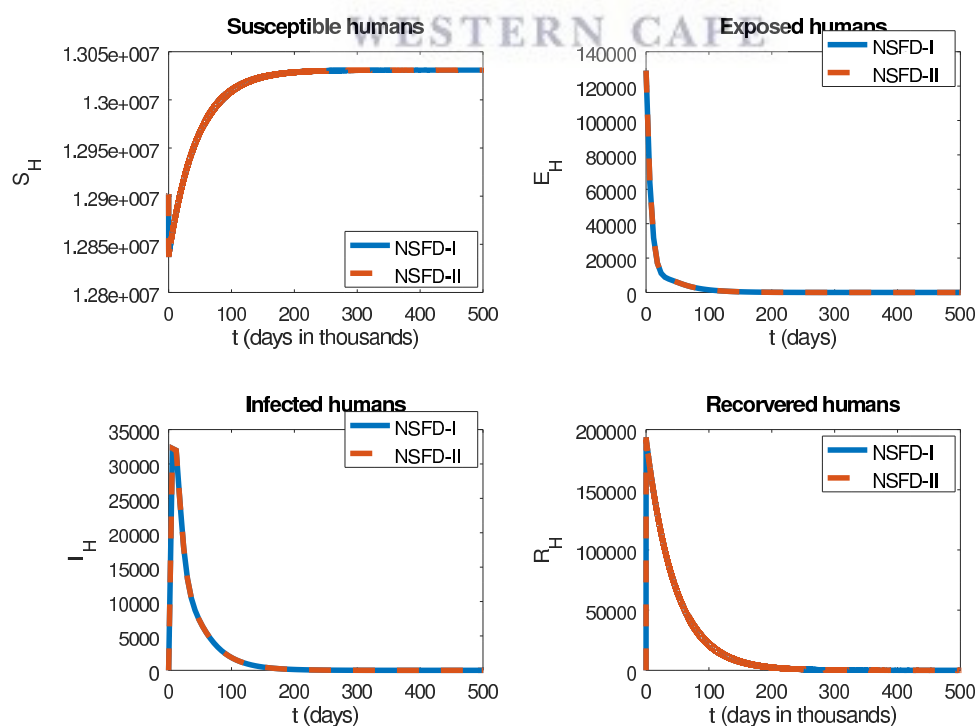


Figure 4.0.3 Profiles of solutions generated by Euler method (a) and by method NSFD-I and NSFD-II (b) for the vector population of patch 1 with  $R_{0,1} = 0.57855$  and  $\ell = 0.5$ .



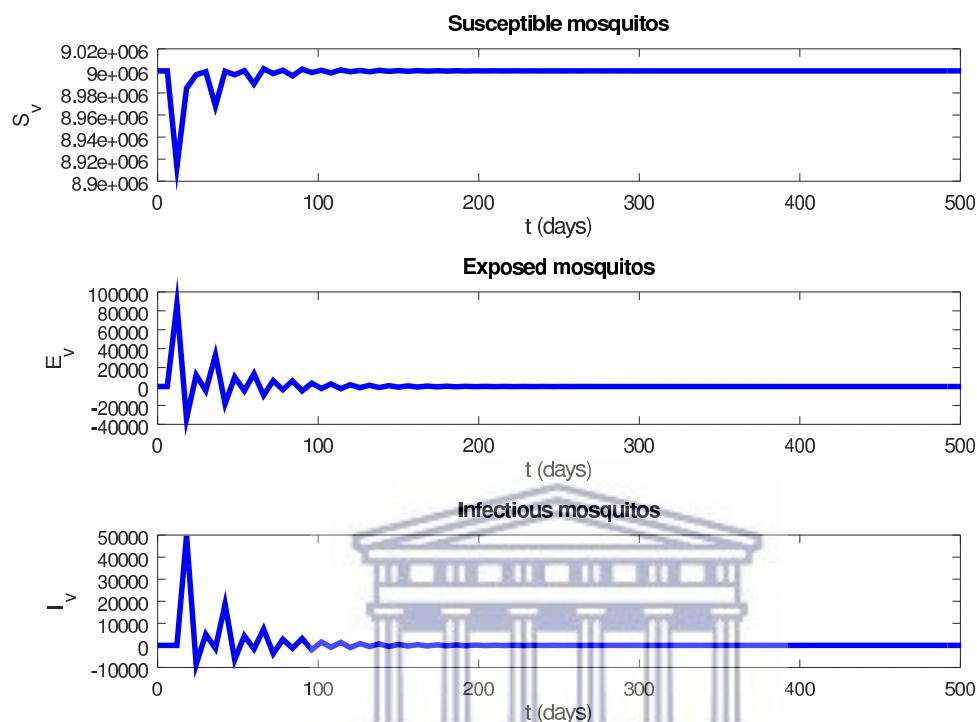
(a)



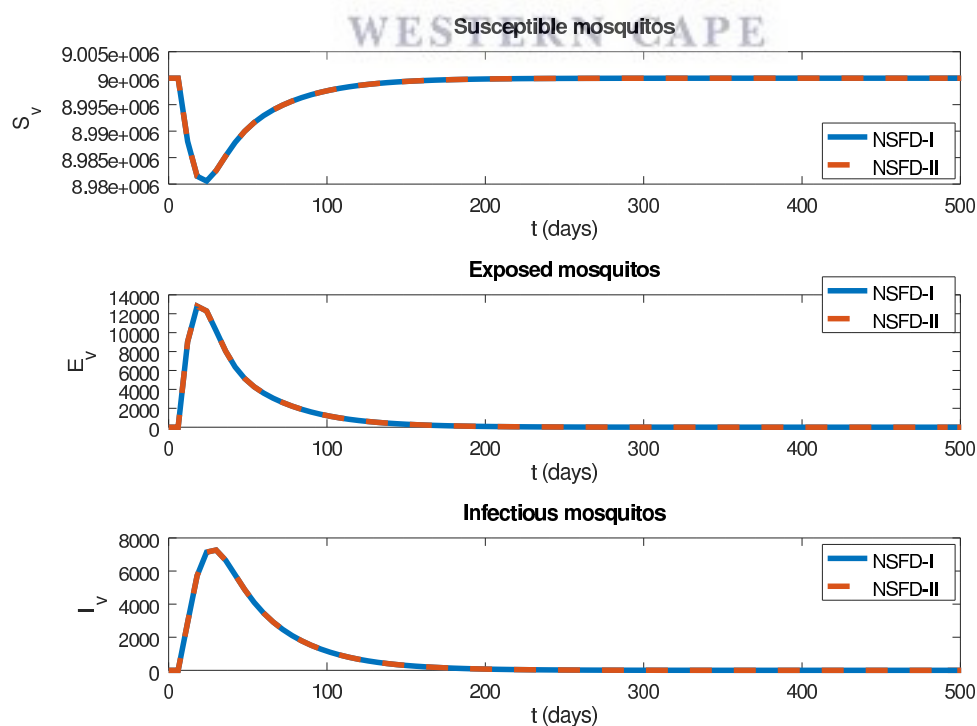
(b)

Figure 4.0.4 Profiles of solutions generated by Euler method (a) and by method NSFD-I and NSFD-II (b) for the human population of patch 1 with  $R_{0,1} = 0.57855$  and  $\ell = 6$ .



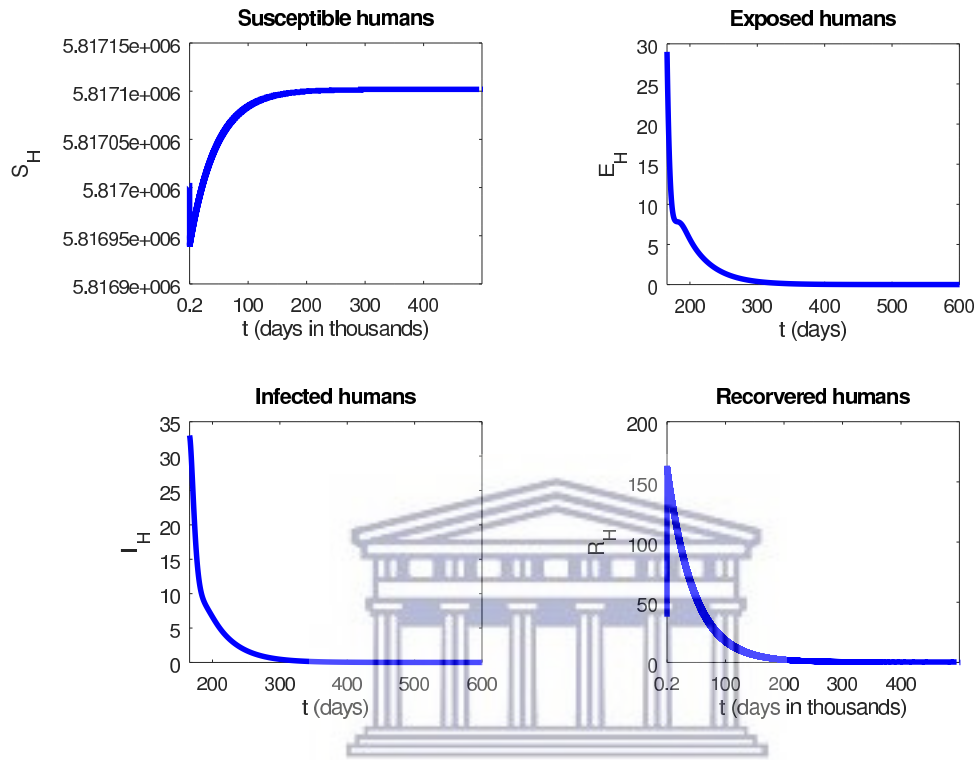


(a)

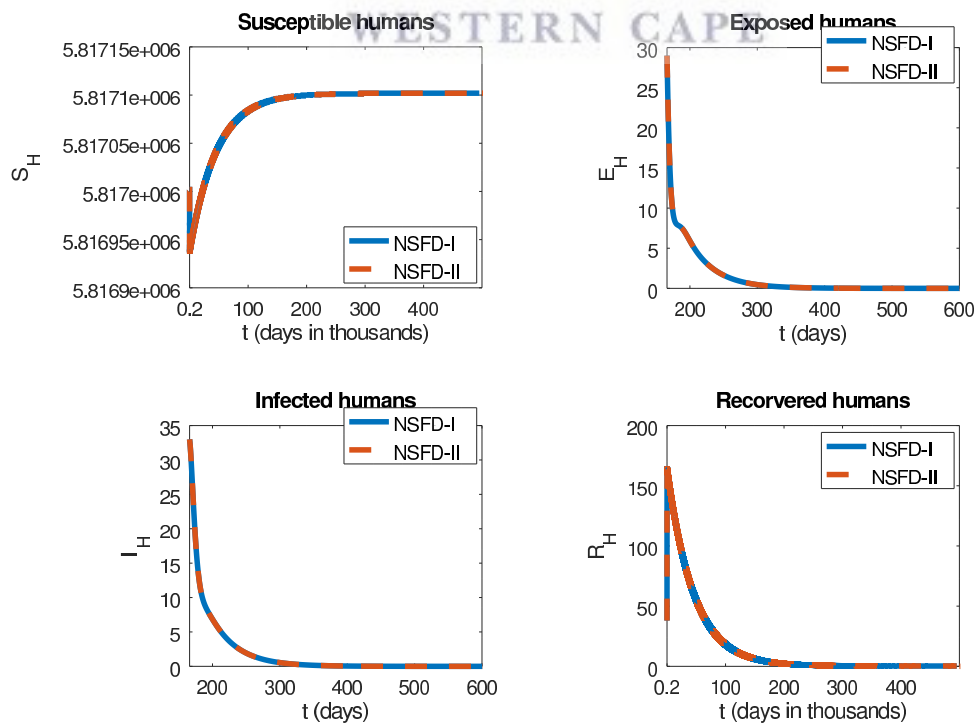


(b)

Figure 4.0.5 Profiles of solutions generated by Euler method (a) and by method NSFD-I and NSFD-II (b) for the vector population of patch 1 with  $R_{0,1} = 0.57855$  and  $\ell = 6$ .

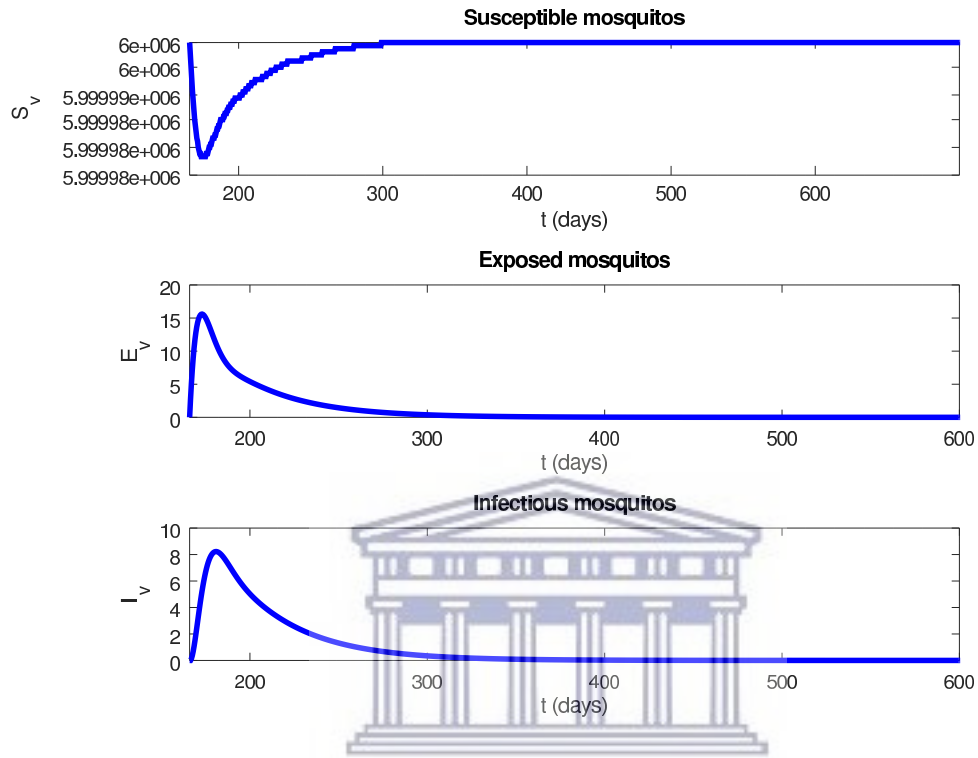


(a)

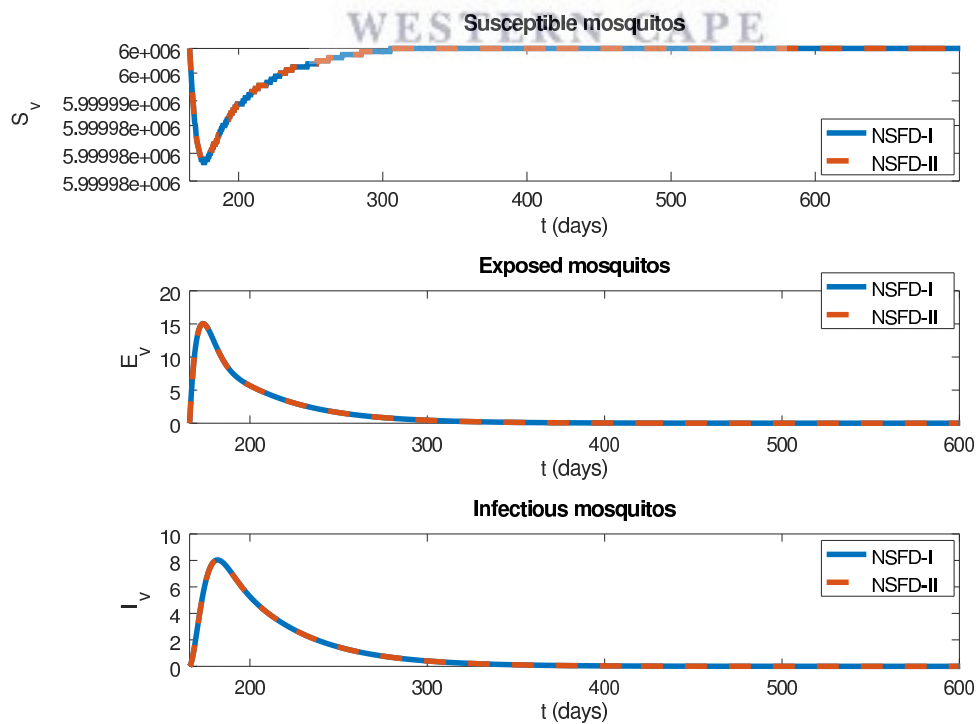


(b)

Figure 4.0.6 Profiles of solutions generated by Euler method (a) and by method NSFD-I and NSFD-II (b) for the human population of patch 2 with  $R_{0,2} = 0.70703$  and  $\ell = 0.5$ .

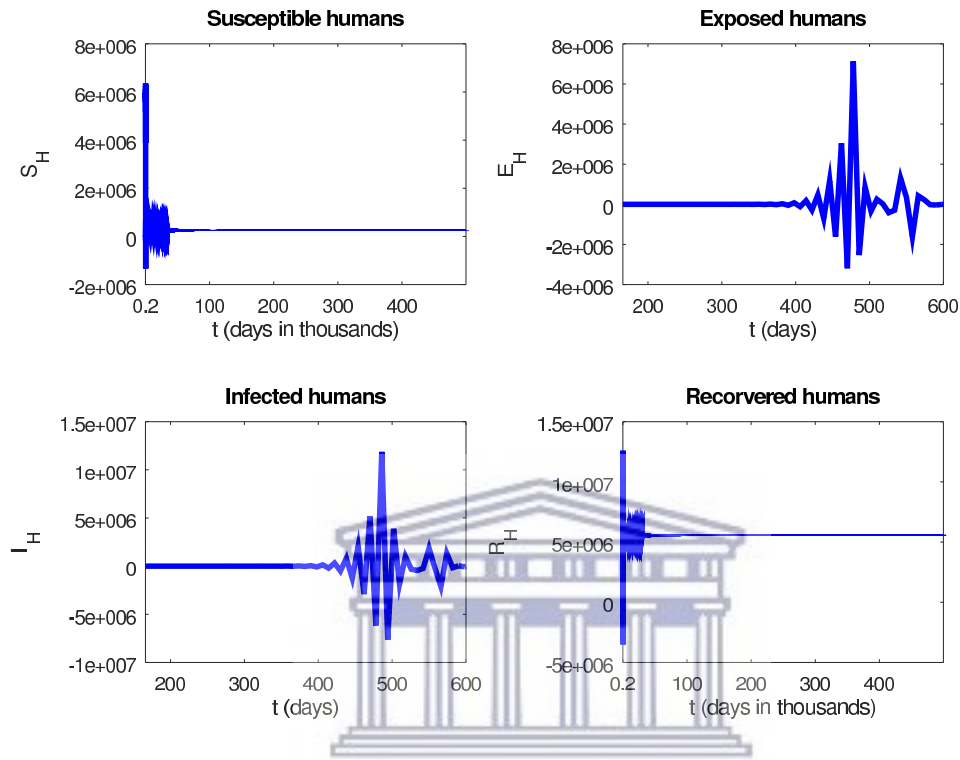


(a)

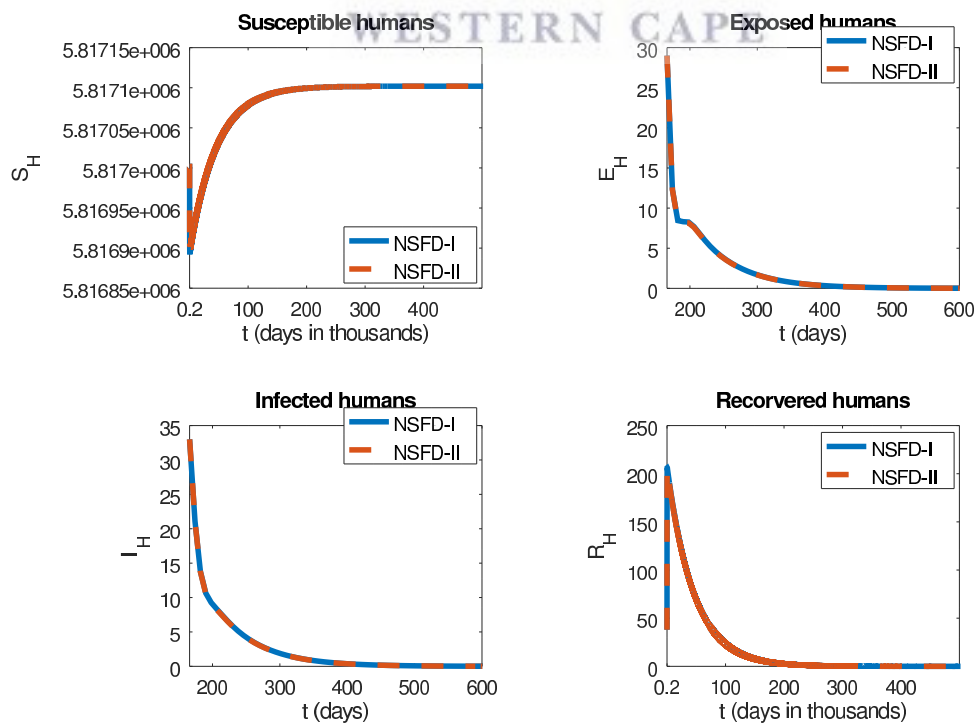


(b)

Figure 4.0.7 Profiles of solutions generated by Euler method (a) and by method NSFD-I and NSFD-II (b) for the vector population of patch 2 with  $R_{0,2} = 0.70703$  and  $\ell = 0.5$ .

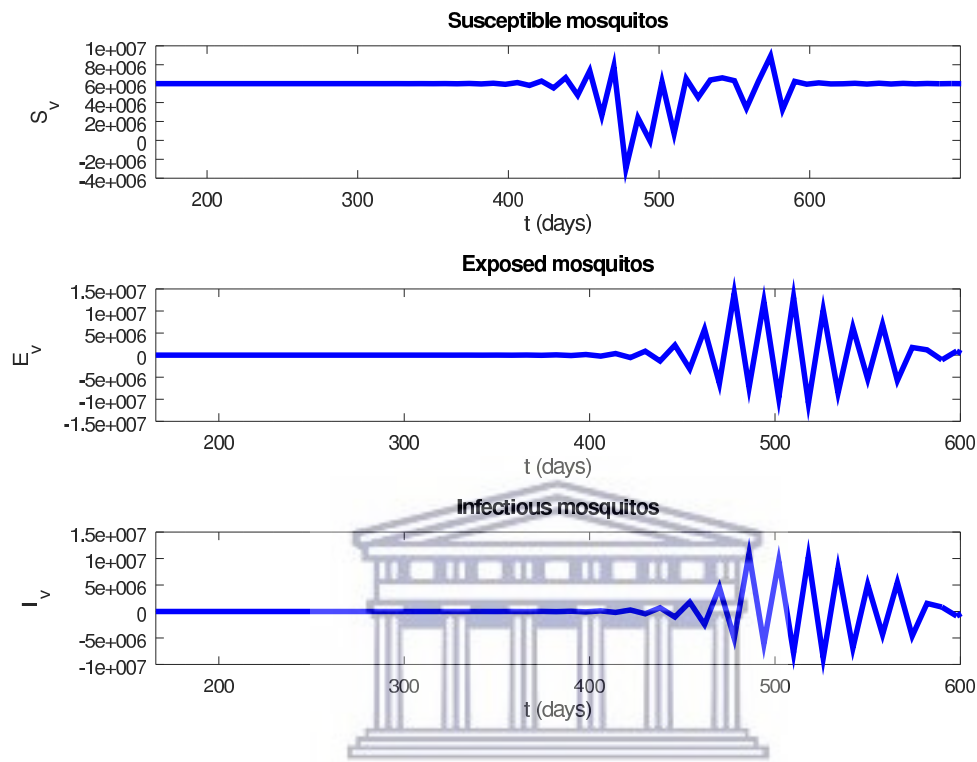


(a)

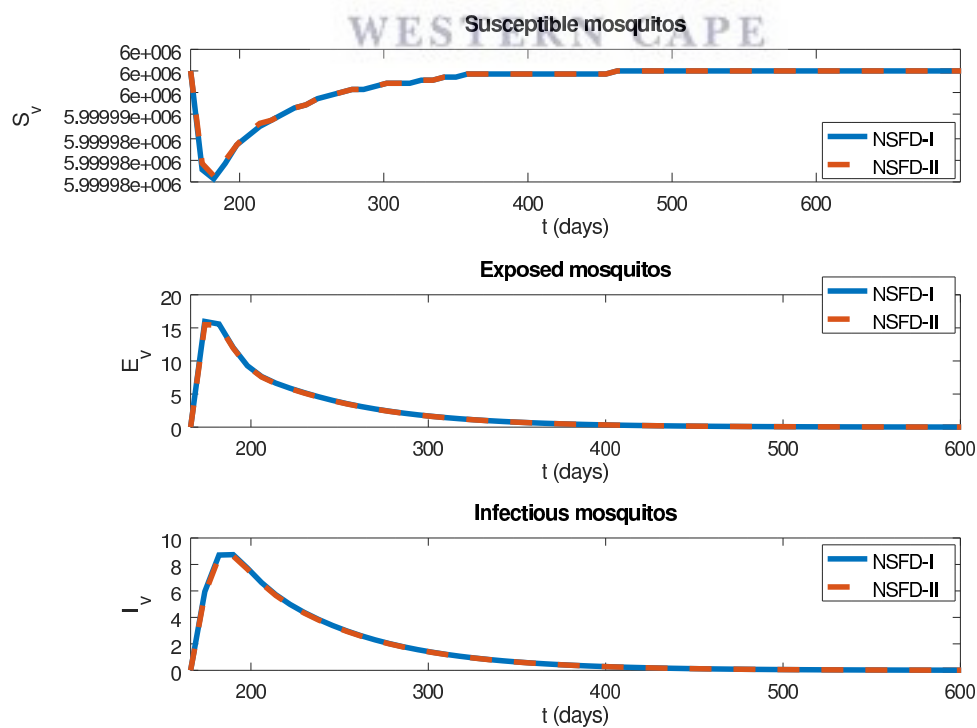


(b)

Figure 4.0.8 Profiles of solutions generated by Euler method (a) and by method NSFD-I and NSFD-II (b) for the human population of patch 2 with  $R_{0,2} = 0.70703$  and  $\ell = 8$ .



(a)



(b)

Figure 4.0.9 Profiles of solutions generated by Euler method (a) and by method NSFD-I and NSFD-II (b) for the vector population of patch 2 with  $R_{0,2} = 0.70703$  and  $\ell = 8$ .

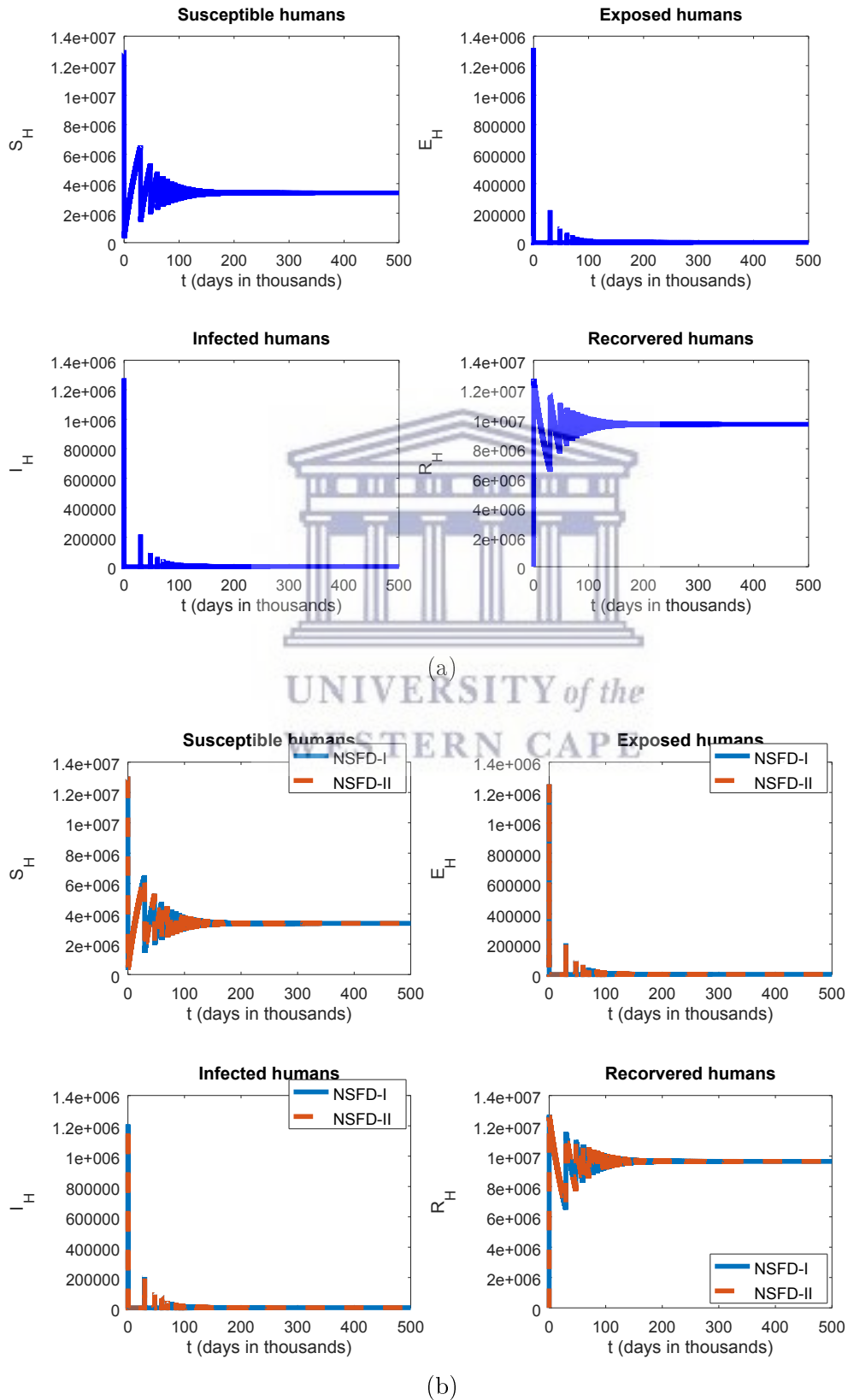
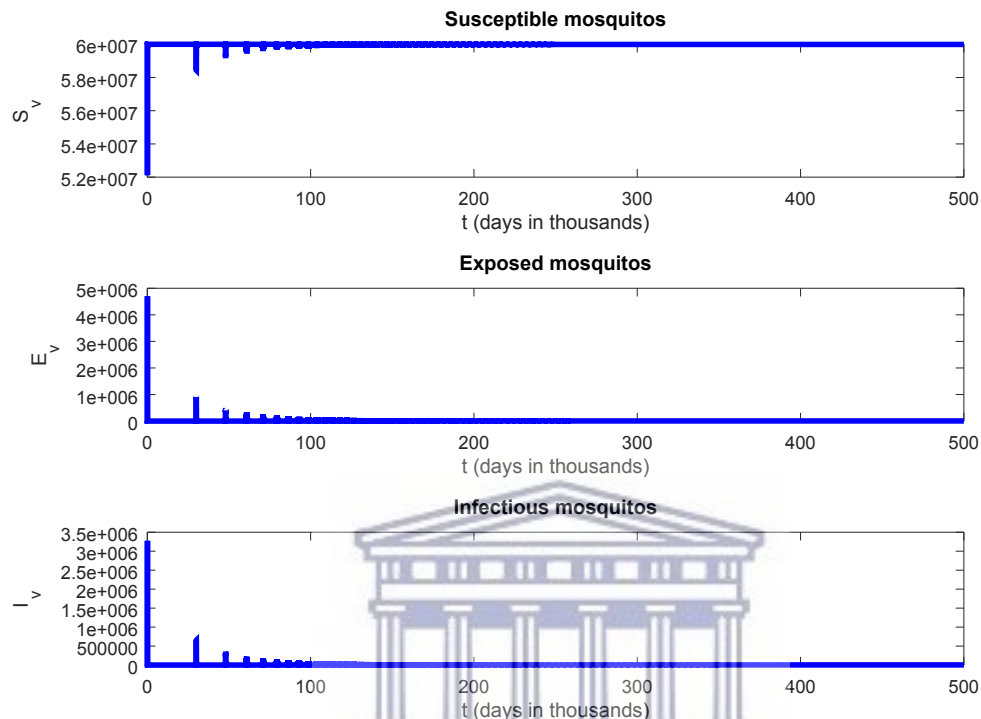
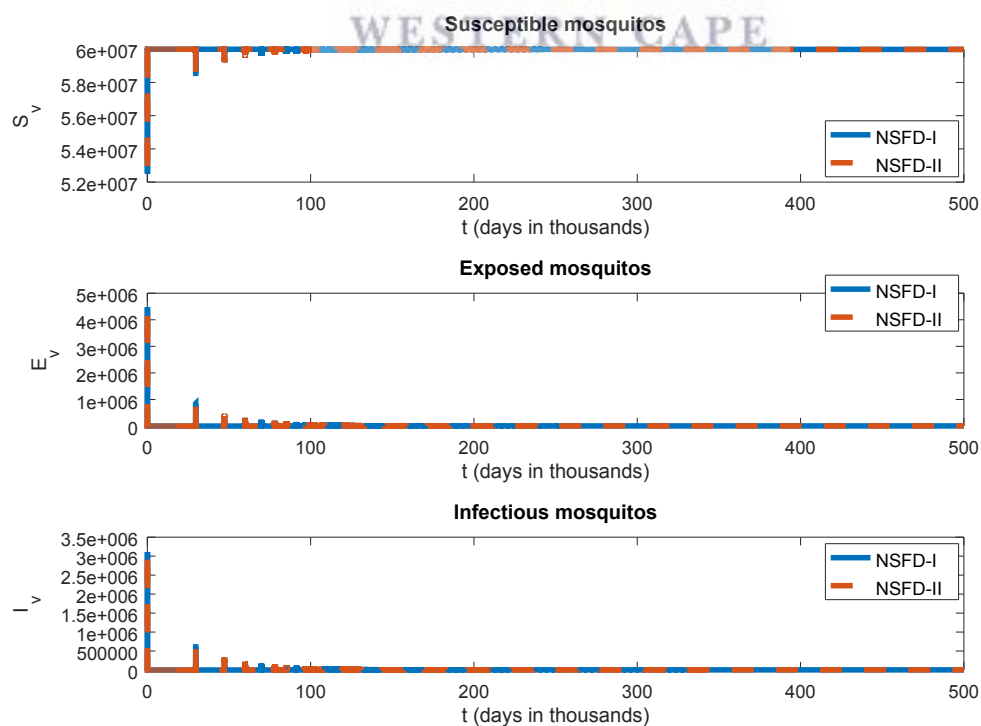


Figure 4.0.10 Profiles of solutions generated by Euler method (a) and by method NSFD-I and NSFD-II (b) for the human population of patch 1 with  $R_{0,1} = 1.9655$  and  $\ell = 0.5$ .

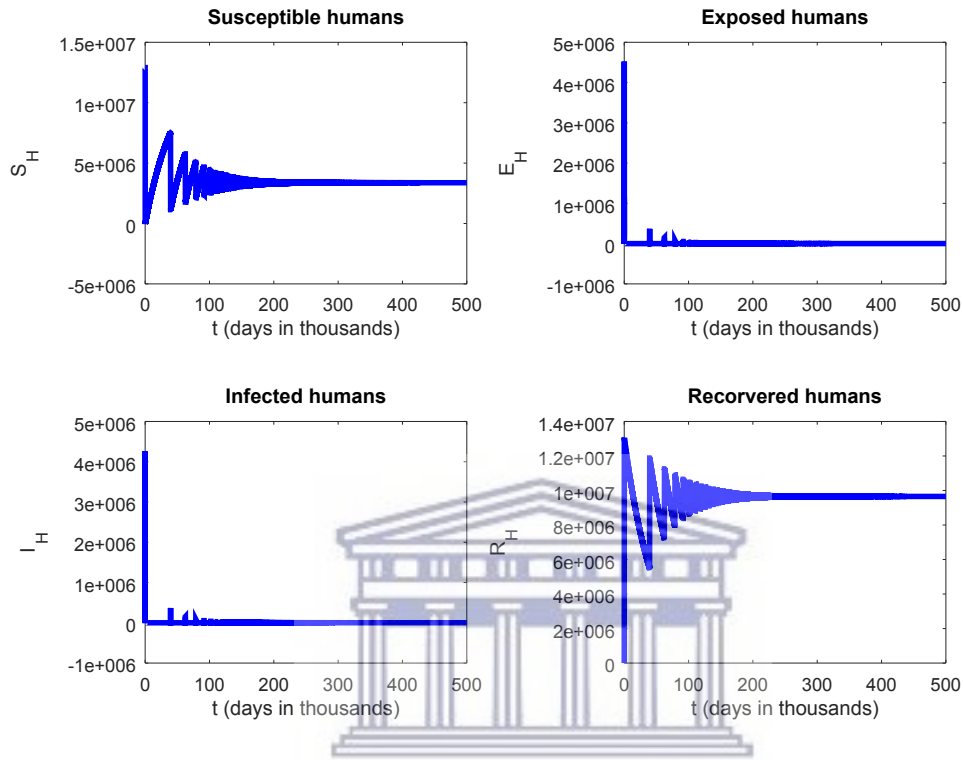


(a)

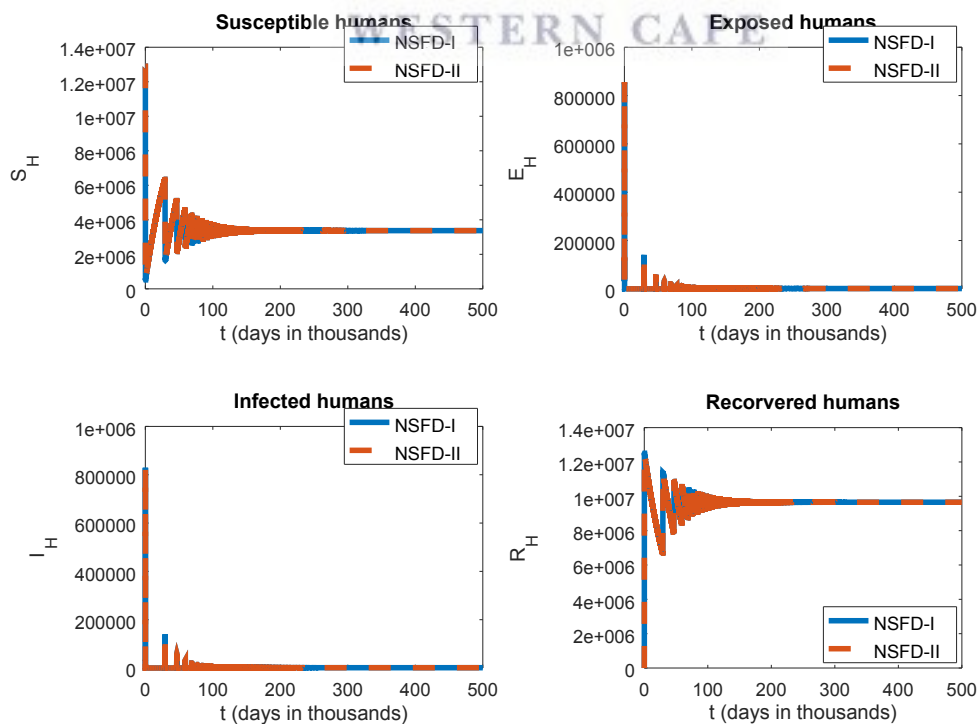


(b)

Figure 4.0.11 Profiles of solutions generated by Euler method (a) and by method NSFD-I and NSFD-II (b) for the vector population of patch 1 with  $R_{0,1} = 1.9655$  and  $\ell = 0.5$ .



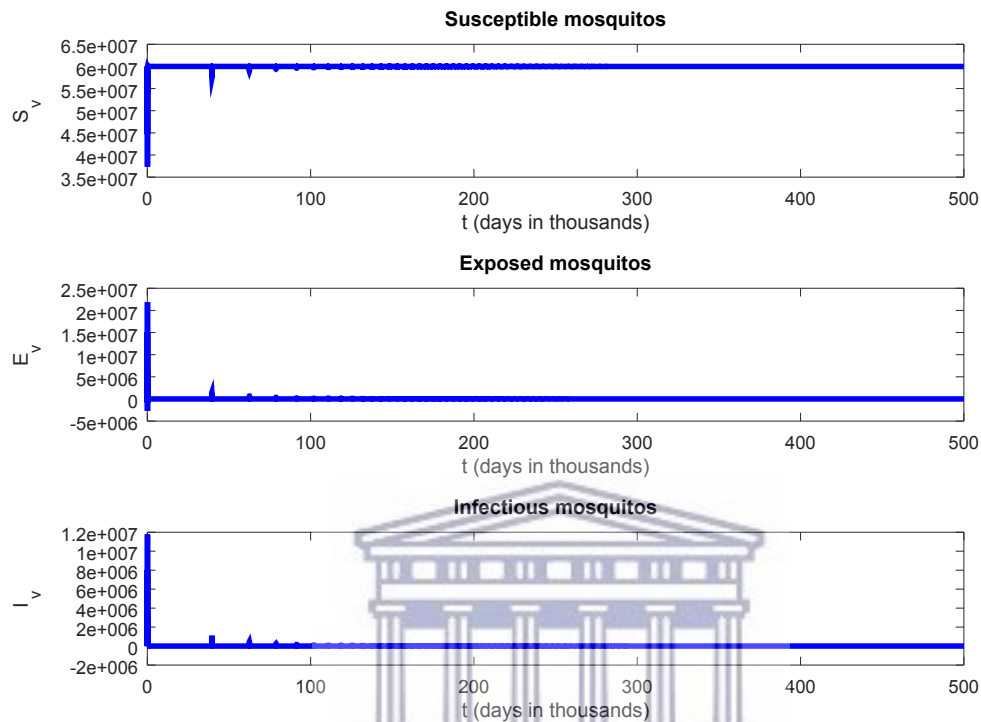
(a)



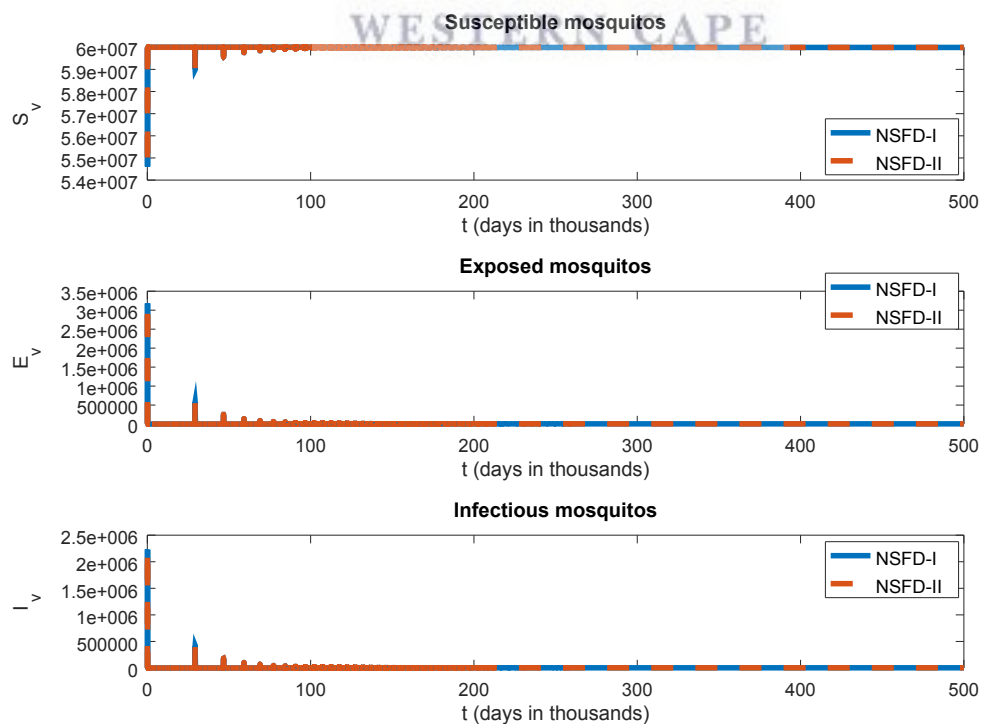
(b)

Figure 4.0.12 Profiles of solutions generated by Euler method (a) and by method NSFD-I and NSFD-II (b) for the human population of patch 1 with  $R_{0,1} = 1.9655$  and  $\ell = 5.55$ .





(a)



(b)

Figure 4.0.13 Profiles of solutions generated by Euler method (a) and by method NSFD-I and NSFD-II (b) for the vector population of patch 1 with  $R_{0,1} = 1.9655$  and  $\ell = 5.55$ .

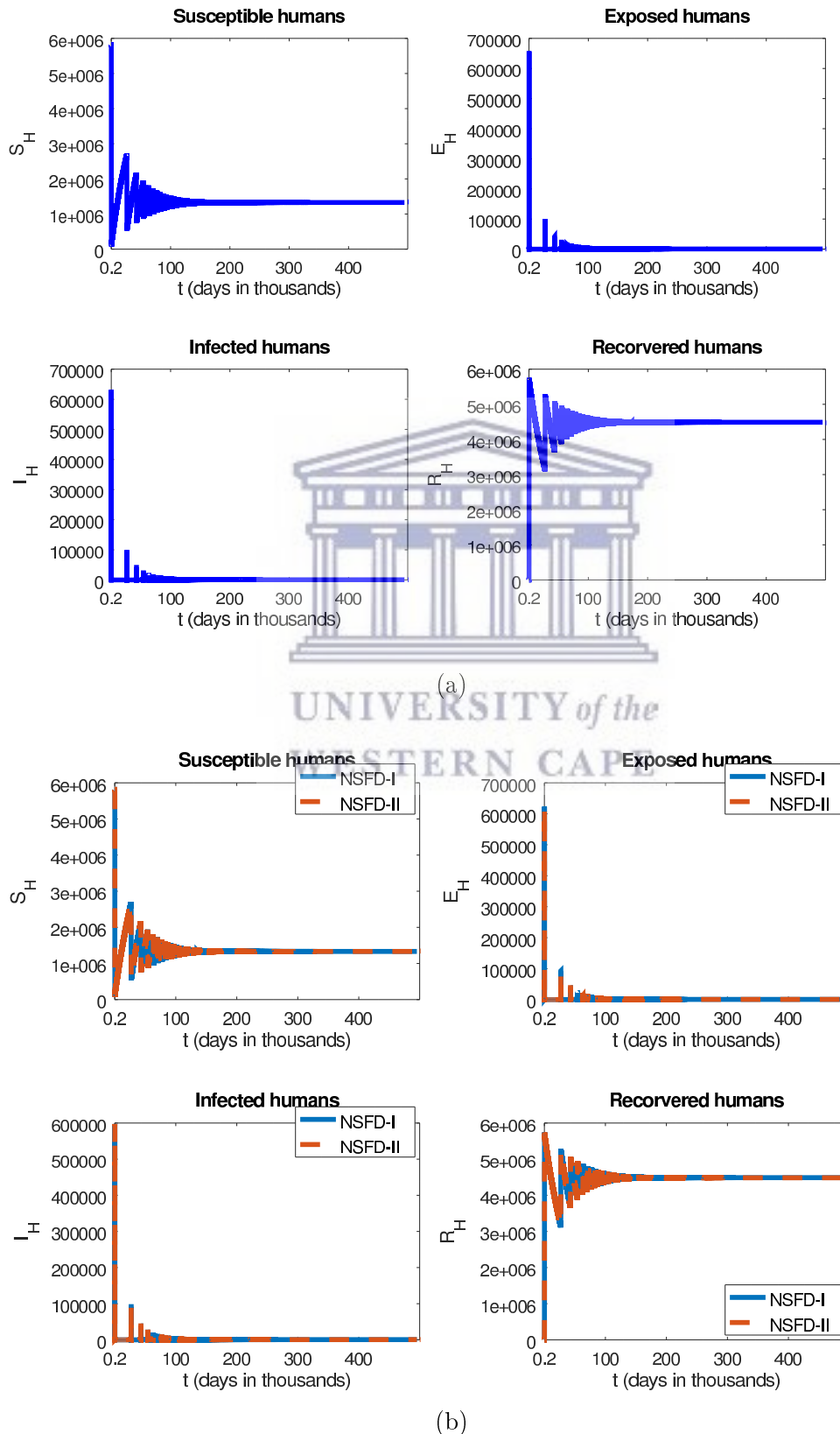
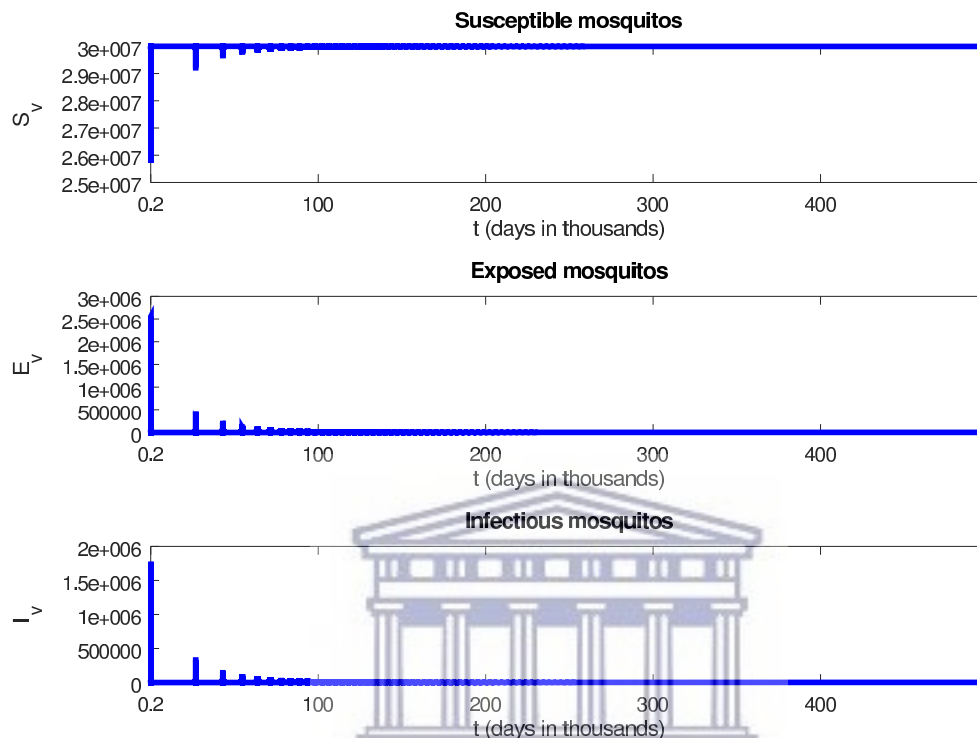
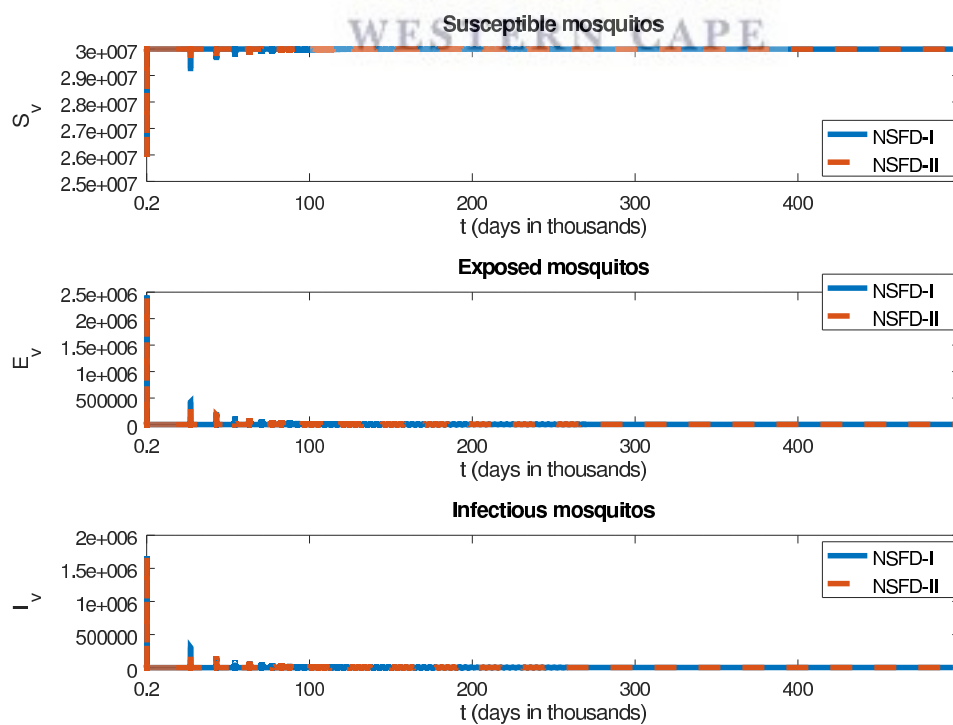


Figure 4.0.14 Profiles of solutions generated by Euler method (a) and by method NSFD-I and NSFD-II (b) for the human population of patch 2 with  $R_{0,1} = 2.0802$  and  $\ell = 0.5$ .

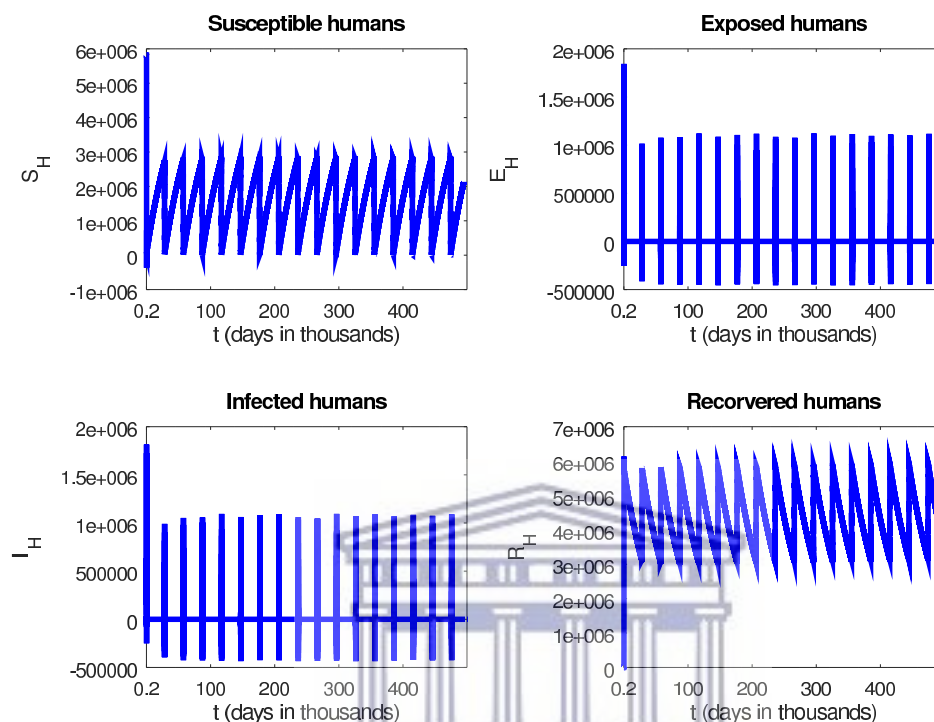


(a)

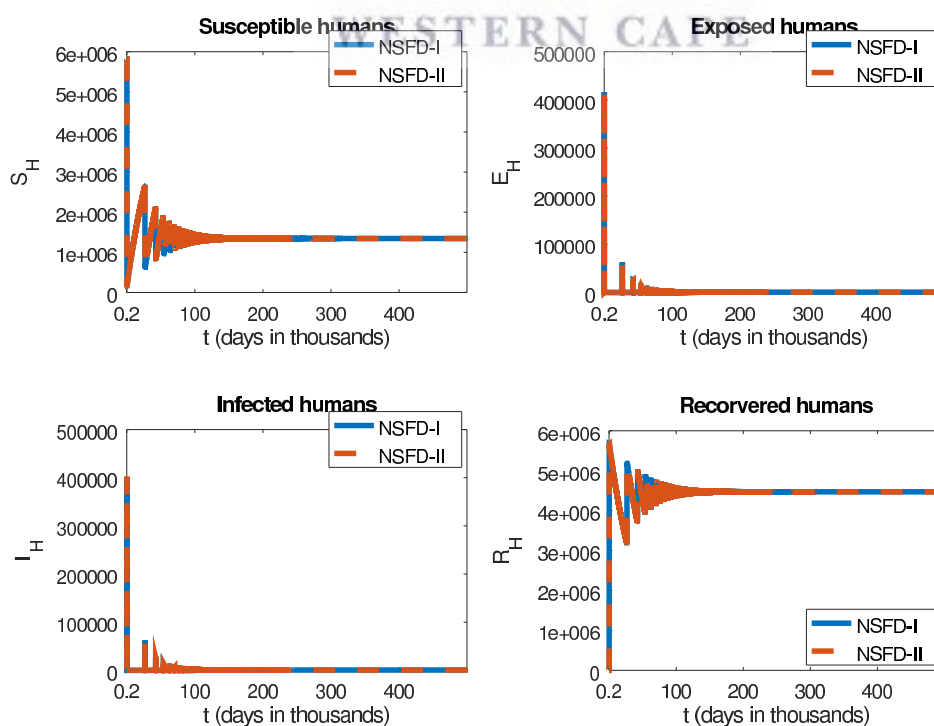


(b)

Figure 4.0.15 Profiles of solutions generated by Euler method (a) and by method NSFD-I and NSFD-II (b) for the vector population of patch 2 with  $R_{0,1} = 2.0802$  and  $\ell = 0.5$ .

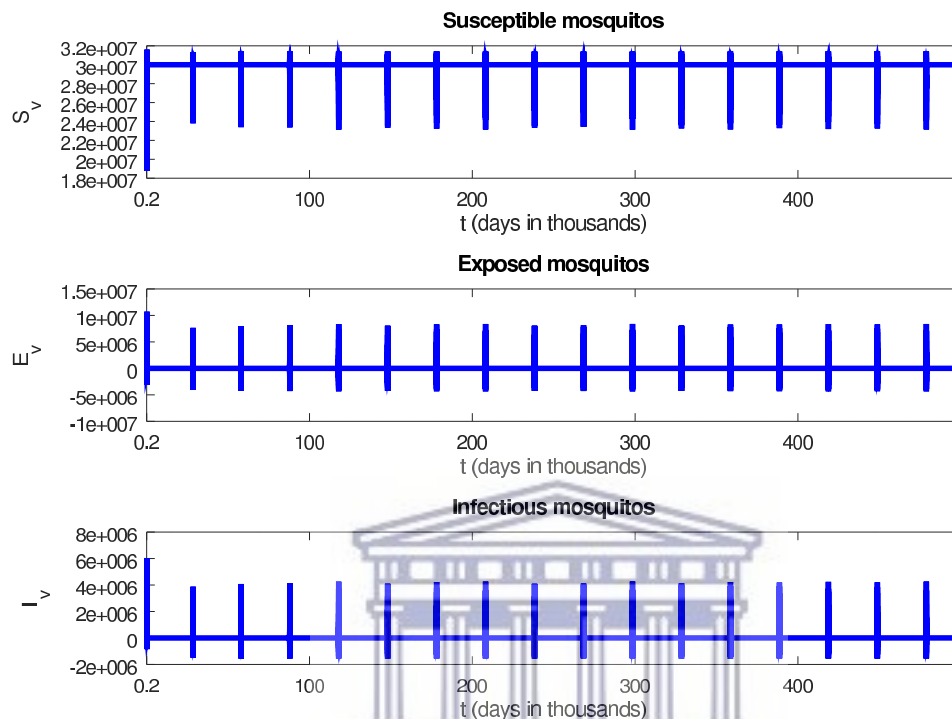


(a)

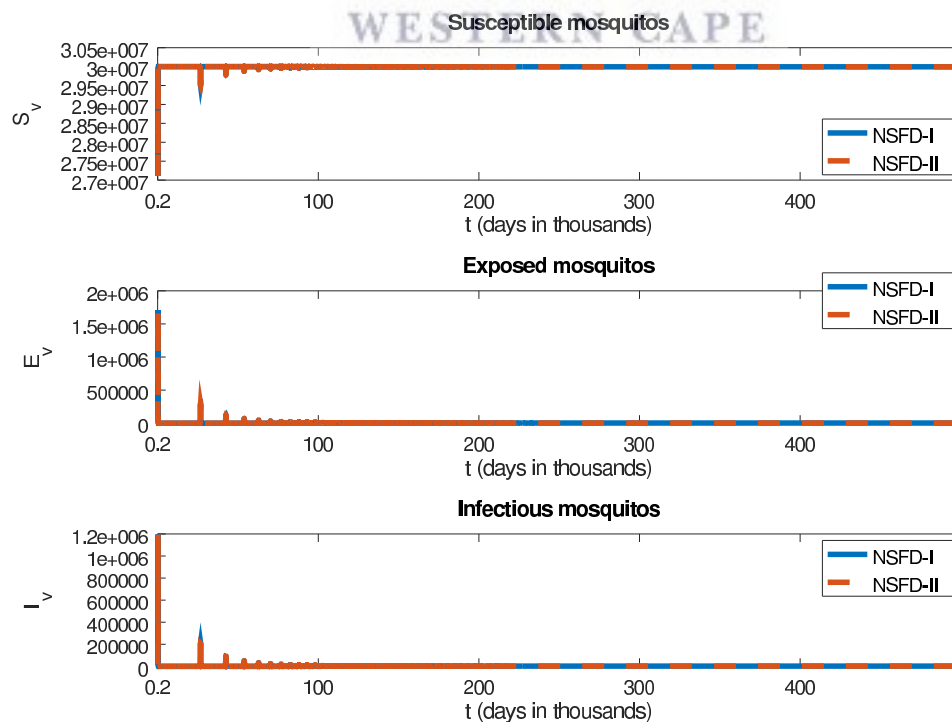


(b)

Figure 4.0.16 Profiles of solutions generated by Euler method (a) and by method NSFD-I and NSFD-II (b) for the human population of patch 2 with  $R_{0,1} = 2.0802$  and  $\ell = 5.8$ .

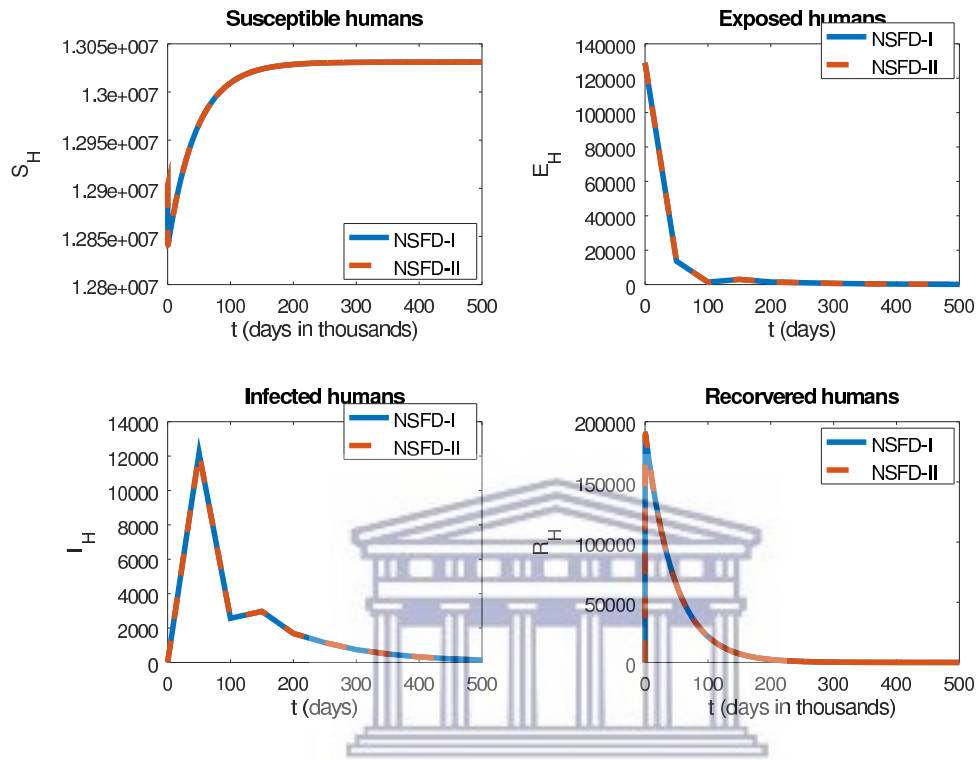


(a)

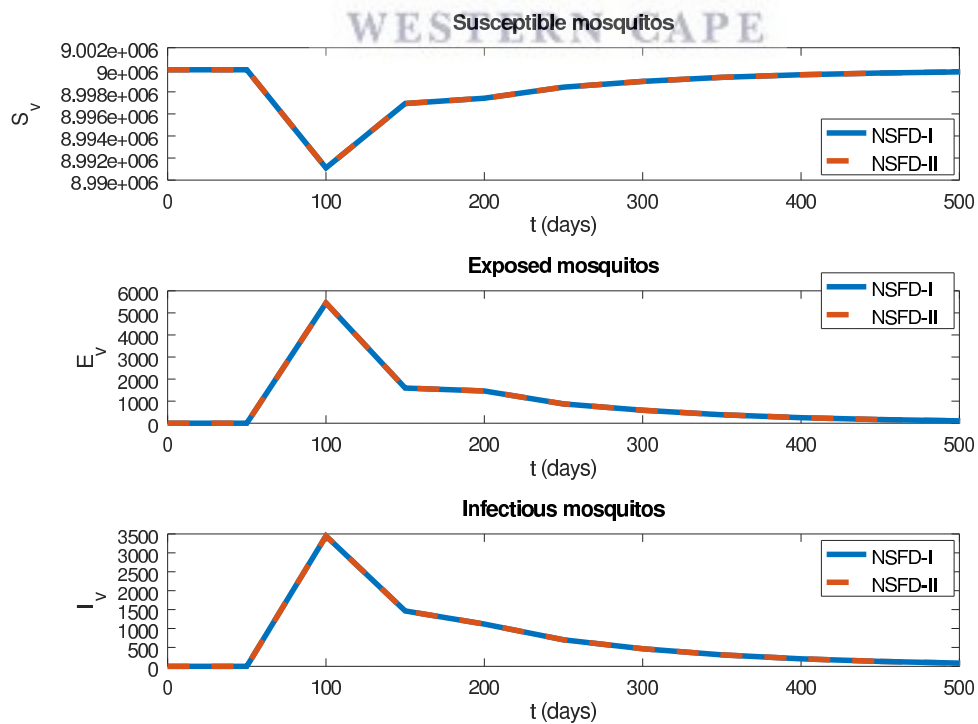


(b)

Figure 4.0.17 Profiles of solutions generated by Euler method (a) and by method NSFD-I and NSFD-II (b) for the vector population of patch 2 with  $R_{0,1} = 2.0802$  and  $\ell = 5.8$ .

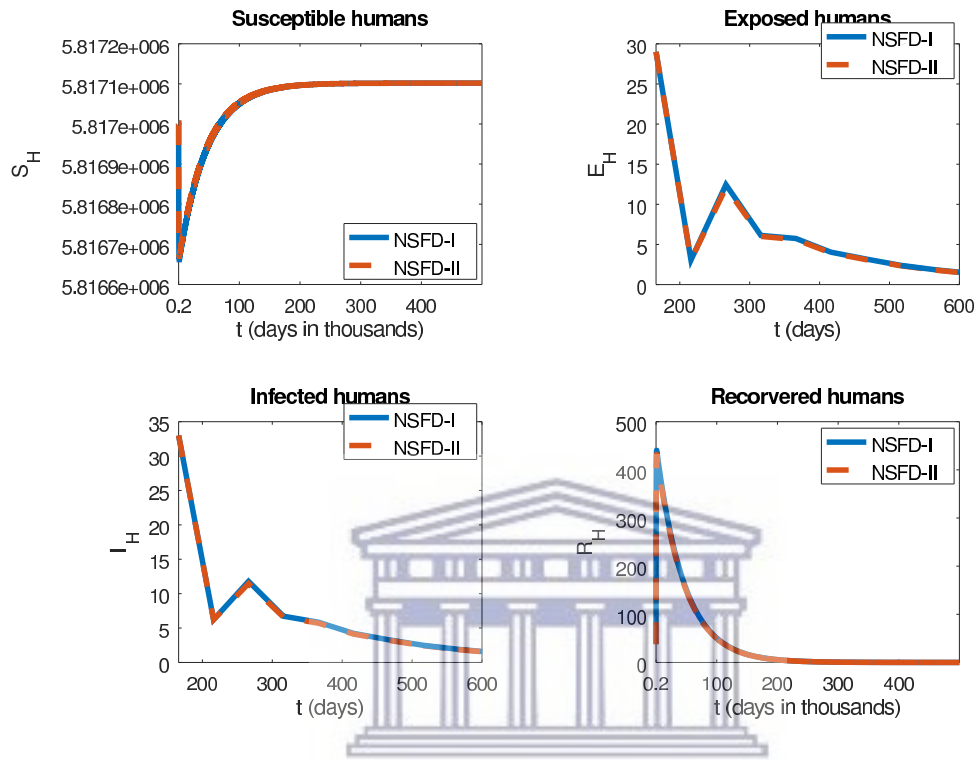


(a)

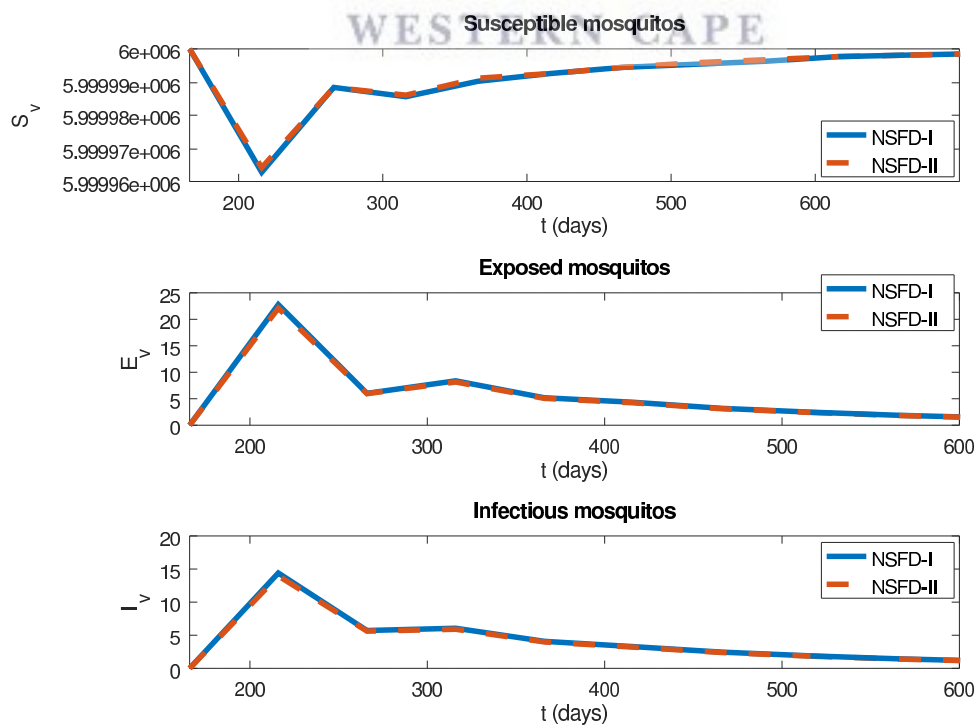


(b)

Figure 4.0.18 Profiles of solutions generated by method NSFD-I and NSFD-II for the human and vector populations of patch 1 with  $R_{0,1} = 0.57855$  and  $\ell = 50$ .



(a)



(b)

Figure 4.0.19 Profiles of solutions generated by method NSFD-I and NSFD-II for the human and vector populations of patch 2 with  $R_{0,2} = 0.70703$  and  $\ell = 50$ .

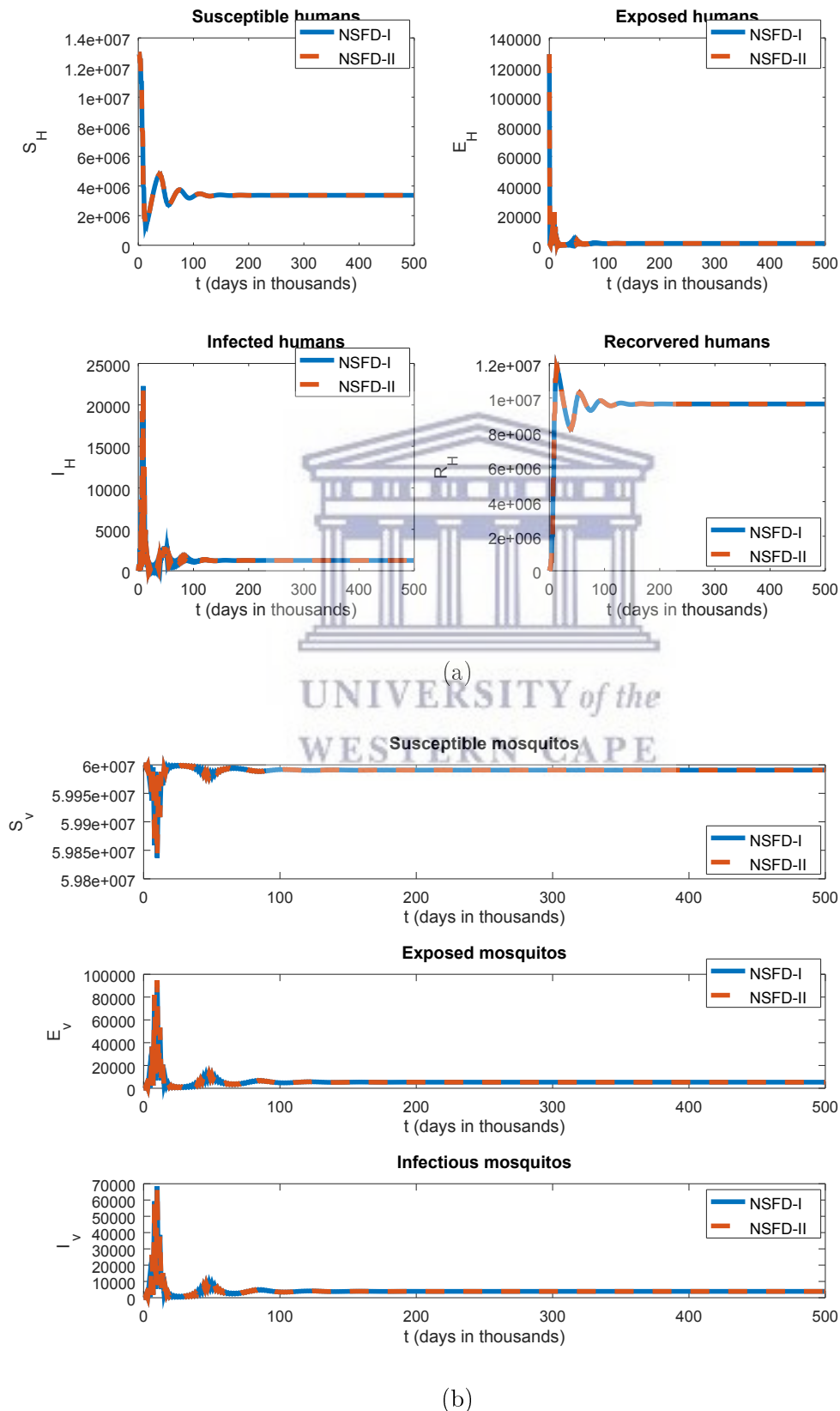


Figure 4.0.20 Profiles of solutions generated by method NSFD-I and NSFD-II for the human and vector populations of patch 1 with  $R_{0,1} = 1.9655$  and  $\ell = 1000$ .



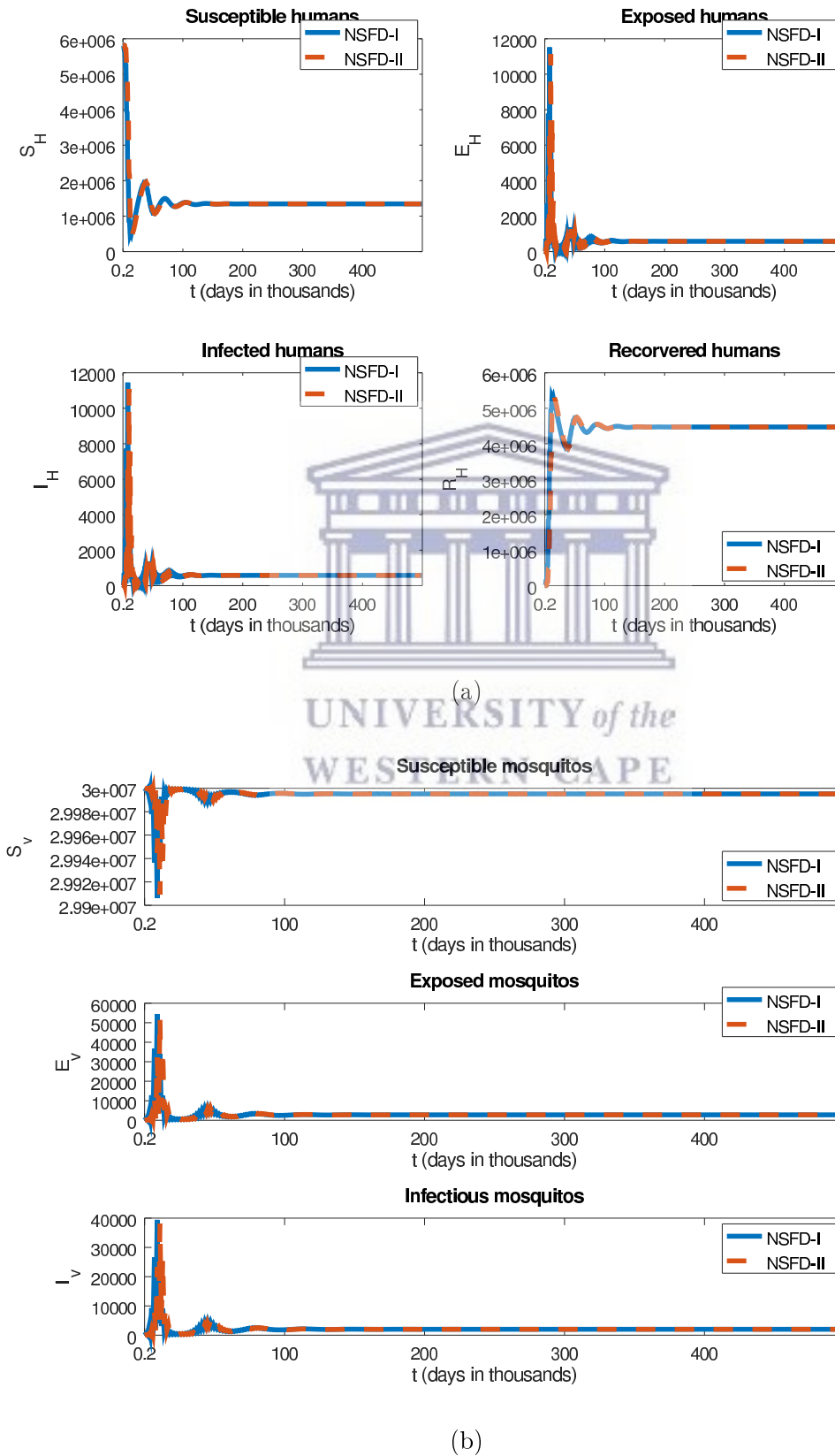
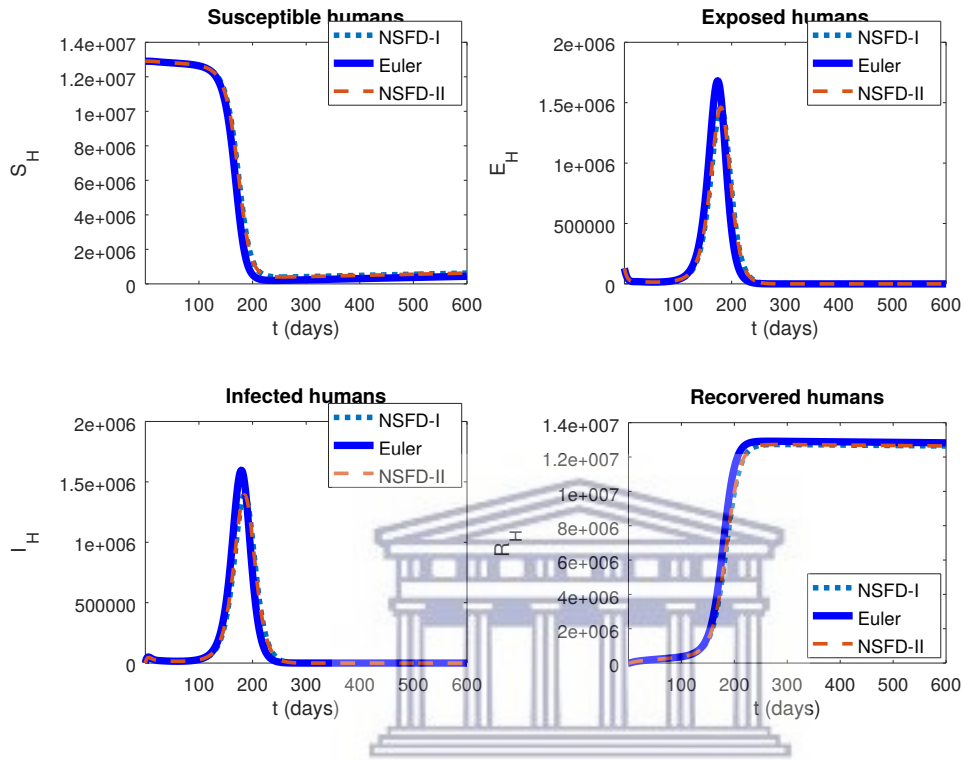
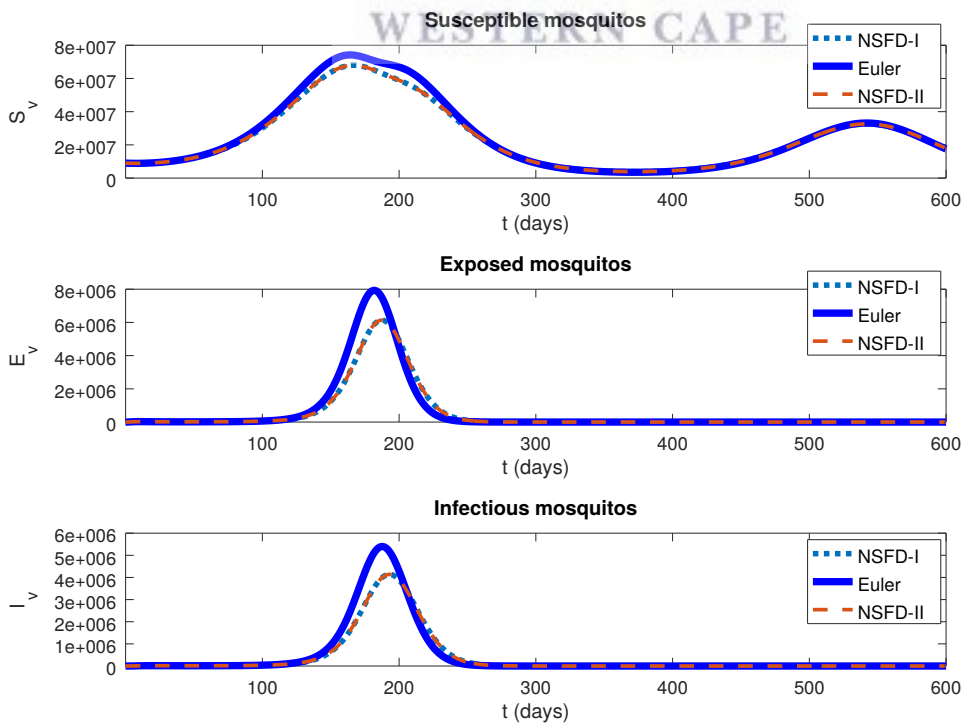


Figure 4.0.21 Profiles of solutions generated by method NSFD-I and NSFD-II for the human and vector populations of patch 2 with  $R_{0,2} = 2.0802$  and  $\ell = 1000$ .



(a)



(b)

Figure 4.0.22 Profiles of solutions generated by Euler, method NSFD-I and NSFD-IIs for the human and vector populations of patch 1 with  $b_v = 0.5$  and  $\ell = 0.5$ .

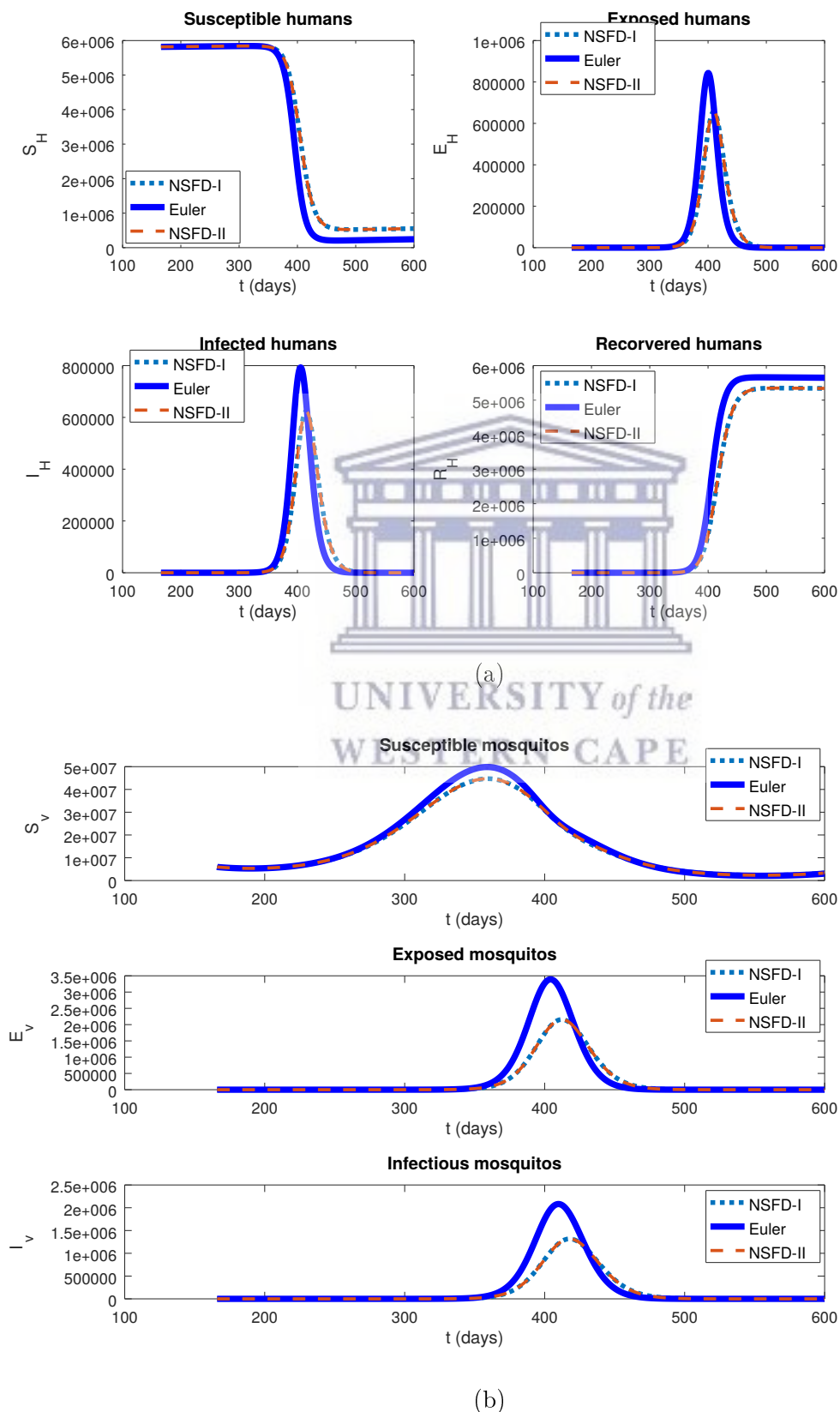


Figure 4.0.23 Profiles of solutions generated by Euler, method NSFD-I and NSFD-IIs for the human and vector populations of patch 2 with  $b_v = 0.5$  and  $\ell = 0.5$ .

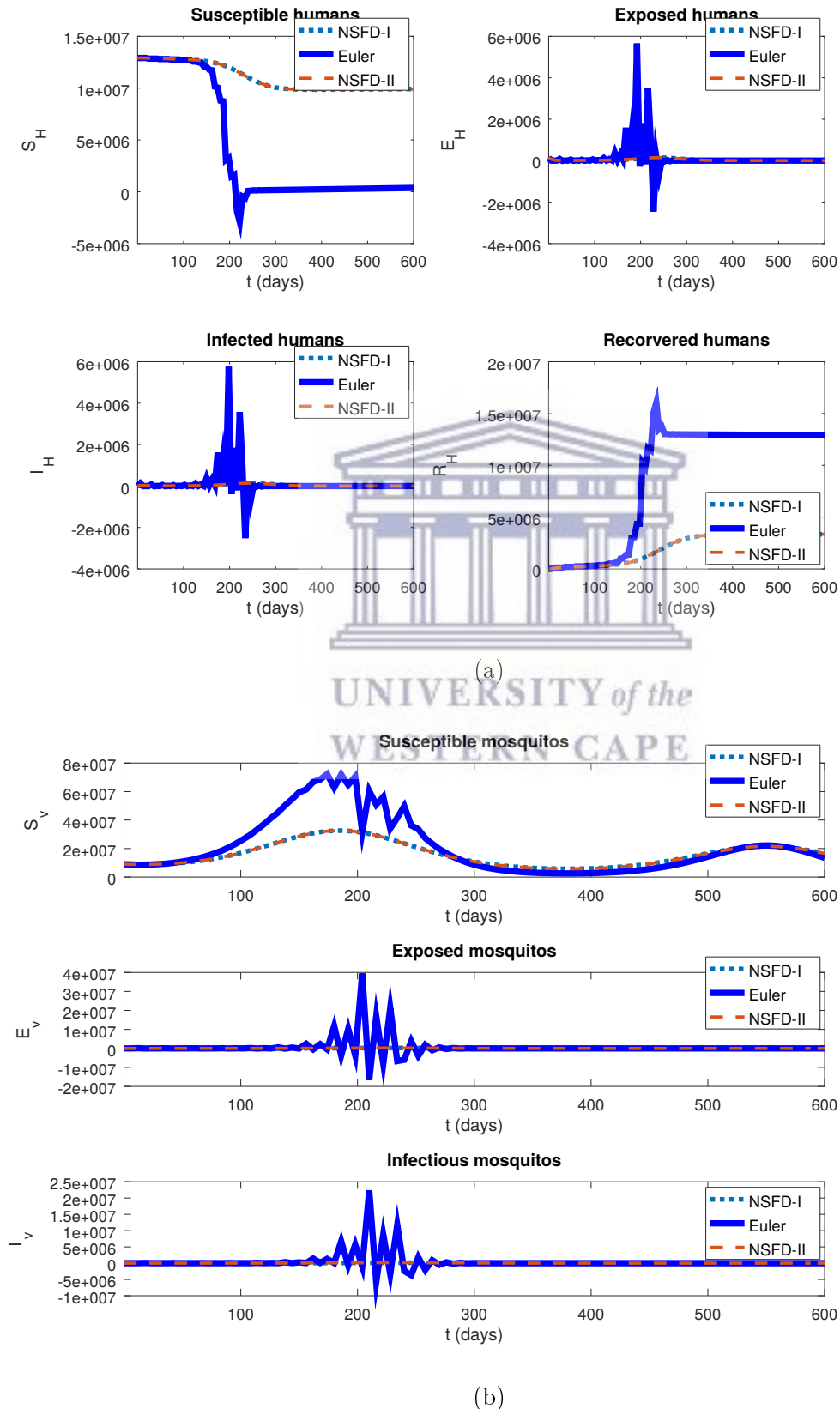
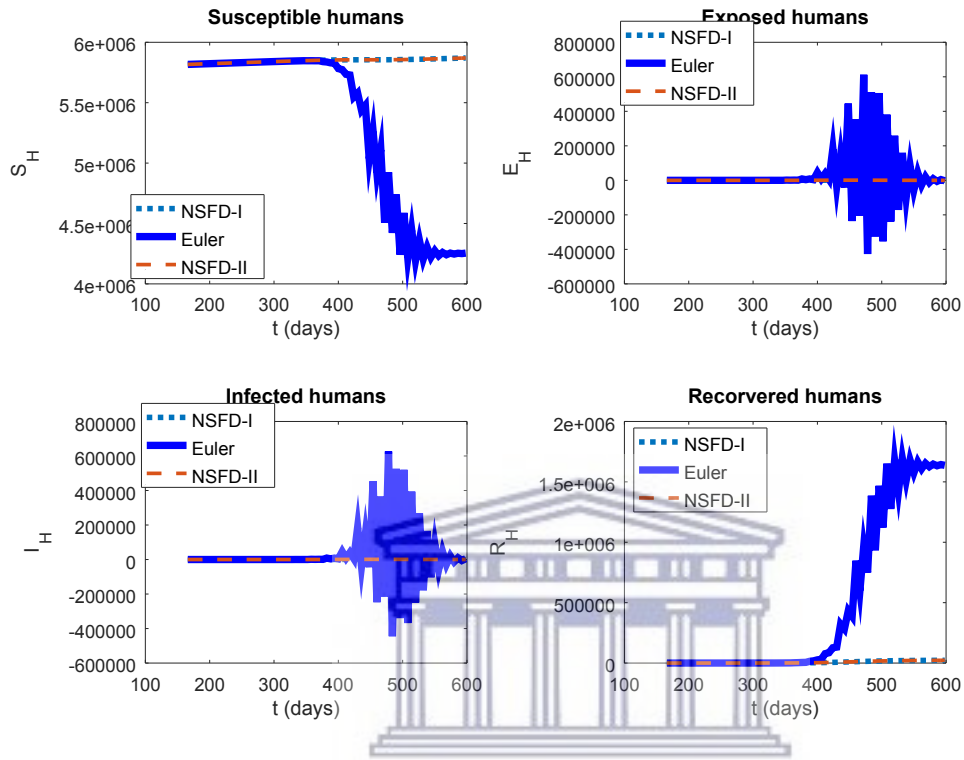
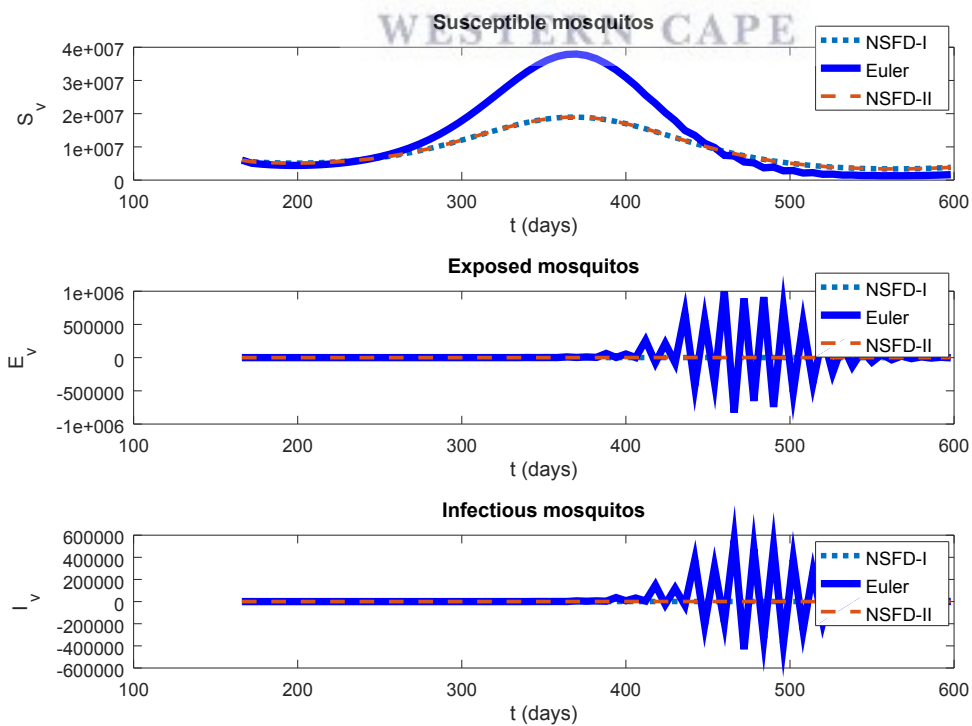


Figure 4.0.24 Profiles of solutions generated by Euler, method NSFD-I and NSFD-IIs for the human and vector populations of patch 1 with  $b_v = 0.5$  and  $\ell = 6$ .

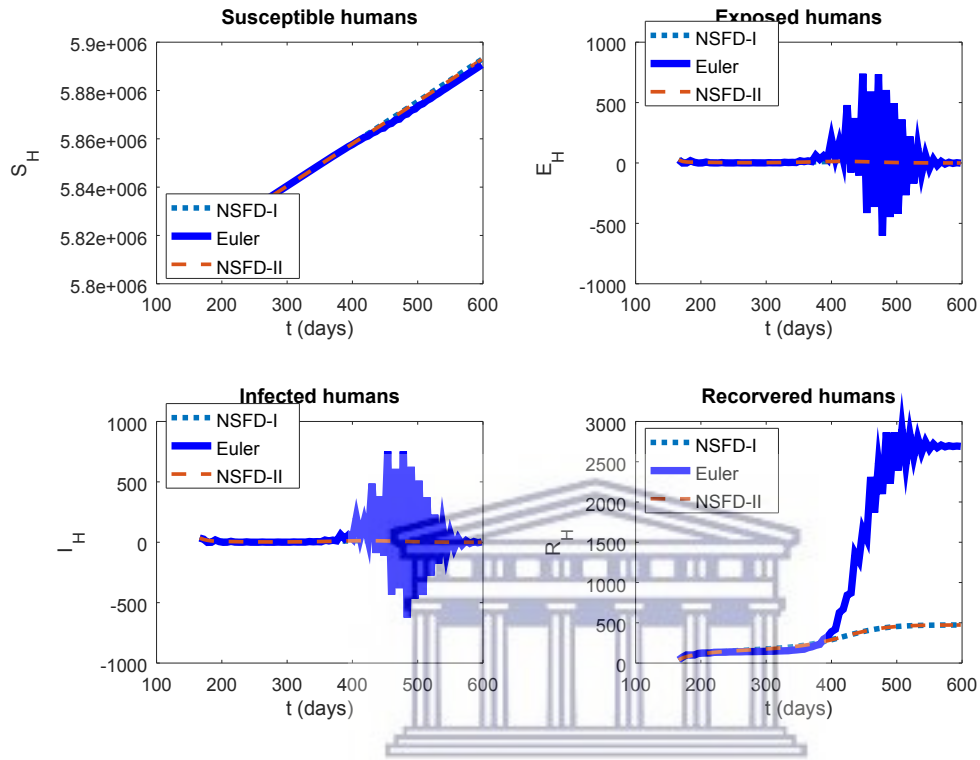


(a)

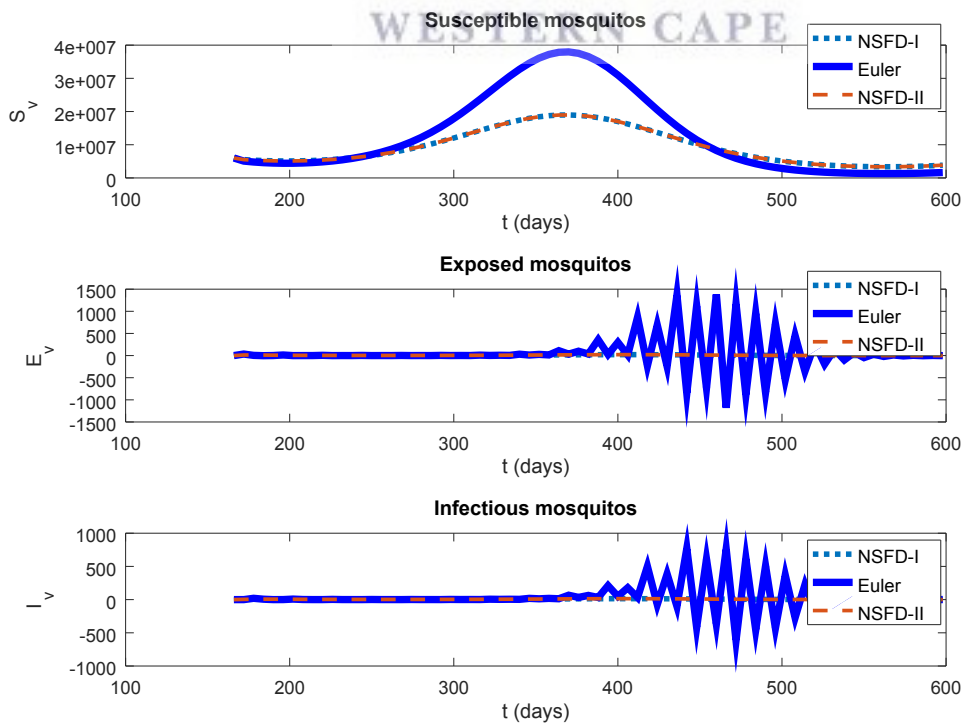


(b)

Figure 4.0.25 Profiles of solutions generated by Euler, method NSFD-I and NSFD-IIs for the human and vector populations of patch 2 with  $b_v = 0.5$  and  $\ell = 6$ .



(a)

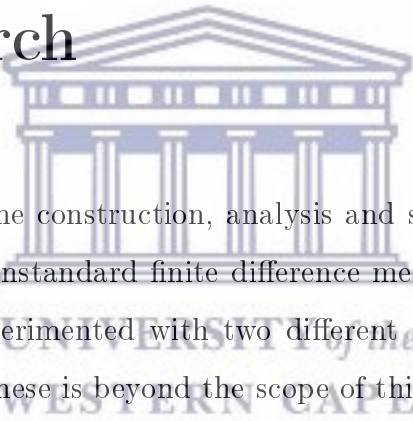


(b)

Figure 4.0.26 Profiles of solutions generated by Euler, method NSFD-I and NSFD-IIs for the human and vector populations of patch 2 with  $b_v = 0.38$  and  $\ell = 6$ .

## Chapter 5

# Concluding remarks and scope for further research



In the thesis we dealt with the construction, analysis and simulation of a robust numerical method called the nonstandard finite difference method to solve a Zika virus disease model. We have experimented with two different NSFDMs to explore their features. Further details on these is beyond the scope of this work.

In the first chapter, we gave a brief introduction on Zika virus disease, its history, symptoms, transmission, prevention and control. We then proceeded by giving literature review on the studies already done on the Zika virus modelling and provided a list of Zika models developed by several authors.

In Chapter 2, we studied the qualitative features of the model developed in [57]. These qualitative features included the positivity of the solution, equilibrium points of the model, the basic reproduction number  $R_{0,i}$  and both the local and global stability of the equilibrium points. In the local stability of the disease free equilibrium point  $E_{0,i}$ , we found that when analysing the eigenvalues of the Jacobean matrix at the disease free point  $E_{0,i}$ , with the aid of the Routh Hurwitz principle, the equilibrium point is locally asymptotically stable whenever  $R_{0,i} < 1$ . In the local stability of the endemic equilibrium point  $E_e^{*,i}$ , we found that the endemic equilibrium point exist and

is unique whenever  $R_{0,i} > 1$  and by studying the sign patterns of the Jacobean matrix at the endemic equilibrium  $E_e^{*,i}$ , we concluded that it is locally asymptotically stable. In global stability of the equilibrium points, we constructed a Lyapunov function to study the global stability of both the equilibrium point and concluded that the disease free equilibrium point will be globally asymptotically stable whenever  $R_{0,i} < 1$  and the endemic equilibrium point is globally asymptotically stable whenever  $R_{0,i} > 1$ .

In Chapter 3, we constructed a numerical method for a typical Zika virus model. This method is referred to as the nonstandard finite difference (NSFD) method. We started by looking at the general philosophy of the NSFD methods. We then proceeded by designing the numerical method for the model and presented both the implicit and explicit form of the discrete model. We then found that in the explicit form of the discrete model, the positivity of the solution is reflected. Following the work in [55], we presented two cases for the step-size function. In case 1, the NSFD-I we set  $\phi(\ell) = \ell$  and case 2, the NSFD-II we set  $\phi(\ell) = \frac{e^{\ell\mu_H^i} - 1}{\mu_H^i}$ . We then established the fixed points of the discrete model and found that the discrete model has the same fixed points as the continuous model. Due to the complexity of finding the eigenvalues of the Jacobean matrix analytically for the discrete model, we then calculated the eigenvalues of the Jacobean matrix at the fixed point numerically by using the perimeters provided by in [57] which are in Table 1.3.1 with  $\phi(\ell) = \ell = 0.5$ . It was then established that for  $R_{0,1} = 0.76125$  the modulus of the largest eigenvalue is less than a unit and therefore the disease free equilibrium point  $E_0^{m,1}$ , is stable and for  $R_{0,2} = 2.9419$  the modulus of the largest eigenvalue is less than a unit and therefore the endemic equilibrium  $E_{e,2}^m$  point is stable. Lastly, as a conventional method, we constructed the Euler method for the model and we also provided its explicit form.

In Chapter 4, we first provide Figure 4.0.1 containing the plot for the basic reproduction number  $R_{0,1}$  and  $R_{0,2}$  obtained using the NSFD-I for both patches showing the effect of the cyclical mosquito death rate  $\mu_v^i$  on the basic reproduction number.



In order to study the convergence of the numerical methods to the fixed points of the system, we assumed a constant vector population by equating the vector death rate  $\mu_v^i$  and birth rate  $\nu_v^i$  and took it to be the average between the maximum vector death rate  $\mu_v^{max,i}$  and the minimum vector death rate  $\mu_v^{min,i}$ . We then provided spectral radii in Table 4.0.1, 4.0.2, 4.0.3 and 4.0.4 showing the spectral radii obtained for the Jacobian matrices evaluated at the disease free and endemic equilibrium points for both patch 1 and 2 using different step-sizes. It is noted from these tables that the Euler method will only converge for a conveniently small step-size, but as the step-size become larger it will fail to converge. This is shown by the spectral radii becoming larger than 1 as the step-size is increased. For the NSFD methods (NSFD-I and NSFD-II), the table shows that the spectral radii will always remain less than 1 even for a larger step-size and therefore the numerical method will converge even for a larger step-size. We then provided figures to support the results shown in the tables by offering plots obtained using the NSFD-I, NSFD-II and Euler methods. We also noted that not only will the Euler method fail to converge for a larger step-size but it also fails to preserve the positivity property of the solution while the NSFD methods does. We then conclude the chapter by offering plots obtained from the numerical methods with a cyclical death rate  $\mu_v^i$  for  $\ell = 0.025$ ,  $\ell = 1$  and  $\ell = 6$  which shows that the methods NSFD-I and NSFD-II provide reliable results as  $\ell$  increases.

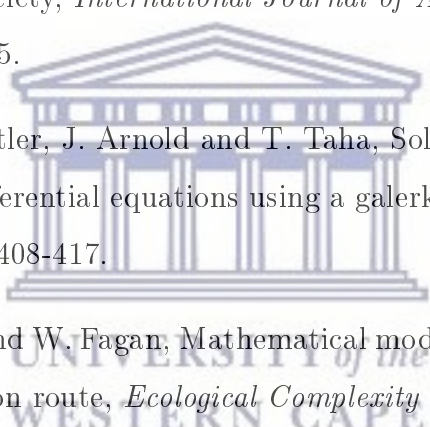
As far as **the scope for further research** is concerned, I wish to mention that

- In this thesis we could only concentrate on the construction of a robust numerical method. The focus was on the effect of the step-size on the performance of the numerical methods. However, to make such methods more robust, we also wish to investigate the effect of the change of parameters and initial conditions to the model.
- We also wish to explore higher order versions of NSFDs and to compare the results with other contemporary higher order methods. This requires a substantial amount of time and should I have a chance to pursue my PhD studies, this

will be one of my plans.



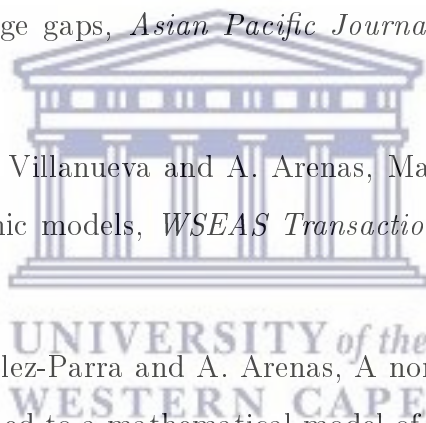
# Bibliography

- 
- [1] A. Ahmad, M. Farman, F. Yasin and M. Ahmad, Dynamical transmission and effect of smoking in society, *International Journal of Advanced and Applied Sciences* **5(2)** (2018) 71-75.
- [2] A. Al-Omari, H. Schuttler, J. Arnold and T. Taha, Solving nonlinear systems of first order ordinary differential equations using a galerkin finite element method, *IEEE Access* **1** (2013) 408-417.
- [3] F. Agosto, S. Bewick and W. Fagan, Mathematical model for Zika virus dynamics with sexual transmission route, *Ecological Complexity* **29** (2017) 61-81.
- [4] F. Agosto, S. Bewick and W. Fagan, Mathematical model of Zika virus with vertical transmission, *Infectious Disease Modelling* **2** (2017) 244-267.
- [5] J. Anaya, Y. Rodríguez, D. Monsalve, D. Vega, E. Ojeda, D. González-Bravo, M. Rodríguez-Jiménez, C. Pinto-Díaz, P. Chaparro, M. Gunturiz, A. Ansari, M. Gershwin, N. Molano-González, C. Ramírez-Santana and Y. Acosta-Ampudia, A comprehensive analysis and immunobiology of autoimmune neurological syndromes during the Zika virus outbreak in Cúcuta, Colombia, *Journal of Autoimmunity* **77** (2017) 123-138.
- [6] M. Ayana and P. Koya, The impact of infective immigrants on the spread and dynamics of Zika virus diseases, *American Journal of Applied Mathematics* **5(6)** (2017) 145-153.

- [7] A. Arenas, G. González-Parra and B. Chen-Charpentier, A nonstandard numerical scheme of predictor-corrector type for epidemic models, *Computers and Mathematics with Applications* **59** (2010) 3740-3749.
- [8] G. Benelli, Spread of Zika virus: The key role of mosquito vector control, *Asian Pacific Journal of Tropical Biomedicine* **6(6)** (2016) 468-471.
- [9] I. Bogoch, O. Brady, M. Kraemer, M. German, M. Creatore, S. Brent, A. Watts, S. Hay, M. Kulkarni, J. Brownstein and K. Khan, Potential for Zika virus introduction and transmission in resource-limited countries in Africa and the Asia-Pacific region: a modelling study, *The Lancet Infectious Diseases* **16(11)** (2016) 1237-1245.
- [10] E. Bonyah and K. Okosun, Mathematical modeling of Zika virus, *Asian Pacific Journal of Tropical Disease* **6(9)** (2016) 673-679.
- [11] S. Bowong, J. Tewa and J. Kamgang, Stability analysis of the transmission dynamics of tuberculosis models, *Stability analysis of the transmission dynamics of tuberculosis models* **7(2)** (2011) 83-100.
- [12] N. Chaikham and W. Sawangtong, Optimal control of Zika virus infection by vector elimination, vector-to-human and human-to-human contact reduction, *Advances in Difference Equations* **1** (2017) 177.
- [13] G. Cruz-Pacheco, L. Esteva and C. Ferreira, The spread of Zika as a vectorial and sexual transmitted disease: a mathematical model analysis, *Journal of Biological Systems* (2019) 1-23.
- [14] Q. Cui, J. Xu, Q. Zhang and K. Wang, An NSFD scheme for SIR epidemic models of childhood diseases with constant vaccination strategy, *Advances in Difference Equations* **1** (2014) 172.

- [15] Q. Dang and M. Hoang, Lyapunov direct method for investigating stability of nonstandard finite difference schemes for metapopulation models, *Journal of Difference Equations and Applications* **24(1)** (2018) 15-47.
- [16] E. Dantas, M. Tosin, J. Peterson, V. Lopes and A. Cunha Jr, A mathematical analysis about Zika virus outbreak in Rio de Janeiro, *Conference of Computational Interdisciplinary Science (CCIS 2016)* **4** (2016).
- [17] B. Dawit and P. Kalyani, Application of non-standard finite difference method on logistic differential equation and comparison with standard difference methods, *IOSR Journal of Mathematics (IOSR-JM)* **12** (2016) 2278-5728.
- [18] M. Díaz-Menéndez, E. Trigo, F. de la Calle-Prieto and M. Arsuaga, Zika virus infection during the Olympic Games in Rio: A fear or an actual risk?, *Revista Clínica Española* **3** (2017) 155-160.
- [19] D. Ding, Q. Ma and X. Ding, An unconditionally positive and global stability preserving NSFD scheme for an epidemic model with vaccination, *International Journal of Applied Mathematics and Computer Science* **24(3)** (2014) 635-646.
- [20] C. Ding, N. Tao and Y. Zhu, A mathematical model of Zika virus and its optimal control, *Control Conference* **35** (2017) 2642-2645.
- [21] V. Duong, P. Dussart and P. Buchy, Zika virus in Asia, *International Journal of Infectious Diseases* **54** (2017) 121-128.
- [22] <https://ecdc.europa.eu/en/publications-data/zika-virus-disease-epidemic-preparedness-planning-guide-diseases-transmitted>.
- [23] U. Fatima, M. Ali, N. Ahmed and M. Rafiq, Numerical modeling of susceptible latent breaking-out quarantine computer virus epidemic dynamics, *Heliyon* **4(5)** (2018) e00631.

- [24] W. Fitzgibbon, J. Morgan and G. Webb, An outbreak vector-host epidemic model with spatial structure: the 2015-2016 Zika outbreak in Rio De Janeiro, *Theoretical Biology and Medical Modelling* **14**(1) (2017) 7.
- [25] D. Gao, Y. Lou, D. He, T. Porco, Y. Kuang, G. Chowell and S. Ruan, Prevention and control of Zika as a mosquito-borne and sexually transmitted disease: A mathematical modeling analysis, *Scientific Reports* **6** (2016) 28070.
- [26] Y. Gebre, N. Forbes and T. Gebre, Zika virus infection, transmission, associated neurological disorders and birth abnormalities: A review of progress in research, priorities and knowledge gaps, *Asian Pacific Journal of Tropical Biomedicine* **6**(10) (2016) 815-824.
- [27] G. Gonzalez-Parra, R. Villanueva and A. Arenas, Matrix nonstandard numerical schemes for epidemic models, *WSEAS Transactions on Mathematics* **9**(11) (2010) 840-850.
- [28] F. Guerrero, G. González-Parra and A. Arenas, A nonstandard finite difference numerical scheme applied to a mathematical model of the prevalence of smoking in Spain: a case study, *Computational and Applied Mathematics* **33** (2014) 13-25.
- [29] K. Gurski, A simple construction of nonstandard finite-difference schemes for small nonlinear systems applied to SIR models, *Computers and Mathematics with Applications* **66** (2013) 2165-2177.
- [30] V. Hall, W. Walker, N. Lindsey, J. Lehman, J. Kolsin, K. Landry, I. Rabe, S. Hills, M. Fischer, J. Staples, C. Gould and S. Martin, Update: noncongenital Zika virus disease cases - 50 U.S. states and the District of Columbia, 2016, *Morbidity and Mortality Weekly Report* **67**(9) (2018) 265.
- [31] H. Harapan, A. Aletta, S. Anwar, A. Setiawan, R. Maulana, N. Wahyuniati, M. Ramadana, S. Haryanto, A. Rodríguez-Morales and K. Jamil, Healthcare

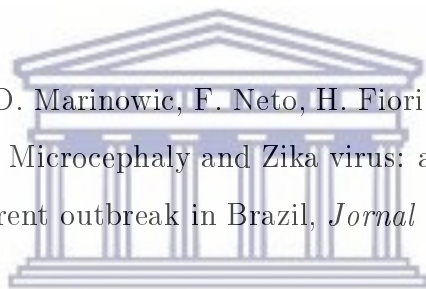


- workers' knowledge towards Zika virus infection in Indonesia: A survey in Aceh, *Asian Pacific Journal of Tropical Medicine* **10(2)** (2017) 189-194.
- [32] A. Huang, P. Shu and C. Yang, A new reportable disease is born: Taiwan Centers for Disease Control's response to emerging Zika virus infection, *Journal of the Formosan Medical Association* **115** (2016) 223-225.
- [33] S. Ioos, H. Mallet, I. Goffart, V. Gauthier, T. Cardoso and M. Herida, Current Zika virus epidemiology and recent epidemics, *Médecine et Maladies Infectieuses* **44** (2014) 302-307.
- [34] M. Khalid, F. Khan, Stability analysis of deterministic mathematical model for Zika virus, *British Journal of Mathematics and Computer Science* **19** (2016) 1-10.
- [35] N. Khanh, Stability analysis of an influenza virus model with disease resistance, *Journal of the Egyptian Mathematical Society* **24** (2016) 193-199.
- [36] S. Khongwicht, N. Wikan and P. Auewarakul, D. Smith, Zika virus in Thailand, *Microbes and Infection* **20** (2018) 670-675.
- [37] A. Kucharski, S. Funk, R. Eggo, H. Mallet, W. Edmunds and E. Nilles, Transmission dynamics of Zika virus disease in island populations: A Modelling Analysis of the 2013-14 French Polynesia Outbreak, *PLOS Neglected Tropical Diseases* **10(5)** (2016) e0004726.
- [38] M. Kumar, K. Krause, F. Azouz, E. Nakano and V. Nerurkar, A guinea pig model of Zika virus infection, *Virology Journal* **14(1)** (2017) 75.
- [39] J. Lamwong and P. Pongsumpun, The Zika virus transmission model, *International Journal of Bioscience* **7(2)** (2017) 66-73.
- [40] J. Lamwong and P. Pongsumpun, Age structural model of Zika virus, *International Journal of Modeling and Optimization* **8(1)** (2018).

- [41] J. LaSalle, Stability theory for ordinary differential equations, *Journal of Differential Equations* **4(1)** (1968) 57-65.
- [42] E. Lee, Y. Liu and F. Pietz, A compartmental model for Zika virus with dynamic human and vector populations, *AMIA Annual Symposium Proceedings* **2016** (2016) 743.
- [43] H. Li and S. Guo, Dynamics of a SIRC epidemiological model, *Electronic Journal of Differential Equations* **121** (2017) 1-18.
- [44] S. Liao and W. Yang, A nonstandard finite difference method applied to a mathematical cholera model, *Journal of Computational Analysis & Applications* **26** (2019) 1.
- [45] G. Liuzzi, E. Nicastrì and V. Puro, Zika virus in saliva-New challenges for prevention of human to human transmission, *European Journal of Internal Medicine* **33** (2016) e20-e21.
- [46] D. Lo and B. Park, Modeling the spread of the Zika virus using topological data analysis, *PLOS One* **13(2)** (2018) e0192120.
- [47] R.E. Mickens, *Nonstandard Finite Difference Models of Differential Equations*, World Scientific, Singapore, 1994.
- [48] R. Mickens, Determination of denominator functions for a NSFD scheme for the Fisher PDE with linear advection, *Mathematics and Computers in Simulation* **74** (2007) 190-195.
- [49] R. Mickens and T. Washington, A note on an NSFD scheme for a mathematical model of respiratory virus transmission, *Journal of Difference Equations and Applications* **18(3)** (2012) 525-529.
- [50] J. Mlakar, M. Korva, N. Tul and M. Popović, Zika virus associated with microcephaly, *New England Journal of Medicine* **374(10)** (2016) 951-958.

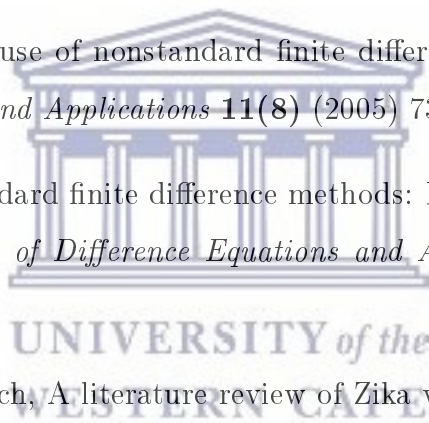


- [51] A. Momoh and A. Fügenschuh, Optimal control of intervention strategies and cost effectiveness Analysis for a Zika Virus Model, *Operations Research for Health Care* **18** (2018) 99-111.
- [52] E. Moya and R. Plata, Mathematical model of diffusion-advection for Zika, *Proceeding Series of the Brazilian Society of Computational and Applied Mathematics* **7(1)** (2018).
- [53] A. Muñoz, H. Colorado and C. Abello, Numerical analysis of the prevention with vaccination against Zika virus (ZIKV), *Contemporary Engineering Sciences* **12(1)** (2019) 33 - 40.
- [54] M. Nunes, C. Carlini, D. Marinowic, F. Neto, H. Fiori, M. Scotta, P. Zanella, R. Soder and J. da Costa, Microcephaly and Zika virus: a clinical and epidemiological analysis of the current outbreak in Brazil, *Jornal de Pediatria* **92(3)** (2016) 230-240.
- [55] H. Obaid, R. Ouifki and K. Patidar. An unconditionally stable nonstandard finite difference method applied to a mathematical model of HIV infection, *International Journal of Applied Mathematics and Computer Science* **23(2)** (2013) 357-372.
- [56] C. Oeser and S. Ladhani, An update on Zika virus and congenital Zika syndrome, *Paediatrics and Child Health* **29(1)** (2019) 34-37.
- [57] C. Oleson and M. Artzrouni, A Patch Model for the transmission dynamics of Zika virus disease from Rio de Janeiro to Miami during Carnival and the Olympics, (2016). DOI:10.1137/16S015425
- [58] T. Oluyo and M. Adeyemi, Mathematical analysis of Zika epidemic model, *IOSR Journal of Mathematics* **12** (2016) 21-33.
- [59] E. Oluwaseun, C. Harley and B. Jacobs, Nonstandard finite difference method applied to a linear pharmacokinetics model, *Bioengineering* **4(2)** (2017) 40.



UNIVERSITY of the  
WESTERN CAPE

- [60] M. Onguna and N. Ozdogan, A nonstandard numerical scheme for a predator-prey model with Allee effect, *Journal of Nonlinear Sciences & Applications (JNSA)* **10(2)** (2017).
- [61] M. Onuorah, A. Ademu, E. Obi and A. Hasheem, Deterministic mathematical model of Zika virus, *Researchjournal's Journal of Mathematics* **3(3)** (2016) 1-15.
- [62] P. Padmanabhan, P. Seshaiyer and C. Castillo-Chavez, Mathematical modeling, analysis and simulation of the spread of Zika with influence of sexual transmission and preventive measures, *Letters in Biomathematics* **4(1)** (2017) 48-166.
- [63] K.C. Patidar, On the use of nonstandard finite difference methods, *Journal of Difference Equations and Applications* **11(8)** (2005) 735-758.
- [64] K.C. Patidar, Nonstandard finite difference methods: Recent trends and further developments, *Journal of Difference Equations and Applications* **22(6)** (2016) 817-849.
- [65] A. Plourde and E. Bloch, A literature review of Zika virus, *Emerging Infectious Diseases* **22(7)** (2016) 1185.
- [66] D. Shutt, C. Manore, S. Pankavich, A. Porter and S. Del Valle, Estimating the reproduction number, total outbreak size, and reporting rates for Zika epidemics in South and Central America, *Epidemics* **21** (2017) 63-79.
- [67] A. Srivastav, J. Yang, X. Luo and M. Ghosh, Spread of Zika virus disease on complex network—A mathematical study, *Mathematics and Computers in Simulation* **157** (2019) 15-38.
- [68] P. Suparit, A. Wiratsudakul and C. Modchang, A mathematical model for Zika virus transmission dynamics with a time-dependent mosquito biting rate, *Theoretical Biology and Medical Modelling* **15(1)** (2018) 11.



- [69] A. Suryanto, A nonstandard finite difference scheme for sis epidemic model with delay: stability and bifurcation analysis, *Applied Mathematics* **3** (2012) 528-534.
- [70] N. Sweilam and T. Assiri, Non-standard finite difference schemes for solving fractional order hyperbolic partial differential equations with Riesz fractional derivative, *Journal of Fractional Calculus and Applications* **7(1)** (2016) 46-60.
- [71] W. Tang, M. Young, A. Mamidi, J. Regla-Nava, K. Kim and S. Shresta, A mouse model of Zika virus sexual transmission and vaginal viral replication, *Cell Reports* **17(12)** (2016) 3091-3098.
- [72] Y. Teng, D. Bi, G. Xie, Y. Jin, Y. Huang, B. Lin, X. An, Y. Tong and D. Feng, Model-informed risk assessment for Zika virus outbreaks in the Asia-Pacific regions, *Journal of Infection* **74** (2017) 484-491.
- [73] P. Van den Driessche and J. Watmough, Reproduction numbers and sub-threshold endemic equilibria for compartmental models of disease transmission, *Mathematical Biosciences* **180** (2002) 29-48.
- [74] S. Weaver, F. Costa, M. Garcia-Blanco, A. Ko, G. Ribeiro, G. Saade, P. Shi and N. Vasilakis, Zika virus: History, emergence, biology, and prospects for control, *Antiviral Research* **130** (2016) 69-80.
- [75] World Health Organization, The history of Zika virus: <http://www.who.int/emergencies/zika-virus/timeline/en/>.
- [76] L. Wong, H. Alias, J. Hassan and S. AbuBakar, Attitudes towards Zika screening and vaccination acceptability among pregnant women in Malaysia, *Vaccine* **35(43)** (2017) 5912-5917.
- [77] S. Wong, R. Wing-Shan, P. Sally and C. Wong, Zika virus infection-the next wave after dengue?, *Journal of the Formosan Medical Association* **115** (2016) 226-242.

- [78] J. Xu and Y. Geng, A nonstandard finite difference scheme for a multi-group epidemic model with time delay, *Advances in Difference Equations* **2017(1)** (2017) 358.
- [79] J. Xu and Y. Geng, Dynamic consistent NSFD scheme for a delayed viral infection model with immune response and nonlinear incidence, *Discrete Dynamics in Nature and Society* **2017** (2017).
- [80] H. Yang, The basic reproduction number obtained from Jacobian and next generation matrices – A case study of dengue transmission modelling, *BioSystems* **126** (2014) 52-75.
- [81] C. Zanluca and C. Duarte dos Santos, Zika virus-an overview, *Microbes and Infection* **18** (2016) 295-301.
- [82] Q. Zhang, K. Sun and M. Chinazzi, Spread of Zika virus in the Americas, *Proceedings of the National Academy of Sciences* **114(22)** (2017) E4334-E4343.
- [83] S. Zibaei and M. Namjoo, A nonstandard finite difference scheme for solving fractional-order model of HIV-1 infection of CD4 T-cells, *Iranian Journal of Mathematical Chemistry* **6(2)** (2015) 169-184.
- [84] A. Zeb, M. Khan, G. Zaman, S. Momani and V. Ertürk, Comparison of numerical methods of the SEIR epidemic model of fractional order, *Zeitschrift für Naturforschung A* **69(1-2)** (2014) 81-89.
- [85] Z. Zhang, H. Wang, C. Wang and H. Fang, Modeling epidemics spreading on social contact networks, *IEEE Transactions on Emerging Topics in Computing* **3(3)** (2015) 410-419.